SIMULATION MODELS FOR INVESTIGATING EAST COAST FEVER AND OTHER PARASITIC DISEASES.

W. BYROM.

Ph.D. Thesis.

Department of Statistics and Modelling Science
University of Strathclyde
GLASGOW, U.K.

1990.

CONTENTS

ACKNOWLEDGEMENTS v

ABSTRACT vi

CHAPTER 1. INTRODUCTION 1

CHAPTER 2. COMPETITION MODELS FOR SIMPLE PARASITE SYSTEMS 11

2.1 Introduction 11

2.2 Single species model 13

2.3 Two species commensalism model 19

2.4 Two species competition model 23

2.5 Rules for the coexistance of N competing species 27

2.6 Conclusions 28

CHAPTER 3. EAST COAST FEVER 29

3.1 East Coast fever 29

3.2 Life cycle of the tick 31

3.3 Life cycle of the parasite 33

3.4 Clinical features of the disease 36

3.5 Disease control 37

CHAPTER 4. MODELS BASED ON EXPERT RULES FOR PARASITE BEHAVIOUR 40

4.1 Quantitative studies on the life cycle 41

4.2 Simple mathematical model 42

4.3 Deterministic model for the behaviour of the level of infection amongst a tick population 50

4.4 Further models 62

4.5 Discussion 85

CHAPTER 5. SIMULATION MODELS OF TICK AND CATTLE POPULATIONS AND DISEASE TRANSMISSION 87

5.1 The tick model 87

5.2 The ECF model 108

5.3 The dipping model 112
5.4 The chemotherapy model 113
5.5 Conclusions 115
CHAPTER 6. GENERATION OF WEATHER SEQUENCE DATA 116
6.1 Introduction 116
6.2 Existing models for rainfall and temperature 116
6.3 Simulation model requirements 122
6.4 Materials and methods 122
6.5 Simulation models 123
6.6 Conclusions 153
CHAPTER 7. ECFXPERT: AN INTEGRATED MODEL 154
7.1 ECFXPERT environment and knowledge base 155
7.2 Programming details 156
7.3 The ECFXPERT package 160
CHAPTER 8. RESULTS 161
8.1 Validation of models 162
8.2 The observed variation in model output 163
8.3 The effects of the tick attachment probability on
tick populations and ECF 165
8.4 The effects of infective period and carrier status on disease 166
8.5 The effects of climatic change on tick populations and ECF 166
8.6 The effects of grass length on tick populations and ECF 170
8.7 The effects of dipping on tick populations and ECF 172
8.8 The effects of chemotherapy on disease 175
8.9 The effects of the carrier infectivity rate on disease 177
8.10 Conclusions 177
CHAPTER 9. DISCUSSION 179
REFERENCES 183

ACKNOWLEDGEMENTS

I would like to thank my supervisor, Dr. George Gettinby, for his tireless source of help and advice, and for his enthusiastic encouragement throughout the course of this project. I would also like to thank my colleague, Steven Hazelwood, for his invaluable help in enhancing the computer programs.

Grateful thanks are due to the staff of the International Laboratory for Research on Animal Diseases, Nairobi, for their support, and especially to Dr. T. Dolan, Dr. I. Morrison, Dr. S. Morzaria and Dr. A. Norval for their expert advice concerning the biological aspects of this thesis. Thanks also to Dr. N. McHardy of Cooper Pitman-Moore Animal Health Ltd., Berkhamsted, for kindly supplying chemotherapy data, and to Dr. D. Berkvens of the Belgian Animal Disease Control Project, Zambia and Dr. B. Perry of the International Laboratory for Research on Animal Diseases, Nairobi, who supplied climatic data for many of the sites in this study.

Finally, but by no means least, thanks to Mrs. Lynne Westwood for her skill and patience in preparing this thesis.

I gratefully acknowledge the financial support of the Overseas Development Administration, U.K.

ABSTRACT

Parasitic diseases of animals place a large constraint on livestock production world-wide. The parasite *Theileria parva*, and the disease East Coast fever it produces, are responsible for the deaths of thousands of cattle each year in central and eastern Africa. Disease control is one way in which agricultural production can be improved, and is a matter of fundamental importance to developing countries where levels of nutrient intake are dangerously low over the majority of the population.

This thesis presents computer simulation models to study East Coast fever and its control. Models are constructed based on expert rules extracted from over 80 years of scientific literature concerning the disease. Rules are translated into programming code, and their outcome investigated by computer experimentation. The models are climate driven, and one chapter of this thesis concerns the development of a model to generate sequences of daily weather data from minimal datasets.

This thesis also contains deterministic models studying the dynamics of other, more general, parasitic diseases, and also the competition between similar species of parasite. These models are constructed using difference equations and analysed analytically and by simulation. This approach is adopted further to specifically consider the behaviour of the level of *Theileria parva* infection amongst vector and host populations.

1. INTRODUCTION

"Now, here, you see, it takes all the running you can do, to keep in the same place. If you want to get somewhere else, you must run at least twice as fast as that!"

Lewis Carroll, *Alice Through the Looking-Glass.*

In Africa the average nutrient intake per member of the population is 30% to 40% below that of the rest of the world. Predictions indicate that the future will bring increased food shortages as the growth of the human population exceeds that of food production. In 1960 the human population of Africa was around 200 million, by 1985 the population had risen to 460 million, more than doubling in 25 years. It is estimated that the population will increase annually by 3%, reaching 730 million by the end of the century, and 1.8 billion by the middle of the next century. Achieving a corresponding 3% annual increase in agricultural production in Africa is a formidable, yet essential, task. But even if a 3% annual increase in food production could be achieved, many people would remain undernourished.

African food crop yields remain extremely low despite increasing on a global scale. Between 1965 and 1987 world yields of sorghum and millet increased by 46% and 26% respectively, yet in Africa production remained constant. Yields of wheat, maize and rice have increased globally by 93%, 65% and 58% respectively over the same time period, but in Africa the yields of all three crops were lower in 1987 than in 1965. The cattle population of Africa, responsible for dairy and beef production, has risen little. In 1958 the number of cattle was estimated as around 106 million, which rose to around 170 million in 1985, representing an annual increase of about 2.5% per year. Disease remains the most important constraint on livestock productivity in tropical regions, even with the development of vaccines, antibiotics and anthelmintics that act against viruses, bacteria and parasitic worms. In Africa, trypanosomiasis is by far the most important disease of livestock. It is estimated to affect livestock production over an area of 10 million km^2 (Murray and Gray, 1984). In such areas, human populations may be devastated by serious epidemics of sleeping sickness (Duggan, 1970). East Coast

fever, described as the second most important cattle disease in Africa (Morrison, *et al.*, 1986), puts at risk around 25 million cattle in Central and Eastern Africa.

In other continents, disease and agricultural pests also place a massive constraint on livestock production. In Australia, the cattle tick *Boophilus microplus*, and the disease babesiosis it vectors, are their greatest threat to cattle, and cost the industry annually around A$40 million in control costs and production losses (Anon., 1975). Without control, the production losses, already around A$27 million, would be vastly increased. In Queensland, 80% of the national loss is incurred (Sutherst and Dallwitz, 1979), and the tick is regarded as the major restraint on the dairy and beef industries. In the UK, yearly losses due to fascioliasis, liver fluke disease, are estimated to be in excess of £60 million (Gettinby, 1974). Not only are the effects of disease and pests devastating, but major and important diseases such as malaria, trypanosomiasis and schistosomiasis are increasing in prevalence. Global warming trends indicate that the habitats of many pests and disease vectors are extending. Average temperature increases of 2^oC and the south of England could become favourable to mosquitos, bringing malaria to Britain. Given the threat and importance of diseases, how can mathematics possibly be of help in their understanding and shed light on their control?

The indications are that mathematics can and does aid in our understanding of biological processes. Early work by Mendel on the genetic variation observed in breeding experiments with peas, has led to the mathematical laws governing genetics. If mathematics can improve our understanding of disease, then improved understanding may lead to improved methods of control. Mathematical models for disease have already proved useful in aiding the control of malaria in West Africa (Molineaux and Gramiccia, 1980).

Early models

Early models for disease were constructed to describe the passage of epidemics by extending previous theory on birth and death processes. A population would be considered to contain susceptible, infective and removed individuals. Susceptibles are those members of the population who are at risk from the disease; infectives are those who have contracted the disease and are infectious to other individuals; and removed members are those who have either recovered or died from the disease and cannot become reinfected. A susceptible becoming infected is equivalent to a 'death' within the susceptible population, and a 'birth' within the infective population. Denoting $x(t)$, $y(t)$ and $z(t)$ as the number of susceptibles, infectives and removed cases respectively at

time t, β as the infection rate of susceptibles and γ as the removal rate of infectives leads to the simple continuous time epidemic model (Bailey, 1975):

$$\frac{dx}{dt} = -\beta xy,$$
$$\frac{dy}{dt} = \beta xy - \gamma y,$$
$$\frac{dz}{dt} = \gamma y.$$

Examination of these equations showed that the behaviour of the infection was dependent on the initial number of susceptibles $x(0)$, and the value of the relative removal rate $r = \gamma/\beta$. If $r \leq x(0)$ then no epidemic could occur, only a small number of susceptibles becoming infected. However, if $r > x(0)$ then an epidemic does occur. The profile of the epidemic can be predicted for different initial conditions, along with other theoretical properties such as the epidemic intensity – the proportion of initial susceptibles that eventually contract the infection. This model assumes that the population is of constant size and homogeneously mixing, and that a susceptible becomes infectious instantaneously. Later models were constructed to deal with non-homogeneously mixing groups, and susceptibles encountering a latent period before becoming infectious.

Assuming a constant latent period and a short infectious period, properties common to many diseases such as mumps and measles, discrete time epidemic models can be produced. The time-step between observations being the latent period of the disease, and the infectious period being a single point in time.

These early models were deterministic, providing a precise and unique disease profile, soley dependent on the initial conditions. However, when considering small populations this deterministic approach was seen to be inadequate. Mollison (1981) stated that when considering populations where there are periods of time when only a small number of individuals exist, differential equations will adequately describe the main course of the process, but stochastic analysis is needed for the critical periods when numbers are small. Chance contacts between infectives and susceptibles are an important factor in the spread of disease, especially when the population is small. Chain binomial models were constructed, where the number of new infectives at time $t+1$ was assumed to follow a binomial distribution. A number of different formulae for the probability of an individual susceptible becoming infected, p, have been proposed, such as the Greenwood model where p depends only on the presence or absence of infection; or the Reed-Frost model where p is dependent on the number of infectious

individuals. These models could be used not only to predict the most likely outcome of the epidemic, but also the theoretical probability distribution of the total number of susceptibles contracting the disease, and the frequency of different routes of disease transfer. Data on the spread of measles amongst small households in Providence, Rhode Island during 1929–1934 was used to test the fit of the models, which appeared inadequate (Bailey, 1975).

In fact, many of these early models, although of mathematical interest, shed little light on forecasting and controlling specific diseases. They did, however, provide the inspiration for the development of realistic disease models. With the aim of accurate disease prediction, rather than elegant or interesting mathematics, modelling parasitic diseases of animals developed in two directions towards index models and analytical and simulation models.

Index models

Index models arose from early disease studies which revealed that key environmental factors seem to correlate well with the incidence of disease. It was therefore attractive to try to combine these factors into a simple quantitative index which could be used to predict the incidence or occurrence of disease. Historically the most important of these was developed by Ollerenshaw and Rowlands (1959). They used a simple M_t index of wetness as an aid to predicting the risk of fascioliasis, liver fluke disease, amongst sheep and cattle in different parts of Britain. The parasite life cycle is complex. As an adult it exists in the liver of its host, but immature stages exist on the pasture and within the snail host *Lymnaea truncatula*. Two important factors in the development of the parasite are temperatures in excess of $10°C$, essential for the development of the egg and intra-snail stages, and the presence of surface water which is essential if the parasite is to succeed in finding a snail to infect. Thus, Ollerenshaw and Rowlands (1959) assumed temperatures were too low for parasite development in the winter, and so the M_t index was proposed to assess whether or not the habitat was wet enough for the parasite for each month from May to October:

$$M_t = (R - P + 5)n$$

where R is the rainfall in inches, P is the potential transpiration and n is the number of rain days for a specific month t. A weighted sum of the M_t index for each month provided a measure of fascioliasis risk, and could be useful in assessing the need for taking preventative control measures.

For ostertagiasis in sheep, Thomas and Starr (1978) obtained good predictions for the onset of peak pasture contamination using an algorithm with day and night rainfall measurements and the number of sunshine hours per day. Donnelly and MacKellar (1970) suggested that the incidence of redwater fever could be predicted from the mean monthly maximum air temperatures recorded 14 days earlier. Further discussion of these and other models can be found in Gettinby and Gardiner (1980) and Gibson (1978).

More recently, the ecoclimatic index, EI, calculated by the Climex model (Sutherst and Maywald, 1985) has proved useful in the study of African ticks (Lessard *et al.*, 1990), which vector many important parasitic diseases of cattle such as East Coast fever, anaplasmosis, and heartwater. This index is produced from the product of two indices: a growth index, calculated from temperature, moisture and daylength data, and a survival probability reflecting the success of the species through the unfavourable season. This probability is calculated from the values of hot stress, cold stress, wet stress and dry stress estimated for the species at a particular site. The study of Lessard *et al.* (1990) showed that areas where ticks were known to exist produced favourable values of the EI. However, many areas where high EI values were predicted represented areas where ticks were absent. The EI only accounts for climatic suitability of an area to a specific species, and does not account for other factors that influence the distribution of the species such as vegetation type. Lessard *et al.* (1990) used a normalised difference vegetation index, $NDVI$, to distinguish areas containing vegetation suitable to ticks. This index was estimated from measurements of infrared and red reflectance obtained by satellite, and is known to be effective in determining vegetation cover. When the two indices were used together, the predicted distribution of ticks was very close to that observed. Some favourable areas still uninfested by ticks were identified as areas where caution must be taken in preventing future introduction of the tick.

Analytical and simulation models

Although many index models have been sufficiently accurate to make disease predictions possible, they do, however, represent an oversimplification of the dynamics of the parasitic life cycles. Analytical and simulation models, on the other hand, have attempted to accurately predict the incidence of disease by modelling all factors that have a bearing on the parasitic life cycle. These models have the disadvantage of being more complex than the simple index models, but have the flexibility of being able to not

only predict levels of disease but quantify the intensity of infection. This provides the potential to assess disease control strategies leading to effective disease management.

MacDonald (1965) developed a probabilistic model for the disease of man, schistosomiasis, caused by the trematode worms *Schistosoma mansoni* and *S. haematobium*. By modelling the parasite and host populations and their interactions, the relative benefits of various disease control strategies were contrasted. The study proved useful in showing that the provision of safe water supplies was of greater importance than the building of latrines. This followed from the prediction that a reduction in the number of times humans became exposed to the parasite was more effective in control than a comparable reducion in the intensity of contamination present. The model also highlighted that improving sanitation alone is not a sufficient measure by which to eliminate the parasite. However, the disease could be successfully controlled by intensive treatment of infected individuals alongside improved sanitation. Application of a simple density-dependent model for general host-vector-parasite systems to model schistosomiasis (Deitz, 1988) yielded similar results. When the model was applied to malaria it was concluded that a vaccine developed to attack the parasite at the sporozoite stage would be more effective than a vaccine attacking it at the later gametocyte stage. Much work on modelling aspects of schistosomiasis has been presented by Anderson (Anderson, 1978, Anderson and May, 1979, Anderson *et al.*, 1982), with special reference to the prevalence of parasite infection within the intermediate snail host. The approach of Anderson has been to consider experimental studies presented in the literature, and, based on these, to develop simple mathematical models to capture the biological features of the infection. In addition to highlighting areas where more detailed biological data is required, these models have been useful in exploring different hypotheses explaining experimental observations.

Rogers (1988) developed a general mathematical model describing the prevalence of sleeping sickness, Trypanosome infection, amongst two host populations, either man and domestic animals or domestic and wild animals, and a population of tsetse flies, the disease vector. Differential equations were developed to predict the changes in the proportions of hosts and vectors infected.

Letting

x_i = the proportion of hosts infected for species i, for $i = 1$ or 2,

a_i = the biting rate for species i, for $i = 1$ or 2,

b_i = the proportion of infected bites producing infection in the host for species i, for $i = 1$ or 2,

m_i = the ratio of vector to host numbers for species i, for $i = 1$ or 2,

y = the proportion of vectors infected,

w_i = the proportion of hosts currently incubating infection for species i, for $i = 1, 2$,

z_i = the proportion of hosts currently immune to infection for species i, $i = 1, 2$,

r_i = the host recovery rate for species i, for $i = 1$ or 2,

c = the probability that an infected blood meal produces infection in the vectors,

f = the proportion of the vector population incubating infection,

u = the mortality rate of vectors,

T = the incubation time of infection within the vector,

and by assigning a circumflex to parameters to refer to the value of that parameter one incubation period previously, it then follows that $a_i b_i m_i \hat{y}$ is the number of infected bites occurring one incubation period of species i ago, $(1 - \hat{x}_i - \hat{w}_i - \hat{z}_i)$ is the probability that a fly bites a susceptible host of species i, one incubation period ago, and $r_i x_i$ is the proportion of hosts of species i to recover.

Thus

$$\frac{dx_i}{dt} = a_i b_i m_i \hat{y}(1 - \hat{x}_i - \hat{w}_i - \hat{z}_i) - r_i x_i, \quad i = 1, 2.$$

It also follows that $(a_1 \hat{x}_1 + a_2 \hat{x}_2)c$ is the probability that infection is passed on to a fly, one vector incubation period ago, $(1 - \hat{y} - \hat{f})$ is the probability that a specific fly is susceptible to infection one vector incubation period ago, e^{-uT} is the mortality rate of flies during the disease incubation period, and uy is the removal rate of flies, so that

$$\frac{dy}{dt} = (a_1 \hat{x}_1 + a_2 \hat{x}_2)c(1 - \hat{y} - \hat{f})e^{-uT} - uy.$$

Equations were derived for equilibrium disease prevalence and for the basic reproductive rate of the infection, R_0, for each host species. The basic reproductive rate represents the number of new infections that eventually arise from a single current infection. The model was fitted using parameter estimates obtained from the literature, and some interesting results were obtained. By considering the basic reproductive rates for *Trypanosoma brucei* infection amongst man and animals, Rogers inferred that human sleeping sickness cannot be maintained in the human host alone, but requires animal

hosts acting as a reservoir for the disease. This lead to the result that greater reduction in human sleeping sickness may be achieved by treating the animal population rather than the human population.

A more complicated model for trypanosomiasis was presented by Milligan and Baker (1988) which allowed for differences in susceptibility to infection of tsetse flies of different ages, seasonality and imigration and emigration in the tsetse fly population, and chemotherapy of infected domestic host.

Gettinby, Hope-Cawdery and Grainger (1974) developed a model for *Fasciola hepatica* development, and later Gettinby and McLean (1979) developed a more complex model based on Leslie matrices (Leslie, 1945) to assess control of the infection in sheep. The optimal timings of molluscicide and flukicide application were concluded. Gettinby, Bairden, Armour and Benitez-Usher (1979) developed a simulation model for *Ostertagia ostertagi*, the nematode worm responsible for the disease ostertagiasis in sheep and cattle. Daily rainfall and temperature data were used to predict the survival and development of the parasite in its free-living stages. Predicted levels of larval contamination showed good correlation with observed levels of larvae on pasture. Gettinby, Soutar, Armour and Evans (1989) developed a model for *O. circumcincta* to study the onset of genetic resistance to anthelmintic drugs. The model was designed to serve as a decision tool for use at farm level.

A model for the Australian cattle tick *B. microplus* was discussed by Sutherst and Dallwitz (1979), and later a more complex network model for the African cattle tick *Rhipicephalus appendiculatus* was developed (Gettinby, Newson, Calpin and Paton, 1988) where probabilities were incorporated into model decisions by employing random numbers, a method known as Monte Carlo simulation. This model used daily temperature data to predict tick development (King, Gettinby and Newson, 1988), and was used to investigate tick resistance to acaricide at different sites and for different hypotheses of genetic selection. In some cases, resistance occurred within a year, whereas in other cases the acaricide could be assumed effective in controlling ticks for over 15 years. More recently, Mount and Haile (1989) developed a simulation model to study the population dynamics of the American Dog Tick, *Dermacentor variabilis*, which is the primary vector of Rocky Mountain spotted fever in the eastern United States. This, and other tick-borne diseases of man such as lymes disease, are becoming increasingly important due to increased suburbanisation and the reversion of farmland to woodland. Both factors increase the contact rate of humans to ticks, and extend

tick habitats. The model uses weather data comprising average weekly temperatures and saturation deficits for one year to simulate tick development and survival, and also accounts for differences in habitat type between different geographical locations. Model predictions showed good agreement with observed seasonal densities of ticks at several locations studied. The model is regarded as the framework for a future model to study the control of Rocky Mountain spotted fever.

Many other simulation models have been developed, and with the advent and accessibility of microcomputers, this has become the age of simulation. Disease prediction and control is not the only area of application. Simulation models are used to predict the allowable mesh sizes for trawling nets in order to maintain fish stocks, the content of oil reservoirs and the optimum drilling sites for oil extraction, and even the predicted effects of nuclear accident on an area in an aid to constructing effective evacuation plans.

Future trends in modelling

Spatial models for the geographical spread of diseases have been developed (Mollison, 1987), such as for the spread of rabies passed by the red fox *Vulpes vulpes* (Ball, 1985). Rabies epidemics may be controlled by erecting barriers to prevent infected foxes from moving into clean areas, and so spatial simulation models are a valuable tool in predicting the rate of spread of an epidemic, and in optimising the positioning of barriers. The stochastic nature of such models is of major importance, as barriers must be located at sites where the epidemic is unlikely to have reached.

With the advent of remote sensing, the potential of index models for estimation of disease risk over vast areas is enormous. Satellites can be employed to measure maximum and minimum temperatures, greenness indexes predicting vegetation type and state, rock and soil types, along with a multitude of other data. Even measurements on the density of puddles in an area could be taken, and compared from day to day to predict suitable mosquito breeding sites. Data can be collected over short time intervals, increasing model accuracy. Remote sensed data has already been used to help identify the habitats of ticks and tsetse flies in Africa, with an aim to aiding disease control (Hugh-Jones, 1989).

Geographical Information Systems (GISs) provide a powerful new tool for manipulating and investigating spatial data. A GIS is a computerised mapping system whereby data obtained from maps, aerial and satellite surveys and mathematical models can be

displayed and investigated. By overlaying different maps, the interactions between different variables can be analysed. This provides great potential in understanding the factors controlling disease prevalence, and producing accurate and sensitive index models to assess disease risk.

The accessibility of microcomputers and powerful software such as GISs, expert system packages and programming languages provides a facility for mathematicians and non-mathematicians to produce predictive models of disease and disease risk. Computer modelling and computer simulation allows models of increased complexity and accuracy, because models need no longer be constrained by their mathematical structure. Computers can be used in providing a framework for performing experiments to investigate the behaviour of models that are too complex to yield analytical solutions. The effect and importance of model parameters can be investigated by comparing model predictions under different parameter values. The concept of computer modelling and computer experimentation is of vital importance in increasing understanding, and improving control, of disease.

Contents

In chapter 2 of this thesis classical modelling techniques are employed to produce simple deterministic models of interactions between species to find conditions for coexistence. Chapter 3 is concerned with East Coast fever, and contains sections on the disease and its control, along with descriptions of the life cycles of the disease vector and parasite. In chapter 4, modelling techniques similar to those presented in chapter 2 are employed to produce models to investigate the infection level in tick populations under different scenarios: constant tick populations, seasonal tick populations, non-uniform tick attachments, resistance of cattle to ticks, resistance of cattle to infection, and chemotherapy of infected cattle. Chapter 5 contains the description of stochastic models for tick populations, the spread of East Coast fever and its control by acaricidal dipping and chemotherapy with antitheilerial drugs. Climatic data is an essential requirement of the models in chapter 5, and so chapter 6 describes methods for generating sequences of daily weather data from monthly mean values, using extreme value distributions and time series analysis. Chapter 7 gives an overview of the operation and philosophy of ECFXPERT, an integrated model designed to investigate East Coast fever and its control, using models developed earlier. Chapter 8 contains the results of a number of computer experiments using ECFXPERT.

2. COMPETITION MODELS FOR SIMPLE PARASITE SYSTEMS

"Government and cooperation are in all things the laws of life;
Anarchy and competition, the laws of death."

John Ruskin, *Unto this last.*

2.1 INTRODUCTION

Over the past ten years chaos has emerged as a new explanation to some of the complexity observed in nature, and has been the subject of interest to scientists working under many disciplines. In mathematical terms, chaos is the randomness generated by simple non-linear dynamical systems. Typically, a system might be expressed in discrete form by:

$$X_{t+1} = f(X_t), \qquad t = 0, 1, 2, \ldots$$

where X_t is an observation on the system at time t and f is a non-linear function of Xt.

Chaotic behaviour is observed when a very small change in the initial conditions, X_0, produces an unpredictably large difference in the resulting sequence $\{X_n; n = 1, 2, \ldots\}$. Such apparent randomness is a feature frequently observed in nature.

It was with the advent and increasing accessibility of microcomputers that the complex behaviour of chaotic systems became apparent. Prior to this, chaos and other complex properties exhibited by even the most simple of dynamical systems remained unexplored. As a simple example, consider the logistic difference equation:

$$X_{t+1} = rX_t(1 - X_t)$$

where r is known as the non-linearity parameter, and represents a growth rate related to food supply, fertility, etc. This is proposed to describe a population growing in a constrained environment. In 1968, the behaviour of this system was described as modelling populations that remain constant or fluctuate "with rather regular periodicity" (Maynard-Smith, 1968).

However, in the following decade, new light was to be shed on this and other non-linear systems, and by using computer methods a new world of complexity was unearthed. May (1976) studied the dynamics of the logistic system, and discovered an amazing variety of possible evolutions as the parameter, r, was varied. By performing repeated iterations at a multitude of different parameter values, the points to which the system settled could be plotted against the value of the non-linearity parameter, r. When the parameter was low, the population became extinct. As the parameter was increased, the level of the population stabilised to a single equilibrium, the value of which increased with the parameter. Under such conditions, the system is said to have a stable fixed point. At a specific parameter value, the equilibrium split in two, and the population began to alternate between two levels. As the parameter was increased further, each equilibrium level split again, producing a stable population which cycled between four levels, then eight, then sixteen, and so on. This phenomenon is known as period doubling, or bifurcation. Mathematical conditions for the stability of such cycles have been derived, and rely upon the application of the Fixed Point Theorem. The plot of the behaviour of the system is termed a bifurcation map, and observation of this showed areas where the system attained no periodic equilibrium. These were areas of chaotic behaviour.

The implications of chaos existing in such simple biological models are immense. If all the laws that govern a system are known, then an exact model can be constructed. But, even if an exact model is produced, the initial conditions of the system must also be known exactly. In nature, such parameters can only be estimated to within a certain order of accuracy. A small difference in initial conditions can cause a huge difference in the resulting model predictions which throws into question the usefulness of such models. On the other hand, these models offer the prospect of explaining the behaviour of systems that appear to be totally random and unpredictable, as evidence now suggests that such behaviour can be produced by models with very simple structures.

In this chapter, three models describing the growth and interactions between species are explored. These models are constructed with specific parasitic systems in mind, although are general enough to be applied to a range of biological systems. The models are represented in the form of network models, as introduced by Lewis (1976), and are analysed using the properties of difference equations, and by computer simulation.

2.2 SINGLE SPECIES MODEL

The protozoan parasite *Entamoeba histolytica* is a serious pathogen producing dysentery in man and some animals. The parasite occurs on a global scale, although is more prevalent in tropical and subtropical regions. Within the vertebrate host, the organism colonises the small and large intestines where it multiplies by binary fission. Parasites spread from animal to animal via a cystic form which is passed in faeces. The growth of the species within a single host is constrained by the capacity of the host to maintain the parasite. The maximum parasite burden, or carrying capacity, of a host will be dependent on parameters such as intestinal size, food intake and the level of the hosts immune response.

Ostertagiasis, haemonchosis and nematodiris are some of the important diseases which are typical of the many nematode worms which infect sheep and cattle producing parasitic gastroenteritis. Adult worms, located in the abomasum of the host, produce eggs daily which are passed onto pasture in faeces. Eggs hatch and develop into an infective L3 larval stage. Ingested L3 larvae develop through a number of stages into adult worms within a number of weeks. The parasite life cycle can be simplified by ignoring the stages spent by the parasite in free existence. Simplistically, adult worms give rise to a daily number of ingested L3 larvae, which may develop into adult worms. The number of worms parasitising any member of the host population will be constrained by the maximum worm burden attainable by the host.

A simple model to describe the dynamics of a parasite population such as *E. histolytica* existing within a single host, or nematodes within a constant and uniform herd or flock can be simply constructed.

2.2.1 Model description

The growth of a species, A, is restricted by the carrying capacity of its environment. The population can never contain more than K members. This represents a maximum parasite burden. On each cycle only a proportion, $R(n)$, of the total population, $A(n)$, is able to successfully reproduce. This proportion is the reproductive potential at the nth cycle and is given by:

$$R(n) = \frac{K - A(n)}{K}$$

which becomes smaller as the population becomes more dense.

When a member of the species reproduces, this gives rise to f progeny. If repro-

duction is asexual then $f = 1 + b$, where b is the number of offspring from one parent. If reproduction is sexual, then the model is confined to the female population only. The male population can then be assumed to be of a size proportional to the size of the female population having taken the ratio of sexes into account. Each member of the population has a probability p of surviving to the next cycle. The life cycle can be represented in network form as shown in Figure 1.

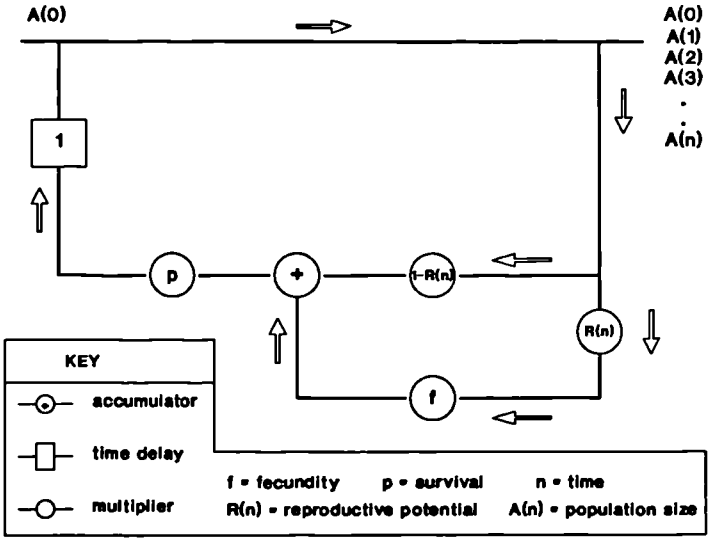

Figure 1. *Network representation of the parasite life cycle.*

In this network a square box refers to a time delay, a circle containing a parameter indicates multiplication and a circle containing a + sign is an accumulator. At first the population contains $A(0)$ members. From these, a proportion $R(0)$ reproduce to give $fR(0)A(0)$ individuals; the remainder do not reproduce. Combining reproducing and non-reproducing members gives the population size after reproduction, and should only a proportion p survive to commence the next cycle, then

$$A(1) = p[fR(0) + 1 - R(0)]A(0)$$

The general system is given by:

$$\begin{aligned} A(0) &= \text{constant} \\ A(n) &= p[fR(n-1) + 1 - R(n-1)]A(n-1), \qquad n = 1, 2, 3 \ldots \end{aligned} \tag{1}$$

2.2.2 Analysis and results

The difference equations (1) can be expressed in terms of the population size for each cycle to give:

$$\begin{aligned} &A(0) = \text{constant} \\ &A(n) = fpA(n-1) - \frac{(f-1)p}{K}A(n-1)^2, \qquad n = 1,2,3\ldots \end{aligned} \tag{2}$$

If the system approaches a single equilibrium point, L, then setting $A(n) = A(n-1) = \ldots = L$ gives $L = G(L)$ where

$$G(L) = fpL - \frac{(f-1)pL^2}{K}.$$

The values of L satisfying this equation are known as the fixed points. Equations described by (2) have fixed points, L, at:

$$L = 0, \qquad \text{and} \qquad L = \frac{K(1-pf)}{p(1-f)}.$$

A fixed point, L, of the system $A(n) = G(A(n-1))$, is described as stable or attractive if, for values $A(n-1)$ close to L, the resulting sequence of values $A(n), A(n+1), \ldots$ tend towards L. Conversely, if the fixed point is unstable or repulsive then a value of $A(n-1)$ close to L results in $A(n)$ being pushed away from the fixed point.

When fp is small, $fp \leq 1$, the population A becomes extinct. The speed of extinction is increasing with smaller fp. However, species with higher survival rates or fecundities, $1 < fp \leq 3$, will attain an equilibrium at a stable limit $L = \frac{K(1-pf)}{p(1-f)}$.

These results follow from the Fixed Point Theorem which states that if $G(L)$ is differentiable in a neighbourhood of a fixed point, L, then if $G'(L)$ evaluated at the fixed point is less than one in absolute value the fixed point is stable. Otherwise the fixed point is unstable. This is a special case of the Principle of the contraction mapping (Goult *et al.*, 1973).

For $fp > 3$, the two fixed points are both unstable. Thus, for species that are prolific, $fp > 3$, no single equilibrium level can be attained, the behaviour exhibited depending on the values of f and p. Two-cycles can be attained when the two non-zero fixed points of the system $A(n+1) = G(G(A(n-1)))$ become stable. The mathematical criterion for this being established by application of the Fixed Point Theorem. Similarly, four-cycles are achieved when the four fixed points of the system $A(n+3) = G^4(A(n-1))$ become stable, and so on.

Letting $a = fp$, and $b = \frac{(f-1)p}{K}$, the system $A(n) = aA(n-1) - bA(n-1)^2$ can be represented as a mapping $ax - bx^2 \longmapsto y$, followed by a mapping $y \longmapsto x$. The fixed points occur at the intersection of the curve $y = ax - bx^2$ with the line $y = x$.

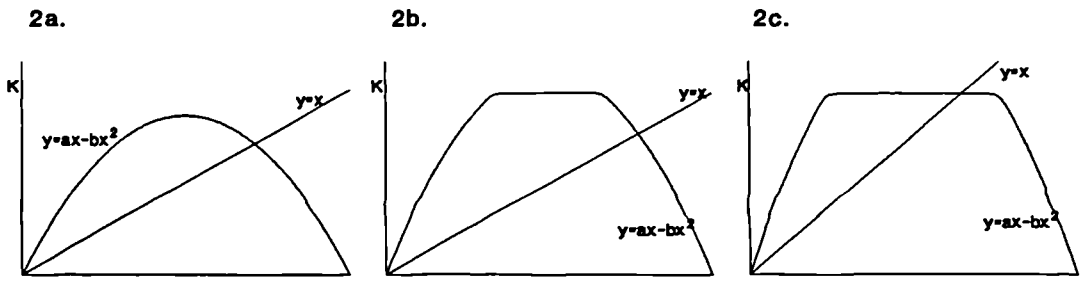

Figure 2. *Fixed points of the system* $A(n) = aA(n-1) - bA(n-1)^2$

When the height of the parabola is less than the carrying capacity K then:

$$3 < fp \leq 2 + 2(1-p)^{1/2}.$$

This is illustrated in (a) of figure 2.

The behaviour of the system within this range has been discussed by May (1976), and can take the form of stable cycles between 2, 4, 8 or more limits, or chaotic behaviour where no period can be established.

When the height of the parabola exceeds K, but the non-zero fixed point is less than K, as illustrated in (b) of figure 2, then:

$$fp > Max\{3, 2 + 2(1-p)^{1/2}\}, \qquad \text{and} \qquad p < 1.$$

The parabola appears truncated because if the population $A(n)$ ever exceeds the carrying capacity K, then a number $A(n) - K$ is removed as there are not the resources to accommodate them.

The presence of the carrying capacity K in the model has a stabilising effect on the behaviour observed. In this case, the behaviour exhibited by the system becomes increasingly more stable with larger values of fp, and eventually stabilises into a cycle between two limits, K and Kp, when fp is large enough.

When the height of the parabola reaches K, the value of fp reaches a critical value, given by $C = 2 + 2(1-p)^{1/2}$. If the survival probability is high, $p \geq 0.75$, then this critical value is less than 3 meaning that the parabola reaches a height of at least K before the non-zero fixed point becomes unstable. In this case the population will cycle between K and Kp. The smaller the survival probability p, the larger the critical

value C becomes, and so the more complex behaviour the system can exhibit. This is illustrated by comparison of Figure 3a with Figure 3b. Figure 3a shows a bifurcation map for a system with carrying capacity $K = 50$, and survival probability $p = 0.3$. Figure 3b shows a similar bifurcation map for a system with carrying capacity $K = 50$, and survival probability $p = 0.4$. In each case, the value of fp is increased by altering the fecundity f.

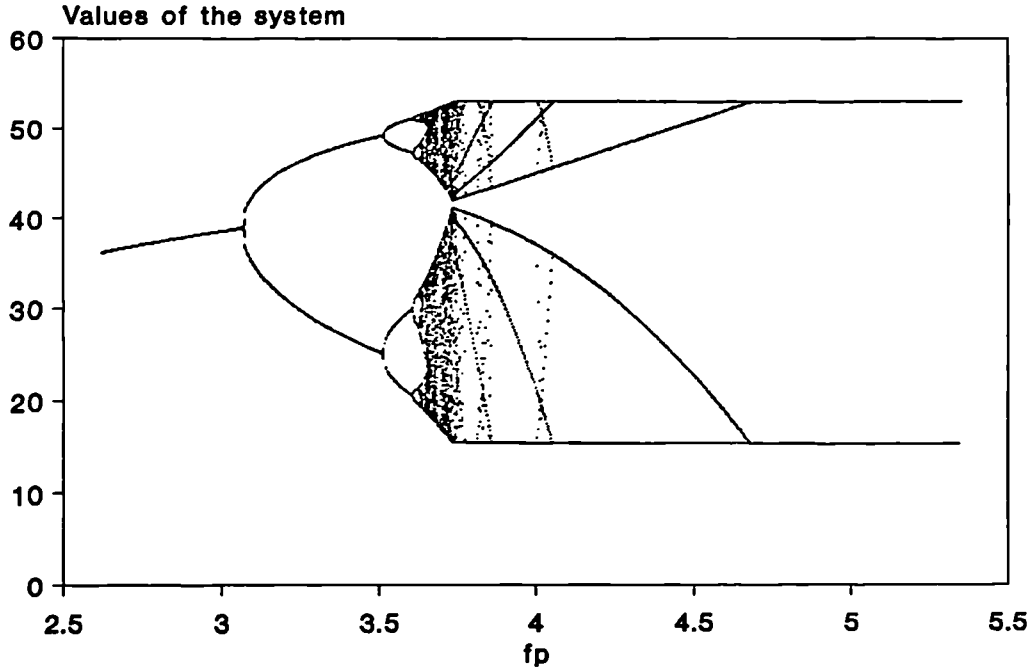

Figure 3a. *Behaviour of the system under increasing f when $K = 50$ and $p = 0.3$*

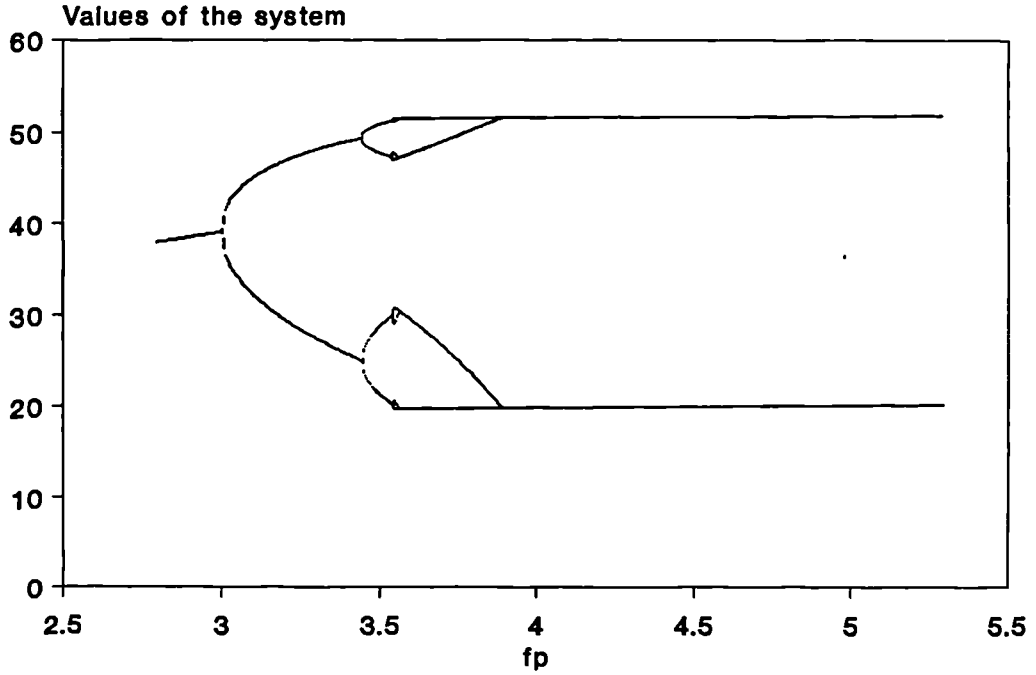

Figure 3b. *Behaviour of the system under increasing f when $K = 50$ and $p = 0.4$*

The single line at the start of each bifurcation map refers to the single limit that would be obtained if $fp < 3$. More than one point at a value of fp indicates a cycling between points, and a scatter of points could refer to chaotic behaviour.

In Figure 3a where $p = 0.3$, the critical point $C = 2 + 2(1-p)^{1/2}$ is given by C equal to 3.67. Values of fp lower than 3.67 permit the system to attain stable cycles between 2, 4, 8 and higher numbers of points. In particular, a cycle between two points occurs at $fp = 3.3$, and a cycle between four points at $fp = 3.5$. A cycle between 4 limits is shown in Figure 4. Chaotic behaviour appears to occur at $fp = 3.66$.

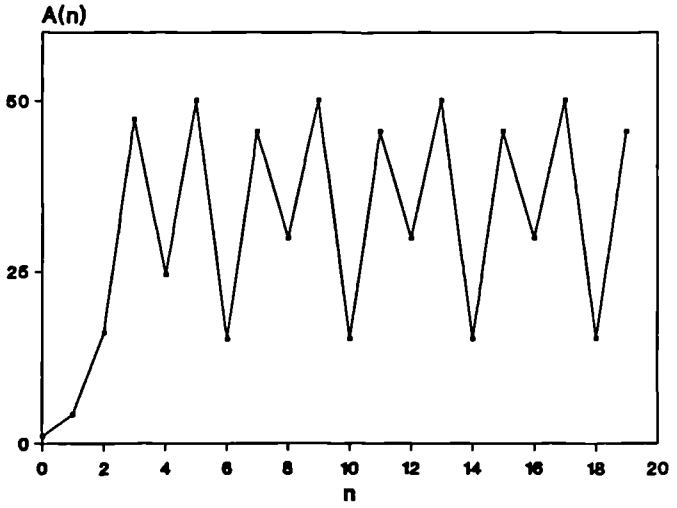

Figure 4. *A stable cycle between 4 limits for* $fp = 3.5$.

However, for $p = 0.4$ in Figure 3b, the critical point occurs at C equal to 3.55, meaning that much of the more complex behaviour is avoided.

Finally, figure 2(c) illustrates the situation in which the height of the parabola and the non-zero fixed point both exceed K. The conditions are:

$$fp > 3, \qquad \text{and} \qquad p = 1,$$

and a single equilibrium level at K is attained.

Species with a very high fecundity, f, usually have a correspondingly low survival probability, p. For example, nematode worms produce a very high number of eggs, but few of them survive to reproduce as adults. High f and low p means that the critical value of $C = 2 + 2(1-p)^{1/2}$ is close to 4. This means that nearly all of the complex behaviour described by May (1976) can occur, all except extinction by catastrophe which requires critical values of 4. Clearly, having an environmental carrying capacity has a beneficial effect to a species, as however prolific the population is, it is unable to fatally destroy itself through catastrophe.

On the other hand, species with a low reproductive rate and high survival rate, such as *E. histolytica*, are likely to exhibit little complex behaviour, and attain stable cycles between a small number of limits for most values of fp.

Increasing the survival chances of a species by making the environment more favourable, has the effect of making the population more stable and therefore more predictable.

2.3 TWO SPECIES COMMENSALISM MODEL

Glossina, or tsetse flies, are important blood sucking flies which transmit several species of trypanosomes which cause fatal diseases in man and animals. The habitat of tsetse flies is confined to the subtropical and tropical areas of Africa. Female tsetse flies produce a single larva at a time. The larva develops in the uterus of the female, and when eventually deposited, submerges itself in the soil and develops into a pupa. Pupae develop into adult flies. Adult flies rely on regular blood meals from their hosts. Some species of host are more suitable than others, and the prevalence of flies is dependent on the number and suitability of their hosts (Soulsby, 1982). *G. palpalis* feeds mainly on humans, which maintain a relatively constant and static population. *G. morsitans*, however, is dependent mainly on big game and cattle, the density of which can be strongly affected by migration and disease. In the Transvaal, the fly disappeared when the big game were devastated by serious outbreaks of rinderpest (Soulsby, 1982). Such observations indicate the existence of a maximum challenge level per host, producing a constraint on the fly population.

Maxima to the burden levels of Ixodid ticks on cattle have been observed (Yeoman, 1966). Beyond a threshold challenge level, the responses of the hosts immune system to ticks feeding, and behavioural changes due to tick irritation and distress are responsible for limiting the numbers of ticks that may remain attached to a host.

A population of tsetse flies or ticks is clearly dependent on the size and state of the host population. Ignoring the possibility of the insects acting as disease vectors, the host population can be assumed unaffected by the size of the insect population.

2.3.1 Model description

The commensalism model describes a system consisting of two species, A and B. Species B is dependent on species A as species A provides the resources necessary for the maintenance of species B. It is assumed that species B does not affect the success of species A, and so the equations describing species A are identical to equations (1)

of the single species model:

$$\begin{aligned} &A(0) = \text{constant} \\ &A(n) = p_A[f_A R_A(n-1) + 1 - R_A(n-1)]A(n-1), \qquad n = 1,2,3\ldots \end{aligned} \tag{3}$$

where, p_A is the survival probability, f_A is the fecundity, $R_A(n) = \frac{K_A - A(n)}{K_A}$ is the reproductive potential, and K_A is the carrying capacity for species A.

The network describing the dynamics of species B is of the same form as that presented earlier in Figure 1. The carrying capacity for species B is dependent on the size of population A. If one member of population A can support at most K_B individuals of species B, then the carrying capacity for species B on the nth cycle is given by $K_B(n) = K_B A(n)$. The reproductive potential $R_B(n)$ is therefore given by:

$$R_B(n) = \frac{K_B A(n) - B(n)}{K_B A(n)}.$$

The fecundity and survival probability of members of species B are f_B and p_B respectively.

The difference equations describing the dependent population, B, are given by:

$$\begin{aligned} &B(0) = \text{constant} \\ &B(n) = p_B[f_B R_B(n-1) + 1 - R_B(n-1)]B(n-1), \qquad n = 1,2,3\ldots \end{aligned} \tag{4}$$

2.3.2 Analysis and results

The system of equations (3) describing the independent population, A, reduce to equations (2) as before:

$$\begin{aligned} &A(0) = \text{constant} \\ &A(n) = f_A p_A A(n-1) - \frac{(f_A - 1)p_A A(n-1)^2}{K_A}, \qquad n = 1,2,3\ldots \end{aligned} \tag{5}$$

The equations (4) describing the dependent population, B, can be expressed in terms of the population size at each cycle by:

$$\begin{aligned} &B(0) = \text{constant} \\ &B(n) = f_B p_B B(n-1) - \frac{(f_B - 1)p_B B(n-1)^2}{K_B A(n-1)}, \qquad n = 1,2,3\ldots \end{aligned} \tag{6}$$

The behaviour of population A is independent of population B and depends on the value of $f_A p_A$ as described earlier. The fixed points of the system describing B are:

$$L_B = 0, \quad \text{and} \quad L_B = \frac{K_B(1 - f_B p_B)}{p_B(1 - f_B)} \lim_{n\to\infty}\{A(n)\}.$$

The fixed point L_B equal to 0 is stable if $f_B p_B \leq 1$. The non-zero fixed point is constant if $A(n)$ reaches a limit as n tends to infinity, which occurs when $1 < f_A p_A \leq 3$, and is stable if $1 < f_B p_B \leq 3$. Thus the overall behaviour of population B can be deduced from the behaviour of population A, and the earlier results:

If species A becomes extinct, $f_A p_A \leq 1$, then species B is forced into extinction, as both fixed points, L_B, are zero and stable.

However, if species A attains a single equilibrium, $1 < f_A p_A \leq 3$, then the dynamics of population B will depend on $f_B p_B$. For low values, $f_B p_B \leq 1$, population B will become extinct, for higher values, $1 < f_B p_B \leq 3$, population B will coexist in equilibrium with species A, the equilibrium level being:

$$L_B = \frac{K_B(1 - p_B f_B)}{p_B(1 - f_B)} L_A,$$

where L_A is the equilibrium level of population A. An example of such an outcome is shown in Figure 5.

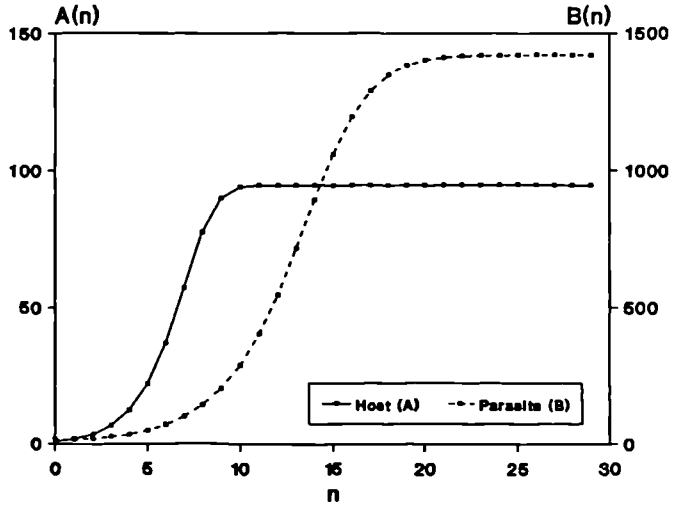

Figure 5. *Parasite and host populations coexisting at equilibrium.*

For $f_B p_B$ still higher, $f_B p_B > 3$, population B coexists with species A but attains no unique equilibrium level; the behaviour exhibited depending on the value of f_B and p_B. As earlier, a high survival rate, $p_B \geq 0.75$, causes the population to cycle between the two limits $K_B L_A$ and $K_B L_A p_B$, or exist at equilibrium at $K_B L_A$ if the survival rate is 1. A lower survival rate, $p_B < 0.75$, causes the behavioural properties of the system to be more complex for lower values of p_B, when $f_B p_B$ is below the critical value $C_B = 2 + 2(1 - p_B)^{1/2}$. For $f_B p_B$ above this critical value, population B will cycle between a small number of limits, just two limits, $K_B L_A$ and $K_B L_A p_B$, if $f_B p_B$ is very large.

If species A has high fecundity and survival, $f_A p_A > 3$, then species B will either become extinct when $f_B p_B \leq 1$, or will coexist with species A when $f_B p_B > 1$. In this case population B cannot attain a single equilibrium level as the non-zero fixed point:

$$L_B = \frac{K_B(1 - f_B p_B)}{p_B(1 - f_B)} \lim_{n \to \infty} \{A(n)\},$$

is not unique, because the system $A(n)$ does not have a unique limit as n tends to infinity. An example of this case is shown in Figure 6, where $f_A p_A > 3$ and $f_B p_B$ lies between 1 and 3.

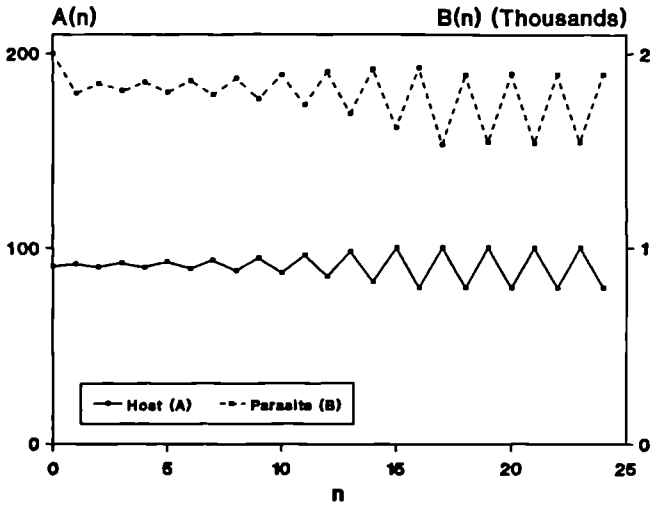

Figure 6. *Parasite and host populations coexisting not at a single equilibrium.*

It is apparent that the behaviour of the host population affects the stability of the parasite population. For example, tsetse flies feeding on stable host populations, such as *G. palpalis* feeding on humans, will exhibit behaviour that appears independent of the host. Tsetse flies have a low reproductive rate and high survival, and so *G. palpalis* are likely to maintain a very stable population. However, a population of *G. mortisans* tsetse flies will be controlled by the large seasonal changes in the density of big game.

One question when dealing with such a parasite or vector systems is how to control, or remove, the parasite population. This model assumes that species B has no serious effect on species A, that species A can maintain species B without causing its fecundity or survival probability to be reduced. Generally, parasites do have a debilitating effect on their host, but not one that would cause death of the host. Normally the effect of a parasite would be to deteriorate the health of its host and lead to production losses. Thus control is an important issue. The four methods of controlling the size of the parasite population, B, are to reduce the host population, A, the parasite fecundity f_B, the parasite survival rate p_B and the carrying capacity per host, K_B.

On pasture, ticks questing for a host remain in very close proximity to the place where they were deposited. Therefore, increasing the grazing area of the host population will have the effect of reducing host density by decreasing the number of potential hosts available to a questing tick, $A(n)$. A decrease in host density also decreases p_B.

Traps employed to distract and kill tsetse flies before they attack potential hosts have a similar effect in reducing p_B.

K_B, the carrying capacity per host, and p_B, can be reduced by drug use which make the environment more hostile to the parasite. Ear tags impregnated with araricide can be attached to cattle which maintain a low concentration of the chemical over the area most vulnerable to tick attack.

2.4 TWO SPECIES COMPETITION MODEL

It is a common observation that a host infected with one species of parasite may also be infected with other strains of the same parasite, or with other species of parasite. Malaria, caused by species of *Plasmodium* protozoa, often occurs as an infection of several species of the parasite, particularly in the tropics where the disease is widespread (Richie, 1988). In a study of field observations on human malaria, Richie (1988) noticed that the number of mixed infections that were recorded was often fewer than expected by chance, suggesting that one parasite has excluded another, or suppressed its parasitaemia to undetectable levels. The suppression hypothesis was supported by experimentation where laboratory animals were inoculated with 2 *Plasmodium* species; many studies have shown that 1 or both species are suppressed. Richie (1988) suggests that a possible cause for this may be competition for host cells or nutrients.

Competition between *Plasmodium* species in a host infected with two species, or between two different nematode species parasitising the same host can be investigated using a simple competition model of a similar form to those described earlier.

2.4.1 Model description

Two species, A and B, are in direct competition for resources. The reproduction success of each species is reduced by the presence of the other species. The reproductive potential for each species is given by:

$$R_A(n) = 1 - \frac{A(n)}{K_A} - \frac{B(n)}{K_B} = R_B(n).$$

In the absence of species B, the reproductive potential for species A is that of a single species. Species have associated with them carrying capacities, K_A and K_B,

survival probabilities, p_A and p_B, and fecundities, f_A and f_B, for species A and species B respectively. The carrying capacities reflect the total number of a species the environment can sustain, in the absence of the other species.

The network representation of each species is similar to that presented earlier in Figure 1.

Difference equations describing the two populations are given by:

$$\begin{aligned} A(0) &= \text{ constant} \\ A(n) &= p_A[f_A R_A(n-1) + 1 - R_A(n-1)]A(n-1), \quad n = 1,2,3\ldots \end{aligned} \tag{7}$$

$$\begin{aligned} B(0) &= \text{constant} \\ B(n) &= p_B[f_B R_B(n-1) + 1 - R_B(n-1)]B(n-1), \quad n = 1,2,3\ldots \end{aligned} \tag{8}$$

2.4.2 Analysis and results

The systems of equations (7) and (8) after substitution became:

$$\begin{aligned} A(0) &= \text{constant} \\ A(n) &= f_A p_A A(n-1) - \frac{(f_A-1)p_A}{K_A}A(n-1)^2 \\ &\quad - \frac{(f_A-1)p_A}{K_B}A(n-1)B(n-1), \quad n = 1,2,3\ldots \end{aligned} \tag{9}$$

$$\begin{aligned} B(0) &= \text{constant} \\ B(n) &= f_B p_B B(n-1) - \frac{(f_B-1)p_B}{K_B}B(n-1)^2 \\ &\quad - \frac{(f_B-1)p_B}{K_A}A(n-1)B(n-1), \quad n = 1,2,3\ldots \end{aligned} \tag{10}$$

The fixed points to which the population may converge, L_A^* and L_B^* for species A and B respectively, are given by:

$$L_A^* = 0, \quad \text{or} \quad L_A^* = \lim_{n\to\infty}\{A'(n)\} - \frac{K_A}{K_B}L_B^* \tag{11}$$

$$L_B^* = 0, \quad \text{or} \quad L_B^* = \lim_{n\to\infty}\{B'(n)\} - \frac{K_B}{K_A}L_A^* \tag{12}$$

where, $A'(n)$ are the sequence of population values for species A in the absence of species B:

$$A'(n) = f_A p_A A'(n-1) - \frac{(f_A-1)p_A}{K_A}A'(n-1)^2,$$

and $B'(n)$ is the analogous system describing population B in the absence of A:

$$B'(n) = f_B p_B B'(n-1) - \frac{(f_B-1)p_B}{K_B}B'(n-1)^2.$$

Denoting the limits as n tends to infinity of these two systems as L_A and L_B respectively, then:

$$\begin{aligned} L_A^* = 0, \quad \text{or} \quad L_A^* = L_A - \frac{K_A}{K_B} L_B^* \\ L_B^* = 0, \quad \text{or} \quad L_B^* = L_B - \frac{K_B}{K_A} L_A^* \end{aligned} \tag{13}$$

For A and B to coexist in equilibrium, L_A and L_B must be non-zero and constant. That is, the systems for each population in the absence of the other must attain a constant non-zero limit. The condition for this is, as determined earlier:

$$1 < f_A p_A, f_B p_B \leq 3.$$

Given L_A and L_B are constant, equations (13) yield L_A^* and L_B^* both non-zero. Species A and B can coexist if:

$$1 - \frac{(1-p_A)}{p_A(f_A - 1)} = 1 - \frac{(1-p_B)}{p_B(f_B - 1)}. \tag{14}$$

Letting the fitness of a population I be:

$$\phi(I) = 1 - \frac{(1-p_I)}{p_I(f_I - 1)}$$

as a measure in $[0,1]$ representing how well adapted a species is to the environment it is placed into; where $(1-p_I)$ is the probability of death, p_I is the probability of survival and $(f_I - 1)$ is the number of new offspring per reproductive act.

Hence coexistence of two species A and B can only occur if:

(a) $f_A p_A > 1$, and $f_B p_B > 1$ and (b) $\phi(A) = \phi(B)$.

Moreover, two species can only coexist, both in equilibrium, if:

(a) $1 < f_A p_A \leq 3$, and $1 < f_B p_B \leq 3$ and (b) $\phi(A) = \phi(B)$.

It can be shown that if $\phi(B) > \phi(A)$ and both $f_A p_A$ and $f_B p_B$ are greater than 1, then species B will dominate and cause the eventual extinction of species A:

If $\phi(B) > \phi(A)$ then:

$$\begin{aligned} 1 - \frac{(1-p_B)}{p_B(f_B - 1)} &> 1 - \frac{(1-p_A)}{p_A(f_A - 1)}, \\ \Rightarrow \frac{p_B(f_B - 1) - (1-p_B)}{p_B(f_B - 1)} &> \frac{p_A(f_A - 1) - (1-p_A)}{p_A(f_A - 1)}, \\ \Rightarrow \frac{(f_B p_B - 1)}{p_B(f_B - 1)} &> \frac{(f_A p_A - 1)}{p_A(f_A - 1)}, \end{aligned}$$

$$\Rightarrow \frac{K_B(1-f_B p_B)}{K_B p_B(1-f_B)} > \frac{K_A(1-f_A p_A)}{K_A p_A(1-f_A)},$$
$$\Rightarrow \frac{L_B}{K_B} > \frac{L_A}{K_A}. \tag{15}$$

Assuming that $\lim_{n\to\infty}\{B(n)\} = 0$ it follows that the fixed point L_B^* equal to zero is stable and the non-zero fixed point is negative. Using equations (13) this condition can be expressed mathematically as:

$$L_B^* = L_B - \frac{K_B}{K_A} L_A^* \leq 0$$

which implies that:

$$L_B \leq \frac{K_B}{K_A} L_A^*. \tag{16}$$

If $\lim_{n\to\infty}\{B(n)\} = 0$, then $L_A^* = L_A$ and equation (16) becomes: $L_B \leq \frac{K_B}{K_A} L_A$. This produces a contradiction, because the condition for $\phi(B) > \phi(A)$ of equation (15) states that $L_B > \frac{K_B}{K_A} L_A$. Thus the initial assumption that $\lim_{n\to\infty}\{B(n)\} = 0$ is incorrect, proving that $\lim_{n\to\infty}\{B(n)\} \neq 0$. Because species A and B are not of equal fitness, and because species B does not become extinct, it follows that species A becomes extinct.

Such an event is illustrated in Figure 7.

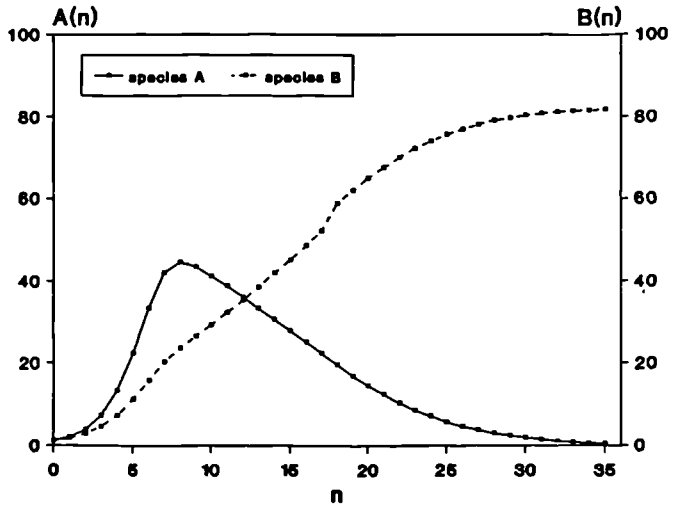

Figure 7. *Species A is suppressed by the competition of species B.*

When condition (14) is satisfied, the equations for non-zero L_A^* and L_B^* reduce to a single equation providing an infinity of possible sets of limits L_A^* and L_B^*. The values of L_A^* and L_B^* obtained on each simulation are unique and depend on the choice of starting conditions $A(0)$ and $B(0)$. It can easily be shown that increasing the starting

value $A(0)$ has the effect of increasing the resulting limit L_A^* and reducing L_B^*, as might be expected:

Equations (9) and (10) describing the size of the two populations A and B at each cycle can be expressed in the following simpler form:

$$\begin{aligned} A(n) &= aA(n-1) - bA(n-1)^2 - cA(n-1)B(n-1) \\ B(n) &= \alpha B(n-1) - \beta B(n-1)^2 - \gamma A(n-1)B(n-1) \end{aligned} \tag{17}$$

Letting $B(0) = A(0) + d$ it follows that:

$$\begin{aligned} A(1) &= (a - cd)A(0) - (b + c)A(0)^2 \\ B(1) &= (\alpha + \gamma d)B(0) - (\beta + \gamma)B(0)^2 \end{aligned} \tag{18}$$

By increasing the value of $A(0)$ by ϵ and keeping $B(0)$ constant such that $B(0) = A(0) + d - \epsilon$ it follows that:

$$\begin{aligned} A(1) &= (a - cd)A(0) - (b + c)A(0)^2 + c\epsilon A(0) \\ B(1) &= (\alpha + \gamma d)B(0) - (\beta + \gamma)B(0)^2 - \gamma\epsilon B(0) \end{aligned} \tag{19}$$

Comparison of equations (18) and (19) shows that an increase in $A(0)$ results in an increase in $A(1)$ and a decrease in $B(1)$. This argument can be continued inductively to produce the required result.

The results can be summarised as follows:

If one species becomes eliminated, species A say, then the behaviour of the other species, B, is as reported for the single species case.

If, however, neither population becomes extinct, $\phi(A) = \phi(B)$, then either both populations will achieve equilibrium, if $1 < f_A p_A \leq 3$ and $1 < f_B p_B \leq 3$, the limits depending on $A(0)$ and $B(0)$; or neither will coexist at a unique equilibrium level, if at least one of $f_A p_A$ and $f_B p_B$ exceeds 3.

2.5 RULES FOR THE COEXISTENCE OF N COMPETING SPECIES

The two competing species model can be extended to N species competing for the same resources. The results obtained are that for N species to coexist then the following two conditions must be satisfied:

(a) Each species must be able to exist in the environment in the absence of the others. I.e. $f_I p_I > 1$, for $I = 1, 2, 3, \ldots N$,

(b) The species must be equally suited to the environment.

I.e. $\phi(I) = \phi(I+1)$, for $I = 1,2,3,\ldots N-1$.

2.6 CONCLUSIONS

Competing species often find environments in which they can happily coexist. It seems that the criterion of equal fitness is rather too strict to occur very often. However, in practice, the environment constantly undergoes small changes which will effect the carrying capacities, survival rates and fecundities of the species contained in that environment. Thus the fitness of a species will be constantly changing with the environment. Competing species with close fitnesses can then coexist as their fitnesses will constantly be becoming greater than and then less than each other. Thus, the species of greatest fitness is given the opportunity to cause the extinction of the others, but due to further changes in the environment, this opportunity is removed before too much damage to any population is done. Only when an advantage can be maintained for any length of time can a species become the victim of the competition of another. Serious environmental changes are often attributable to man, who constantly manufactures the planet into an environment most suitable to him, at the expense of the other occupants.

Final remarks

It is not satisfactory only to be able to predict which, out of a number of different species, can exist together in a given environment. The above sections illustrate that it is impossible to predict analytically the relative frequencies of species existing together, even for the simple models discussed. These models are general models, and represent enormous oversimplifications of the life cycles of specific parasites. If even such simple sets of equations remain insoluble analytically, simulation appears to provide the most rewarding method of analysis of these and more complex systems. In fact, if this is so, then keeping models mathematically simple is a ridiculous concept. If equations cannot be solved, then why keep them simple? Simulation is the way forward in providing useful, practical and meaningful models of biological processes.

3. EAST COAST FEVER

"So, naturalists observe a flea
Hath smaller fleas that on him prey;
And these have smaller fleas to bite 'em,
And so proceed ad infinitum".

Jonathon Swift, *On Poetry: A Rhapsody.*

The models for parasite systems contained in the previous chapter, provide useful insights into patterns of behaviour of populations under different hypotheses. To construct a model of practical value for complex diseases such as East Coast fever, however, it is important to gain a full understanding of the disease process.

3.1 EAST COAST FEVER

Development of agricultural production in Africa has attracted much international interest and investment (Young *et al.*, 1988), due to the problems caused by past and present food shortages. The majority of people living in Africa are subsistence farmers and, due to the lack of long term agricultural planning, periods of environmental mishap, such as drought, can become major disasters. The holding of livestock, in particular cattle, plays an important role in the subsistence way of life, and cattle have become culturally accepted status symbols. Most farming families will hold only a small number of cattle, and the loss of any one member of the herd is regarded of a major financial blow. The development of the livestock industry represents one area where aid is being directed. Disease places a large restraint on such development.

East Coast fever (ECF) has been described as the second most important African cattle disease after trypanosomiasis (Morrison, *et al.*, 1986). The disease is caused by the protozoan parasite *Theileria parva*, which is transmitted to cattle by the three host tick *Rhipicephalus appendiculatus*. The prevalence of ECF is normally restricted to central and eastern Africa – regions where the cattle hosts, *Bos taurus* and *Bos indicus*, the tick vector, and the parasite share the same geographical location. Figure 1 displays the current geographical locations of *R. appendiculatus* and ECF (Lessard *et al.*, 1990).

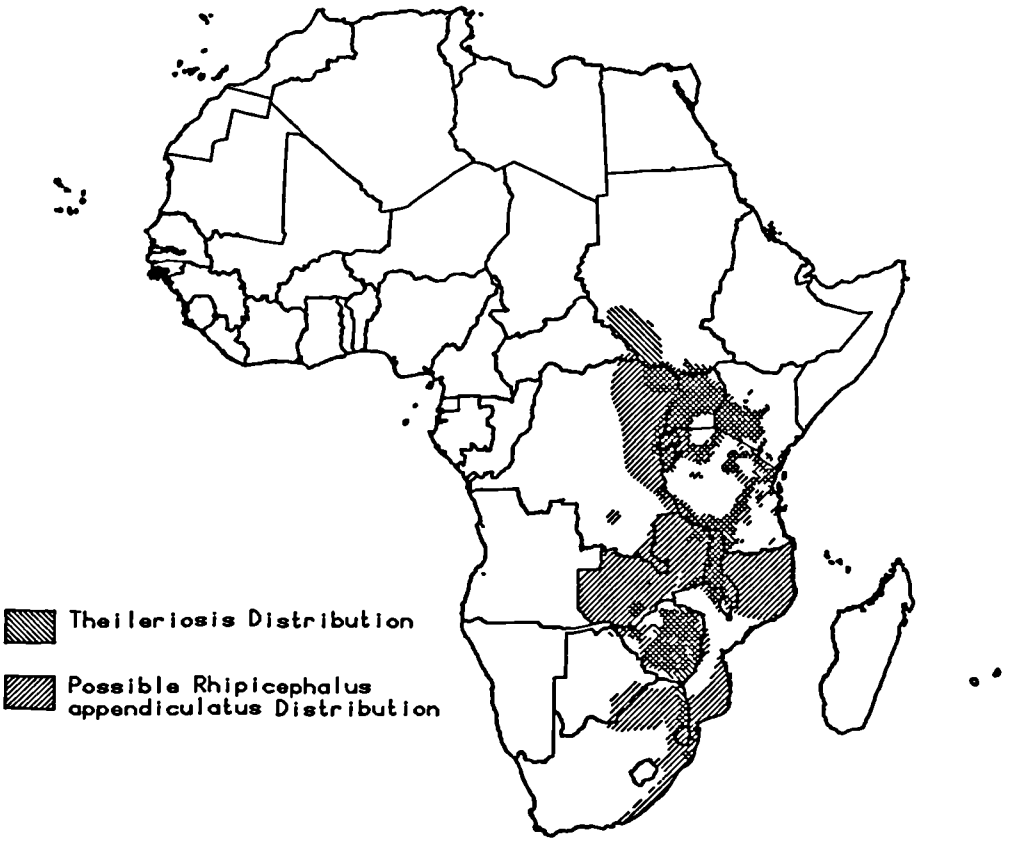

Figure 1. *The geographical location of R. appendiculatus and East Coast fever, reproduced with permission of Lessard et al. (1990). The distribution of R. appendiculatus is based on observations and expert opinion. The distribution of East Coast fever is based on the distribution of T. parva antibodies. It should be noted that the distribution of antibodies to T. parva in southern Sudan was reported on the basis of samples taken from within the administrative boundary, and it is unlikely that T. parva antibodies are found throughout the province.*

ECF is a major economic threat, putting at risk the lives of about 25 million cattle in Burundi, Kenya, Malawi, Mozambique, Rwanda, Sudan, Tanzania, Uganda, Zaire, Zambia, and Zimbabwe. The disease has been reported to be the cause of half a million deaths in cattle per year in East Africa (Miller *et al.*, 1977). In Kenya alone, it has been estimated that 50 – 80% of the national cattle population (currently around 10 million animals) are exposed to the tick, and of these animals 1% die of ECF each year (Dolan 1989). The real figures, however, may be considerably higher. Duffus (1976) claimed that out of 115,000 heifer calves born in Kenya between 1974 and 1975, around 10 – 12% died before they reached a calving age. It should also be noted that these figures take account of the use of tick control methods, without which the disease is

likely to be even more devastating.

Economic losses due to ECF cannot be simply restricted to losses caused by mortality. Losses in the productivity of recovering cattle, and the cost of disease control must also be considered. The presence of ECF also limits the stock of cattle suitable for an area. Higher yielding cattle stocks have been developed by crossing natural stocks with imported European animals. This results in increased milk and liveweight productivity, but also a reduction in natural resistance to local diseases. In areas where ECF is endemic, even intensive tick control may not permit the introduction of such fully susceptible stock (Morrison *et al.*, 1986).

Figure 1 also illustrates that the tick occurs in many areas where the disease is currently absent. As cattle can now be easily transported great distances, the threat of introducing ECF to clean areas, via the importation of infected ticks or cattle, is of great concern. Illegal cattle movements have been responsible for severe outbreaks of the disease in the past (Irvin 1983, Dolan 1989).

Before examining the clinical features of the disease and present control strategies, it is important to understand the life cycles of the vector and the parasite.

3.2 LIFE CYCLE OF THE TICK

Theiler (1904) identified the three host tick *R. appendiculatus* as the principle vector of ECF in cattle. Since this discovery, the importance of the tick in transmitting a major disease has stimulated tick communities to be studied in great detail, and the life cycle of *R. appendiculatus* is now well documented at certain geographical loci. This life cycle is ilustrated in figure 2.

A number of weeks after being deposited, eggs (1) will normally hatch and release larvae (2). The development of eggs before the emergence of larvae is known as the pre-eclosion phase, and the length of time spent in this phase is controlled mainly by temperature (Branagan, 1978). Larvae (2) will initially remain in the vegetation for a number of days whilst the cuticle hardens. Once this is completed, they periodically climb up and down the grasses and scrub, in search of a suitable host (3). This process is known as questing, and ticks can survive unfed in this stage for many days. Questing ticks only move very small lateral distances from where they develop, and so larval ticks are observed in very large clusters close to the area where an egg mass was laid.

When a passing animal comes within range, the questing larvae are able to attach (4). It is believed that ticks can sense the presence of a host by being able to detect

exhaled carbon dioxide (Norval, unpublished). Once attached, the larva makes its way to the head of the animal to feed (4). Here it will spend a few days extracting a blood meal before dropping back to the vegetation (5) to moult into the nymphal form (6). Nymphal ticks repeat the cycle, eventually moulting into adult ticks (7) – (10).

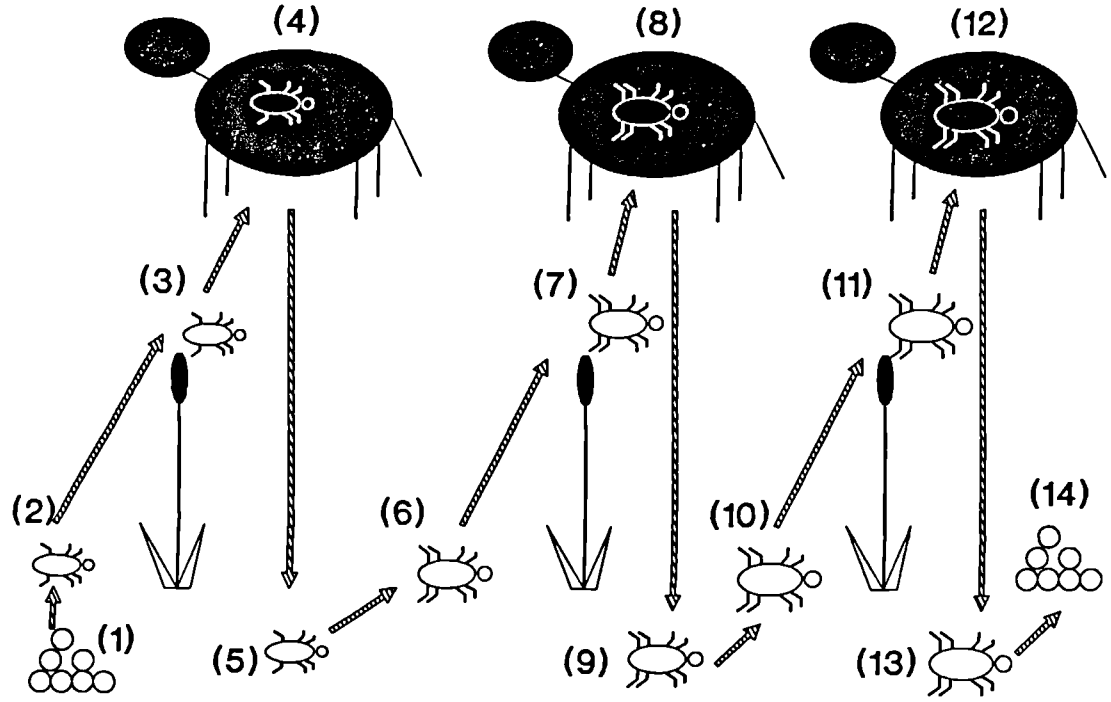

KEY
(1) eggs (2) developing larvae (3) questing larvae (4) attached larvae (5) - (6) larval to nymphal moult (7) questing nymphae (8) attached nymphae (9) - (10) nymphal to adult moult (11) questing adults (12) attached adults (13) preovipositioning females (14) eggs

Figure 2. *Stages in the life cycle of R. appendiculatus.*

The activity of questing adult ticks is dependent on satisfactory conditions of temperature, rainfall and daylength (Short and Norval, 1981). Periods of inactivity in adult ticks are believed to induce the seasonality observed in many tick populations. When questing adult ticks (11) succeed in finding a host (12), they engorge for a few days whilst completing their sexual development. Males then seek receptive female ticks to mate with, and may mate with several females before dropping from the host and dying (13). After mating, females continue to engorge – increasing in weight up to a hundred times. The final weight of the engorged female having a bearing on the

number of eggs it will eventually produce. The engorged female then returns to the vegetation (13) and goes through pre-oviposition, a developmental period when the eggs are produced. Sperm from the male ticks that was stored during mating fertilises the eggs as they are being laid. Eggs are sensitive to desiccation, and so female ticks will normally seek a sheltered, humid place in which to deposit the egg mass (14). This will often be at the base of a grass stalk. Typically, the number of eggs laid per female may be between 4000 and 6000, after which the female dies.

R. appendiculatus is described as a three host tick as it requires three blood meals for successful completion of its life cycle. Usually each meal will be from a different host. The length of the complete life cycle is influenced by various climatic factors, and in a year up to two generations of ticks can be observed (Short and Norval, 1981).

3.3 LIFE CYCLE OF THE PARASITE

The parasite, *Theileria parva*, is maintained in cattle and ticks by a simple host–vector relationship. Ticks contract the infection whilst feeding on cattle infected with the parasite. Infected ticks transmit the infection whilst feeding on uninfected cattle. The parasite is unable to be transmitted through the egg stage of the tick life cycle. Hence, it is only the nymphal and adult tick stages that can transmit *T. parva* to cattle, having received the infection whilst feeding as larvae and nymphae respectively. ECF cannot be naturally passed between cattle without the intervention of the tick vector.

Development of the parasite is well documented, at least qualitatively. Figure 3 shows in detail the life cycle of *T. parva* in the tick and vertebrate hosts, based on the accounts given by Cowdry and Ham (1932) and, more recently, by Mehlhorn and Schein (1984), and Fawcett *et al.* (1985).

The first stage (1) commences at the point of transmission of the parasite from the cow to the tick, when the tick feeds and ingests erythrocytes containing the parasite in piroplasmic form. The piroplasms are released into the gut of the tick (2) and transform into male and female gametes (3a, 3b). The gametes fuse and penetrate the gut epithelial cells to give rise to zygotes (4) which grow into ookinetes (5).

Weeks later, when the tick moults from larva to nymph or nymph to adult, the ookinetes are released from the gut cells into the haemolymph (6), and migrate to the tick salivary glands. The tick is now questing, and the parasite can survive many months whilst the tick remains unfed. A number of acini in the salivary glands may each become infected by a single ookinete when the tick commences feeding (7). Thereafter,

the ookinete differentiates into a multinucleated mass known as a sporoblast (8) which eventually produces numerous sporozoites (9).

On about the fourth day of feeding, the parasitised acini cells rupture, releasing the infective sporozoites into the saliva of the tick (10). The tick becomes clean of the parasite, and cannot transmit ECF to another animal without first ingesting a further dose of parasitised erythrocytes. The length of time a tick is attached to its host does not permit it to induce an ECF infection rapid enough to reinfect itself.

During the blood meal, the sporozoites drain into the lymphatic system of the cow, where they rapidly penetrate the lymphoid cells (11). The sporozoites differentiate into schizonts (12), sometimes referred to as macroschizonts, which induce lymphoid cell division. At this stage the first signs of the disease become apparent in the animal.

Around thirteen days after infection, the schizonts produce merozoites (13) which enter the bloodstream and penetrate the erythrocytes to form piroplasms (14–16). These piroplasms may now infect other feeding ticks, and so the life cycle is maintained.

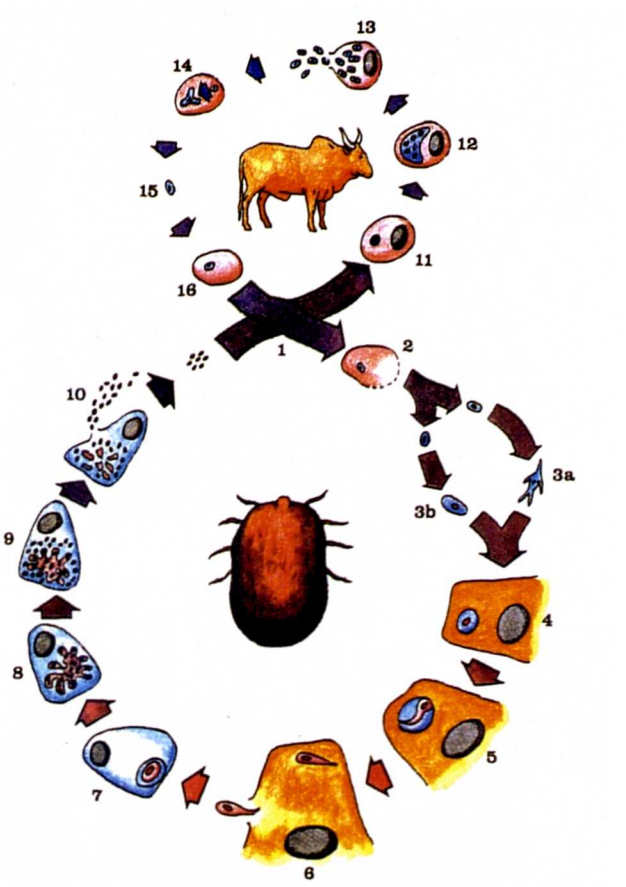

1. Parasite transmission to and from tick and animal.
2. Piroplasms released in gut of tick. 3a,b. Male and female microgametes.
4. Zygote within gut epithelial cells. 5. Developing ookinete.
6. Ookinete released into the haemolymph.
7. Infected acinus cell.
8. Developing sporoblast within an infected acinus cell.
9. Sporoblast produces sporozoites.
10. Sporozoites are released into the tick saliva.
11. Infected lymphocyte. 12. Schizont.
13. Schizont producing merozoites. 14. Piroplasm dividing within a red cell.
15. Free piroplasm. 16. Piroplasm infected red cell.

Figure 3. *Stages in the life cycle of T. parva.*

3.4 CLINICAL FEATURES OF THE DISEASE

Having penetrated the lymphoid cells of the vertebrate host, the parasite initiates these cells to divide, and rapidly engulfs the lymphatic system. Initially animals display a lack of appetite and are dull and listless. Their bodily condition and milk production deteriorates as the parasite infects more and more of the white blood cells. As the preferred sites of tick feeding are the ears and head of cattle, infection is normally first noticed by the swelling of the parotid lymph nodes (Irvin, 1983). These lymph nodes drain the site of the initial sporozoite entry just below the ears. As the infection spreads, all lymph nodes become painfully swollen and hot. Body temperature rises above the normal level, and can approach temperatures in excess of $42°C$ (Irvin, 1983). A febrile response of at least $39.5°C$ is normally reached around ten to fourteen days after infection. The precise timing of this being dependent on the level of schizont parasitisation (Jarrett, 1969).

As the disease progresses, the bodily condition of the animal deteriorates greatly, and animals become reluctant or unable to move. Thirteen days after infection, piroplasms begin to appear in the red blood cells. Animals become anaemic due to erythrocyte destruction.

The terminal stages of the disease are anaemia and severe respiratory distress.

Animals receiving fatal doses will normally die within four weeks of contracting the disease. In those animals that recover, schizonts will normally disappear eighteen days after the initial infection. However, it is unclear as to the persistence of piroplasms in the blood stream of recovered cattle. One school of thought is that piroplasms eventually disappear and the animal ceases to be infective to feeding ticks (Purnell, 1977). Others believe that the parasite levels in the blood of recovered animals persist indefinitely, waxing and waning, producing an infectious carrier state (Dolan, unpublished).

There is general agreement that, on recovery, the animal will become immune to challenge with homologous strains of the *T. parva* parasite (Irvin, 1983). The animal, however, may not be at all resistant to challenge with an unrelated parasite strain. As strains vary between geographical locations, animal stocks that are considered immune to ECF may suffer great losses when transported to other areas.

3.5 DISEASE CONTROL

Due to the devastation caused by ECF in the past, disease control has become a priority issue. Many counties make it illegal for farmers not to adhere to their recommended disease control strategies, as the disease is regarded as a national problem.

Disease control strategies can be divided into two groups: those that control the level of parasite infection by employing various methods of tick control and herd management, or those that attack the parasite, or influence the host response to the parasite.

3.5.1 Tick control and herd management

Tick control strategies are employed in many developing countries, as most of these countries are faced with a multitude of different species of ticks which transmit various tick-borne diseases. Tick control can therefore be used not only to restrict ECF outbreaks, but also to control other major tick-borne diseases such as anaplasmosis, babesiosis and heartwater.

Many countries use acaricidal dips to remove attached ticks from cattle. Acaricides, however, are expensive, and intensive dipping strategies are difficult to sustain. In Kenya the annual budget for acaricidal dipping in 1987 was US$ 6–10 million, and in Zimbabwe the national dipping strategy had to be cut from weekly dips to fortnightly dips due to the costs (Tatchell, 1987).

Dipping cattle has been seen to be of some use in controlling ECF, but does not represent long term control. Tick populations can rarely be eradicated because ticks make use of wild hosts, often buffalo, as well as attaching to domestic hosts. Also, due to new selection pressures, tick populations will eventually become resistant to the acaricide used. The onset of resistance is often speeded up by farmers failing to use the recommended strength of dip solution. Due to the expense of acaricides, using sub-strength dip is an attractive proposition, and has become fairly widespread. Some farmers prefer to use spray races rather than dips to administer acaricide. These appear more conservative on dip solution, as well as being less stressful for cattle.

An alternative to dipping is to use eartags impregnated with acaricide to control ear ticks such as *R. appendiculatus*. These have the advantage of being very easy to administer, unlike the labour intensive dipping strategies. However, they must be treated with some caution as the speed at which ticks become resistant to the acaricide may well be increased. In flies that transmit disease to animals there has been some evidence for the development of resistance by this method in the USA (Young *et al.*,

1988).

Simple management strategies can be used to help control disease. For example, by providing tick proof quarantine quarters for infected cattle, the transmission of the parasite from cow to tick can be controlled. As tick populations are relatively static, the level of *T. parva* infection in a local population can be much reduced. Similar effects can be attained by intelligent management of grazing areas.

Cattle have been seen to have a variable resistance to ticks. Ticks feed more successfully on certain cattle, and tick burdens between members of the same herd can vary substantially. The tick resistant trait is increasingly being seen as important in cattle stock breeding programs, as the tick resistant cattle are less likely to be affected by tick- borne disease.

Finally, work is underway in developing a tick vaccine that can be given to cattle to kill attached ticks. By isolation of various tick antigens from saliva or the midgut, it may be possible to find the specific antigen that produces an immune response in cattle, and thus use this as the basis of a vaccine. This method has recently proved successful in the development of a vaccine for the *Boophilus microplus* tick in Australia.

3.5.2 Parasite control

Theiler demonstrated that cattle could be immunized using splenic and lymphoid cells obtained from ECF cases. Between 1911 and 1914 238,000 cattle in South Africa were immunized by this method. Laboratory tests showed that the immunization procedure proved fatal to 25% of cattle, but out of those that survived, 60% were apparently immune to ECF (Dolan, 1989).

Experiments have been done on the exact dose of schizonts required to successfully immunize cattle, but the results were often very unpredictable. Due to this, and problems of being unable to store living schizonts for any length of time, this method was abandoned.

Immunization of cattle can also be achieved by artificial infections of tick sporozoites from titrated *R. appendiculatus* ticks, followed by drug treatment. This method is known as "infect and treat". It has the advantage that sporozoite suspensions are able to be cryopreserved, making the method much more practical. Due to differences between strains of parasites, a combination of isolates (known as a cocktail) is recommended – such as the "Muguga cocktail" comprised of *Theileria parva parva* (Muguga), *T. p. parva* (Kiambu 5), and *T. p. lawrencei* (Serengeti). Two approaches are possible.

A global cocktail, such as the Muguga cocktail, can be used, or local parasite strains can be isolated and used to produce a local cocktail. A local cocktail has the advantage of being site specific. Cocktails, however, may not always protect against challenge in the field. "Breakthrough" may occur, when an animal immunized against certain strains encounters a different strain. In this event, cattle must be immunised against this other strain by isolating it and adding it to future cocktails.

Cattle that have the disease can also be treated using chemotherapy. Three main antitheilerial compounds are available on the market: Halofuginone, taken orally with water, and Parvaquone (Clexon, Welcome) and Buparvaquone (Butalex, Coopers) administered by intramuscular injection. Each drug is expensive to use. The mode of action of the drug is usually towards attacking the schizont form of the parasite. The drug destroys parasitised lymphocytes, causing the schizonts to be released. These schizonts are vulnerable and degenerate (Mehlhorn and Schein, 1984). Unparasitised lymphocytes remain intact. These drugs consequently have an effect of the piroplasm levels in the bloodstream of infected cattle, which affects the transmission of the parasite to the tick. A major problem with chemotherapy is that the success of a drug relies upon diagnosis of the disease in its early stages.

A schizont vaccine is an area where current research interests are being directed. Such a vaccine could lead to fast and effective disease control. The parasite itself is never likely to be eradicated by such a method, due to the large pool of wild host, many of which are carriers of certain strains. However, the impact of the disease on treated cattle could be significantly reduced. The goal of a schizont vaccine is well founded, as prevention of the disease is regarded as being better than cure.

4. MODELS BASED ON EXPERT RULES FOR PARASITE BEHAVIOUR

"All nature is but art unknown to thee;
All chance, direction which thou canst not see;
All discord, harmony not understood;
All partial evil, universal good;
And, spite of pride, in erring reason's spite;
One truth is clear, 'whatever IS, is RIGHT'."

Alexander Pope, *Essay on Man.*

Construction of a mathematical model requires an intimate knowledge of the biology of the processes being studied. In this modelling approach, expert rules were extracted from published findings and data, or taken from expert opinion, and were translated into a programming language for implementation. This is not dissimilar to the approach of expert systems, where knowledge is stored in a rulebase and conclusions made by chaining through the subset of rules relevant to a particular query. An expert system, in fact, has the advantage that knowledge stored in the rulebase remains in an intelligable form where it can easily be editted to consider the consequences of different hypotheses or opinions. A simple expert system model for *T. parva* was created using Expertech's XiPlus package (Gettinby and Byrom, 1989), but this approach was abandoned as present technology provides only a very limited facility for incorporation of mathematical structures. Future expert systems that can interface qualitative and quantitative knowledge will provide a powerful modelling tool. This chapter illustrates the role of classical modelling in constructing a quantitative model using expert rules extracted from literature on the dynamics of ECF infections. The problem of disease control is briefly considered by investigating a number of simple disease control strategies.

4.1 QUANTITATIVE STUDIES ON THE LIFE CYCLE

The life cycle of the parasite *T. parva* was described in detail in the previous chapter. Along with much qualitative information, numerous studies report data concerning the development of the parasite. The question arises, how best can knowledge be integrated to increase understanding, and to determine viable methods of controlling *T. parva* in areas where the disease is prevalent?

Many studies that report data on the life cycle of *T. parva* have dealt with the effect of drugs and immunization techniques on particular stages of the life cycle. Consequently, the data are not directly useful. However, some papers have specifically addressed the issue of the development of the parasite in the animal and tick, providing suitable data for a numerical study of the life cycle of the ECF parasite. (It may be useful to refer to the life cycle diagram in chapter 3 whilst reading this section).

In 1969, Jarrett *et al.* carried out a detailed study of the kinetics of replication of *T. parva* in high-grade cattle. Cattle were challenged with groups of 10, 100 and 1000 ticks. The ticks were infected with a well defined strain of *T. parva* known as Muguga. Daily observations on blood samples taken from the animals enabled the size of the schizont and piroplasm populations to be estimated. The schizont count was expressed as the macroschizont index (MSI), which is the number of schizonts per 100 lymph cells examined. From these findings, important deductions were possible: the growth rate of schizonts was tenfold every 3 days and independent of the tick challenge; each infected cell from a tick transmitted 5×10^4 infective particles; the day of fever occurred when the number of schizonts reached 7×10^9 and did not depend on the tick challenge; piroplasm counts did not increase after the MSI reached 100%; and piroplasms appeared at the same time irrespective of tick challenge.

A similar study in cattle was reported in 1974 by Radley *et al.*, but instead of natural challenge using ticks, cattle were infected with suspensions of *T. parva* sporozoites. These suspensions were produced by grinding together the salivary glands from a batch of infected ticks. The infective doses received by cattle can be more accurately quantified using this method of infection. From the results it was concluded that the growth rate of schizonts, the time to fever, the length of prepatent period and the survival time of cattle were dependent on the size of the infective dose of sporozoites transmitted in the saliva of the tick, whereas time to piroplasm production did not depend on this. The finding that the growth rate of schizonts was dose-dependent was at variance with that of Jarrett *et al.* (1969), and suggested that immunization could be enhanced by

using a low dose of sporozoites to produce a slowly developing infection.

More recently, Dolan *et al.* (1984) found experimental relationships between the size of an infective sporozoite dose and time to appearance of schizonts, time to febrile response, time to death, probability of death, and time to production of piroplasms. The findings also indicated that time to recovery was not dependent on sporozoite challenge. The day of recovery was defined as being the last day on which schizonts could be detected in the host. Also, Morrison *et al.* (1986) stated that the prepatent period of the infection ends when the MSI reaches 0.05%.

The above findings essentially span the development stages of the parasite from sporozoite to piroplasm within the animal, that is, stages 11 to 16 in figure 3 of Chapter 3. These results suggest that it should be possible to model this part of the life cycle, although no data are present on the merozoite stage.

Few quantitative data are available concerning the development of the parasite within the tick. However, in the study of Purnell *et al.* (1974), nymphal ticks were fed on high-grade cattle infected with *T. parva* (Muguga). The proportion of ticks found to be infective and the average number of infected acini per infected tick were then correlated with the level of piroplasms measured in cattle the day before the ticks completed feeding. Piroplasm counts were expressed as parasitaemia, which was the percentage of piroplasms per 1000 red cells examined. The experiments showed that whether the parasitaemia in cattle was waxing or waning was an important factor, and that variation among ticks was considerable. The findings provide an important and unique data base for the relationship between the infective status of cattle and the degree of infectivity produced in ticks. They also provide sufficient information to link stage 1 of the life cycle, in figure 3 of Chapter 3, to stage 10.

4.2 SIMPLE MATHEMATICAL MODEL

From the reported findings a set of rules can be established as a basis for a model of the *T. parva* life cycle. These are **primary** rules because they are substantiated by published findings. Some of these findings, however, depend on assumptions made by the experimenter, and so affect the accuracy of the model.

Primary rules

P1. The mean total lymphoid cell count per animal is 2.4×10^{12} (Jarrett *et al.*, 1969).

P2. The growth rate of macroschizonts is tenfold every 3 days, and is independent of dose (Jarrett *et al.*, 1969).

P3. Patency occurs when the MSI reaches 0.05% (Morrison *et al.*, 1986).

P4. The first day of fever occurs when the number of macroschizonts first exceeds 7×10^9, i.e. the MSI has reached 0.31% (Jarrett *et al.*, 1969).

P5. Macroschizonts are accurately quantifiable when the MSI reaches 1% (Jarrett *et al.*, 1969).

P6. The day of commencement of piroplasm production is independent of dose, and is 13 days after infection (Radley *et al.*, 1974).

P7. Piroplasm levels increase exponentially, and level out when the MSI reaches 100% (Jarrett *et al.*, 1969).

P8. The growth rate of piroplasms is independent of dose (Jarrett *et al.*, 1969).

P9. An animal is infectious when piroplasms infect more than 1% of the erythrocytes (Purnell *et al.*, 1974).

P10. Death or recovery is dependent on the dose (Dolan *et al.*, 1984).

P11. The day of death is linearly related to the logarithm of the sporozoite dose, and occurs no earlier than 11 days after infection (Radley *et al.*, 1974, Dolan *et al.*, 1984).

P12. The day of recovery is independent of dose, and does not occur until 18 days after infection (Dolan *et al.*, 1984).

In rule P3, patency is defined as the day on which schizonts become detectable in a non-regional lymph node. Schizonts are likely to be detected one or two days earlier in the regional lymph node. The lymphoid cell count in rule P1 was derived from observations on young adult cattle. Rules P9, P10, and P11 are derived from observations on indigenous African Boran cattle; the other rules from observations on European stock.

Two issues arise. First, the consequences of certain rules may be of interest or rules may be in conflict, in which case the model can be used to test possible outcomes. The rules of interest or in conflict then become **test** rules. Secondly, the primary and test rules may not form a sufficient set and **secondary** rules must be added to compensate for nonexistent data. These secondary rules should be kept to a minimum and should at least be based on expert opinion.

Test rules

An examination of the papers of Jarrett *et al.* (1969) and Purnell *et al.* (1974) suggests

that the infective status of ticks is important to the transmission of the disease. In the experiments of Jarrett *et al.* (1969), batches of nymphal ticks fed on infected cattle are considered to be 100% infective, each tick having an average of 10 infected acini cells. Ticks are assumed to transmit the bulk of their infection on the fourth day of feeding, so extrapolation of the MSI growth curves to day 4 provides an estimate of the number of sporozoites contained in each infected acinus cell. The estimate given by Jarrett *et al.* (1969) using this method was approximately 5×10^4 sporozoites per infected acinus. This is an estimate of the number of sporozoites per acinus that are successful in penetrating lymph cells. Purnell *et al.* (1974) indicate that ticks fed on infected cattle can be expected to produce an infection rate closer to 40% and each infected tick has on average only 6 infected acini. Similar extrapolation, using the same growth curves, implies each infected acinus will have on average 17.5×10^4 sporozoites. This is much larger than that estimated by Fawcett *et al.* (1985) from comparison of sporozoite to acinus cell volumes. However, Morrison *et al.* (1986) suggest that initial replication of the parasite is at a much faster rate than that estimated by Jarrett *et al.* (1969), causing backward extrapolation of the growth curve to overestimate the number of sporozoites per acinus. The difference in the sporozoite count per infected acinus has implications for the transmission of the disease. Consequently, the model is used to compare challenge from batches of infective ticks where:

Either:

T1. An infective tick has on average 10 infected acini and each acinus transmits 5×10^4 sporozoites (Jarrett *et al.*, 1969);

or:

T2. An infective tick has on average 6 infected acini and each acinus transmits 17.5×10^4 sporozoites (Purnell *et al.*, 1974).

Comparisons are made on the basis of parameters relevant to the course of disease within the animal.

Secondary rules

No data exist on the rate at which a piroplasm population declines in animals which recover. The following rule is proposed:

S1. If an animal recovers, the rate of decay of the piroplasm population is equal to the growth rate observed during the increase phase.

The rule set only provides the relationships between certain stages shown in the life

cycle in figure 3 of Chapter 3. The life cycle can then be represented in the reduced form shown in figure 1 below.

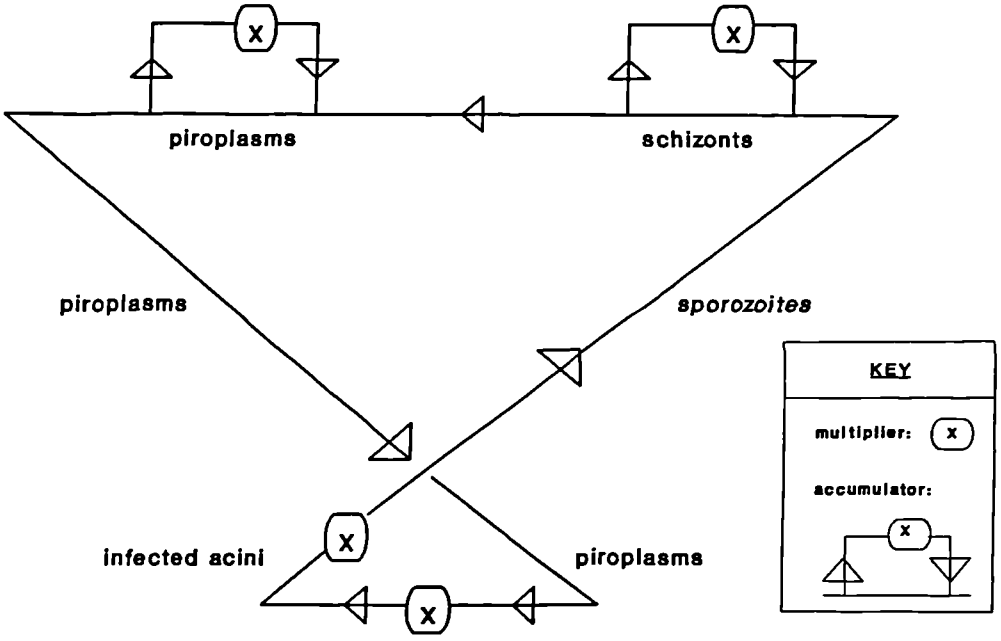

Figure 1. *Mathematical representation of the parasite life cycle.*

The rule set can be programmed, and the growth profiles of the parasite in schizont and piroplasm form can be predicted. A given tick challenge is converted into a sporozoite infection using rules T1 or T2. This sporozoite infection is used to predict the fate of the infected animal, and the timing of death or recovery using rules P10–P12. The initial MSI can be calculated using rule P1, and daily changes in the MSI can be predicted using rule P2. Disease responses such as the timing of patency, first fever and schizont detection can be predicted from the MSI using rules P3–P5. Similarly, the growth profile of piroplasms can be predicted using rules P6–P9 and S1.

In order to test the rules T1 and T2, the model predictions can be compared. Table 1 shows the predictions under rules T1 and T2 when batches of 1, 2, 3, 4, 5, 9, 10, and 20 infective ticks feed on cattle as adults. The rules have been translated into equations and a computer model developed for use on a microcomputer using the programming language Prospero Pascal.

The model shows that under T1 an animal can be expected to die when the tick challenge is 10 or more. An animal is expected to die if the sporozoite dose it receives exceeds the LD_{50}. The prepatent period and days to febrile response decrease as the infective tick challenge increases. Under T2, an animal can be expected to die when the tick challenge is as low as 4 infective ticks. If the tick challenge is any lower the animal

recovers. As challenge increases, the prepatent period and day of fever decrease. The infectious period is short when the tick challenge is low (1-3 infective ticks) and the animal recovers, but also when the tick challenge is high (10 or more infective ticks) because the animal dies shortly after contracting the disease. The latter prediction from the mathematical model is supported by the experimental findings of Branagan (1969), where, in some cases, death reactions were so severe that animals died before producing piroplasms. Moderate tick challenges of 4 to 5 infective ticks produce the largest infectious periods. This suggests it is possible that the severity of the disease is limiting. When the level of infection in the tick population exceeds a threshold, the infectious period in cattle drops due to rapid deaths. Subsequently, the level of infection falls in the tick population.

Table 1. Predicted time in days from infection of disease characteristics in cattle when Rules T1* and T2* are examined using challenges with different numbers of infective ticks.

	Infective Tick Challenge							
	1	2	3	4	5	9	10	20
Rule T1:								
Prepatent period (day)	11	10	9	9	9	8	8	7
Days to febrile response	13	12	12	11	11	10	10	9
Days to 1% MSI	15	14	13	13	12	12	12	11
Day of recovery	18	18	18	18	18	18	-	-
Day of death	-	-	-	-	-	-	20	16
Duration of infectious period	5	5	5	5	5	5	7	3
Rule T2:								
Prepatent period (day)	10	9	8	8	8	7	7	6
Days to febrile response	12	11	11	10	10	9	9	8
Days to 1% MSI	13	13	12	12	11	11	10	10
Day of recovery	18	18	18	-	-	-	-	-
Day of death	-	-	-	21	20	16	16	12
Duration of infectious period	5	5	5	8	7	3	3	0

* See text for explanation.

Contrasting the two rules, the main difference is in the infective tick challenge required to kill the animal. The differences in the other parameters are not so noticeable. In fact, under experimental conditions, the course of the infection would appear similar in animals that recover, irrespective of tick challenge or the infective capacity of each tick. Figure 2 illustrates, under rule T1, the predicted growth curves of the macroschizont index and the percentage piroplasms in an animal which recovers after challenge with 5 infective ticks, assuming each tick has 10 infected acini and each acinus has 5×10^4 sporozoites. Similar growth curves are shown in figure 3, only under rule T2 each tick is assumed to have 6 infected acini and each acinus 17.5×10^4 sporozoites. On day 19 the animal dies.

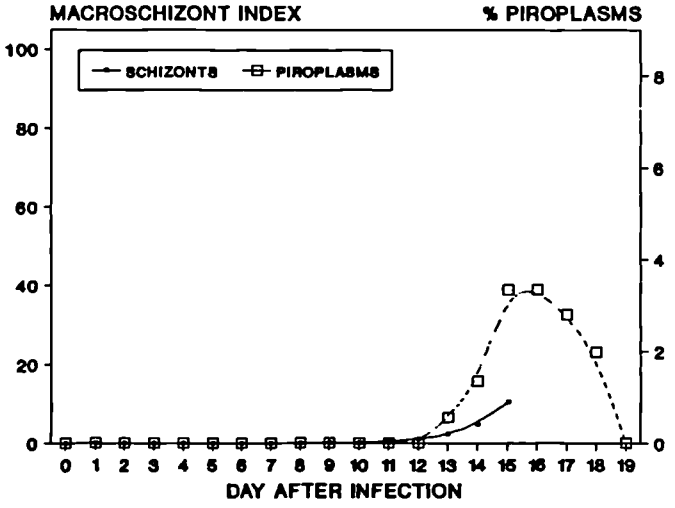

Figure 2. *Predicted parasite growth in animals challenged with 5 ticks under T1.*

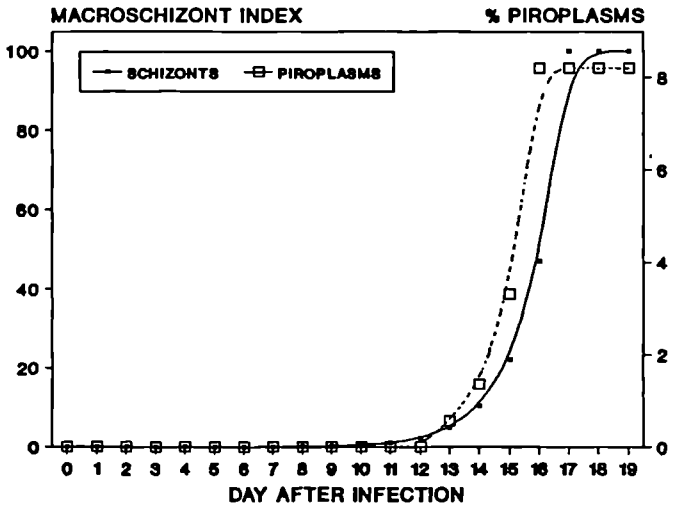

Figure 3. *Predicted parasite growth in animals challenged with 5 ticks under T2.*

The problem now is distinguishing between the two rules to find which provides the results more consistent with reference to other expert knowledge on the disease.

Yeoman (1967) surveyed the density of adult *R. appendiculatus* ticks attached to cattle in various areas of differing ECF disease severity. He found that in areas where the disease is enzootic (that is, where fatalities due to ECF are high in young cattle as they are still susceptible, but low in adult cattle as they have built up a resistance to the disease) an average of 50 adult ticks were observed attached to each animal. He also stated that the average period of attachment for ticks is about 5 days; thus representing an attachment rate of around 10 adult ticks per animal per day. If we assume that larvae, nymphs and adults are found on cattle in similar proportions, then we expect that in an enzootic area 30 ticks attach per animal per day.

Walker *et al.* (1981) in their study of an enzootic area estimated that between 1% and 2% of adult ticks were infected with the parasite. We assume that a similar proportion of nymphs are also infected, say 1.5% of adult and nymphal ticks are infected. Larvae do not have to be considered as they are only capable of contracting infection and not transmitting.

So, in accordance with the above observations, consider the following scenario. Ticks attach at a rate of 30 per animal per day, and drop off after 5 days. The probability of a tick being infected is 0.01. Assume further that the infection transmitted by ticks attaching within the same 5 day interval is that which determines the course of the ECF reaction; and any infected ticks biting after this 5 day interval will have little effect as the disease is already well established. Thus we need only consider a typical 5 day period to compare the two test rules.

From the above results we see that for a death reaction we require a challenge of 10 infective ticks under T1, or 4 infective ticks under T2. Given that 150 ticks are likely to attach in a 5 day period, and the probability of a tick being infective is 0.01, then the number of infective ticks attaching in a 5 day period, X, will follow a binomial distribution with mean 150×0.01 and variance $150 \times 0.01 \times 0.99$. Thus, the probabilities of an animal receiving a fatal tick challenge under the two test rules are:

T1: Prob(10 or more infective ticks attaching out of 150)

$$= P(X \geq 10) \simeq 0.000003.$$

T2: Prob(4 or more infective ticks attaching out of 150)

$$= P(X \geq 4) \simeq 0.19.$$

Infections causing deaths in young cattle are expected to be fairly common in an enzootic area, so the probability of a death under T1 seems much too low; whereas under T2 a death is quite likely. A challenge of less than the fatal number of infective ticks will result in recovery of the animal and solid immunity to subsequent homologous challenge (Irvin, 1983).

Hence, from a modelling viewpoint, T2 appears to best describe the expected disease dynamics, for an enzootic area at least. As stated earlier, the estimated number of sporozoites per acinus under T2 is at variance with experimental observations, but due to initial parasite replication being at a higher rate (Morrison *et al.*, 1981) it provides a more realistic description of the disease dynamics when the replication rate of the parasite within lymphocytes is assumed tenfold every 3 days.

From the model under T2 we see that the duration of an animal's infectious period is dependent on the size of infective tick challenge. This relationship is illustrated in table 2.

Table 2. Predicted duration of the infectious period of cattle under T2 for different infective tick challenges.

Infective Tick Challenge	Infectious period (days)
0	0
1,2,3	5
4	8
5	7
6	6
7	5
8,9	4
10,11	3
12,13	2
14,15,16	1
17 +	0

From challenges of 4 infective ticks or more, the duration of the infectious period decreases almost linearly. If we assume that the infectious period also increases linearly

for tick challenges less than 4 (recovery reactions), then the following function for the infectious period is obtained:

$$F(x) = \begin{cases} 2x; & 0 \leq x \leq 4, \\ 8 - (8/13)(x-4); & 4 \leq x \leq 17, \\ 0; & \text{otherwise}, \end{cases}$$

where, $F(x)$ is the estimated infectious period in an animal receiving a challenge of x infective ticks.

The assumption that infectious periods increase with infective tick challenge for recovery reactions is logical, as for lower tick challenge you might expect fewer piroplasms to be produced.

It is now possible to construct a deterministic model to describe the passage of infection amongst a herd of cattle and a population of ticks. The sporozoite dose to infectious period relationship describes the infection within the herd, and the data presented by Purnell *et al.* (1974) describes the infection within the tick population. The remainder of this chapter concerns the development of such a model. Observations on the behaviour of the expected level of infection in the tick population under various scenarios are reported.

4.3 A DETERMINISTIC MODEL FOR THE BEHAVIOUR OF THE LEVEL OF INFECTION AMONGST A TICK POPULATION

Primary rules

The primary rules P1, P2, P3 and P4 employed by this model are taken from the previous model. Rules P5, P6 and P7 are constructed to deal with a field situation.

P1. The mean total lymphoid cell count per animal is 2.4×10^{12} (Jarrett *et al.*, 1969).

P2. The growth rate of macroschizonts is tenfold every 3 days, and is independent of dose (Jarrett *et al.*, 1969).

P3. The day of commencement of piroplasm production is independent of dose, and is 13 days after infection (Radley *et al.*, 1974).

P4. An animal is infectious when piroplasms infect more than 1% of the erythrocytes (Purnell *et al.*, 1974).

P5. Ticks remain attached on cattle for 5 days before dropping off (Yeoman, 1967).

P6. Infection is passed from animal to tick on the first day of tick feeding (Reichenow, 1940).

P7. Infection is passed from tick to animal on the fourth day of tick feeding (Mehlhorn and Schein, 1984).

Secondary rules

The previous model only contained one secondary rule which was concerned with the decline in piroplasm numbers in a recovering animal. As T1 and T2 have now been tested, T2 becomes a secondary rule (S2). Further secondary rules are required to deal with superinfection. Superinfection occurs when an animal that is already infected receives a further challenge from infective ticks at some time after the initial infection. No experiments looking into the disease reactions following superinfection have been reported. However, Stagg *et al.* (1984) observed in their experiments that an infected lymphocyte may be reinfected with further sporozoites, but offer little information on the infection dynamics as a result of this. Mehlhorn and Schein (1984) in their study of the stages in the *T. parva* life cycle state that when a lymphocyte has multiple infection the size of the resulting schizonts is reduced. This could suggest that the resulting merozoite output of any infected lymphocyte is independent of the number of schizonts contained by the cell. Thus, any sporozoites entering parasitised lymphocytes will not have any influence on the resulting disease dynamics. With reference to the above, rules S3, S4, and S5 were constructed.

S1. If an animal recovers, the rate of decay of the piroplasm population is equal to the growth rate observed during the increase phase.

S2. An infective tick has on average 6 infected acini and each acinus transmits 17.5×10^4 sporozoites.

S3. If a sporozoite penetrates a parasitised lymphocyte then it is assumed not to affect the disease dynamics.

S4. Sporozoites that enter unparasitised lymphocytes become schizonts.

S5. The disease reaction following superinfection is calculated by adding the proportion of the new dose of sporozoites that infect unparasitised lymphocytes to the level of schizonts estimated for that day. Backward extrapolating the schizont growth curve to day 0 will yield the number of sporozoites required to be transmitted on day 0 to bring about this new level of infection. The corresponding infective period can then be calculated.

S6. The duration of infectious period in cattle is given by $F(x)$, where $x =$ the number

of infective ticks in the challenge

$$F(x) = \begin{cases} 2x; & 0 \leq x \leq 4, \\ 8 - (8/13)(x-4); & 4 \leq x \leq 17, \\ 0; & \text{otherwise.} \end{cases}$$

S7. If the infectious period is not an integer, then the animal is assumed infective to feeding ticks for a fraction of a day. This is accounted for by reducing the chance of ticks receiving infection on this day by multiplying the infection probability by this fraction.

S8. The herd size remains constant.

S9. The tick population remains constant.

S10. The time between successive tick attachments is constant.

S11. Tick attachments are constant over the herd.

Rule S6 is a secondary rule because it is taken from the results of the earlier model that relied upon secondary rules.

Test rules

The following three rules become the test rules, as it is by their adjustment that the behaviour of the level of infection in the tick population is dictated:

T1. The number of ticks attaching per animal per day is N.

T2. The probability that a tick receives infection from an infective animal is a.

T3. The probability that an engorged tick survives and reattaches is p.

Analysis of the model

The model rules were translated into program code using the Prospero Pascal programming language. For certain T1, T2, and T3, the number of infective ticks to attach per animal per day is obtained. Moreover, the infection level in the tick population can be studied as time progresses. The time-step employed by the model is the length of time spent by a tick between blood meals. This length of time is defined to be the duration of one cycle of ticks. Because the time between successive attachments is constant, from rule S10, a cohort of feeding ticks will attach on the next cycle with the larvae, nymphae and adults comprising the cohort having developed into nymphae, adults and larvae respectively. Given an initial tick challenge, the resulting "effective tick challenge" on the next cycle of ticks can be obtained. The effective tick challenge is the equivalent number of infective ticks to attach on one day having allowed for superinfection.

For example, to illustrate the chaining of rules, if one infective tick attaches to an animal initially, then by S6 the infectious period of that animal will be 2 days. The number of infective ticks to attach next cycle will be $2Nap$ from T1, T2, T3 and S9. But, as the infectious period was 2 days, this represents challenges of Nap infective ticks on two consecutive days from S10. These challenges of infective ticks are converted to a sporozoite dose, X, for each day using rule S2.

By rules S3 and S4, the number of sporozoites penetrating unparasitised lymphocytes on the first day is X, and on the second day is less than X as some lymphocytes are now parasitised. The proportion of sporozoites successful in penetrating unparasitised lymphocytes is equal to the proportion of unparasitised lymphocytes, q:

$$q = 1 - \frac{X}{2.4 \times 10^{12}} \qquad \text{by rule P1.}$$

Thus, the active sporozoite dose for day 2 is given by:

$$Y = qX$$

Using rules P2 and S4, the number of schizonts on day 2, after superinfection is calculated as:

$$Z = X10^{1/3} + Y.$$

By rules S5 and P2, the number of sporozoites input on day 1 to bring about this level of schizonts on day 2 is given by:

$$A = Z/10^{1/3}$$

The effective tick challenge can finally be calculated by converting this number of sporozoites, A, into a number of infective ticks by using rule S2.

Thus, the initial infective period function can be translated, using the other rules, into a relationship between tick challenge and the effective tick challenge on the next cycle of ticks. Let this relationship be denoted by $G(x)$, where $G(x)$ is the effective tick challenge next cycle, resulting from an effective challenge of x infective ticks this cycle. The form of this transformation of $F(x)$ into $G(x)$ is illustrated in Figure 4.

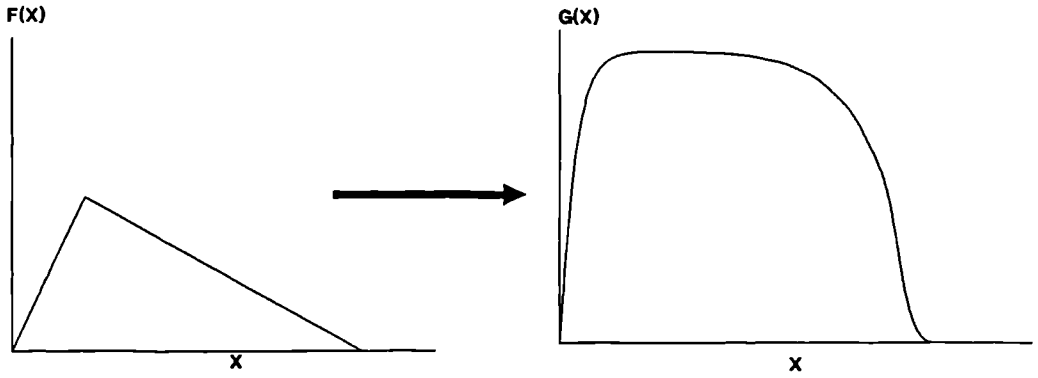

Figure 4. *Transformation of the infective period function $F(x)$ into the effective tick challenge function $G(x)$.*

It is observed that the shape of the function $G(x)$ is always similar. The amplitude of the function, however, varies with choice of the parameters N, a, and p.

The analysis is now simple, as we have obtained the graphical representation of a difference equation scheme. That is, starting with a challenge of x infective ticks per animal, we expect a challenge of effectively $G(x)$ ticks next cycle, followed by a challenge of $G(G(x))$ the next cycle, and so on. Denoting the initial number of infective ticks by A_0, and the effective number of ticks biting on cycle n by A_n; we attain the difference equation scheme:

$$A_{n+1} = G(A_n), \qquad n = 0, 1, 2, \ldots$$

This can be expressed graphically by a vertical mapping of $x = A_n$ onto the function $y = G(x)$; followed by a horizontal mapping of $y = G(A_n)$ onto the line $y = x$, to yield the new number of infective ticks $x = A_{n+1}$. This is repeated, and the behaviour of the level of infection in the tick population can be observed from cycle to cycle for different T1, T2, and T3. An example of this is illustrated in figure 5.

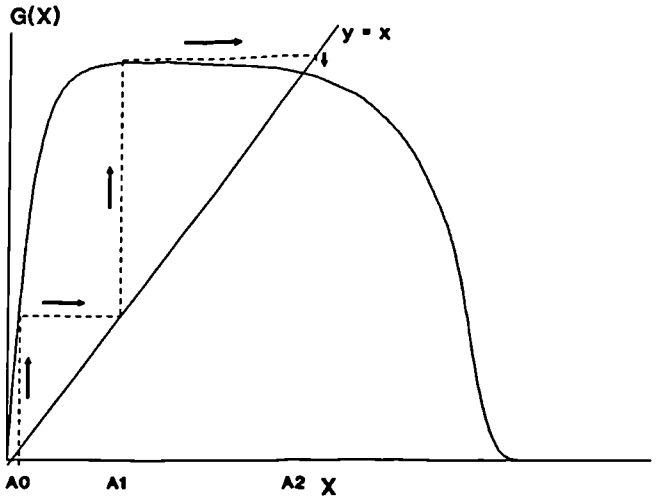

Figure 5. *Graphical representation of the change in the level of infection in the tick population.*

The analysis can now be confined to the analysis of two possible cases, each case represented in figure 6.

The point(s) at which the line $y = x$ crosses the curve $y = G(x)$ are known as stationary points or fixed points. These represent possible limits of the system:

$$A_{n+1} = G(A_n), \qquad n = 0, 1, 2, \ldots \qquad \text{as} \qquad n \to \infty.$$

Whether or not these limits are attained is determined by the Fixed Point Theorem which states that if $G(x)$ is differentiable in a neighbourhood of a fixed point, L, then if $G'(x)$ evaluated at the fixed point is less than one in absolute value the fixed point is stable. Otherwise the fixed point is unstable.

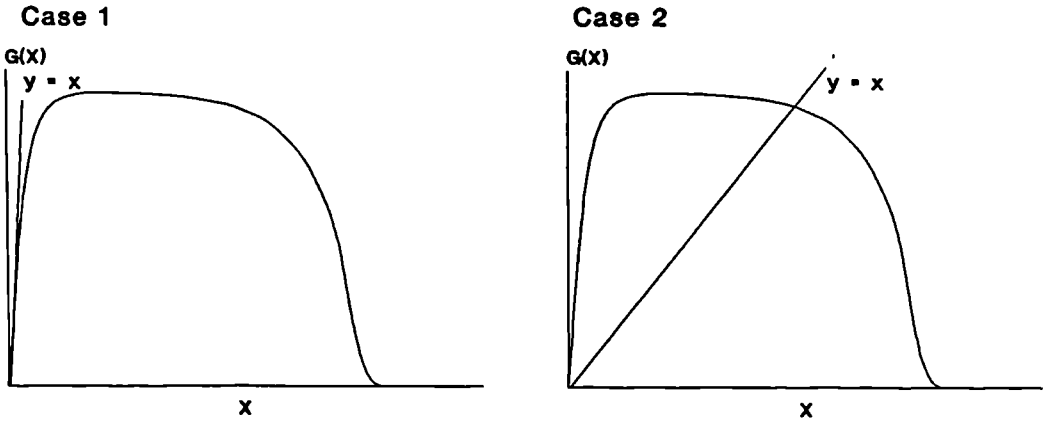

Figure 6. *Two possible cases: one or two fixed points.*

Stability of a fixed point L means that in a neighbourhood of L, the elements of

the series $\{A_n; n = 1,2,3...\}$ tend towards L. That is, L is attractive. Instability implies the converse. Consider the two cases of figure 6 separately.

Case 1

The graph in figure 6 clearly shows that there is only one fixed point, which occurs at $x = 0$. It is also clear that, in this case, this fixed point is stable, because the gradient of $y = G(x)$ is positive and less than 1 (the gradient of $y = x$). In this case, therefore, the eventual extinction of *T. parva* in the tick population is certain. It now remains to find the conditions in T1, T2, and T3 for this case arising.

Define the disease-potential, D, as the number of ticks attached to an infective animal that become infected and will survive to reattach after moulting. From T1, T2, and T3 this can be calculated as $D = Nap$

Now, consider an effective tick challenge of less than 0.5 ticks. This produces an infective period of less than 1 day in the animal (S6). Therefore, the number of new infective ticks resulting from this infection will attach on the same day next cycle (S10), and so superinfection does not occur.

Thus, for $0 \leq x \leq 0.5$

$$F(x) = 2x, \qquad \text{by S6}$$

and $$G(x) = 2xNap \qquad \text{by S10, T1, T2, and T3.}$$

For stability of the fixed point at zero, it is required that:

$$\frac{dG(x)}{dx}\Big|_{x=0} \leq 1$$

Therefore, $2Nap \leq 1$, and the disease-potential, D ≤ 0.5.

Thus, we have the condition that if the disease-potential is less than or equal to a half, then eventually the tick population will become clean of the parasite.

Case 2

The condition for case 2 is therefore that the disease- potential must be greater than a half. If this is so, it follows that the fixed point at zero is now unstable as the gradient of $G(x)$ at the origin is greater than one.

Other properties of the function $G(x)$ are now of interest. The non-zero fixed point may be stable permitting an equilibrium level of infection to be attained in the tick population (figure 7).

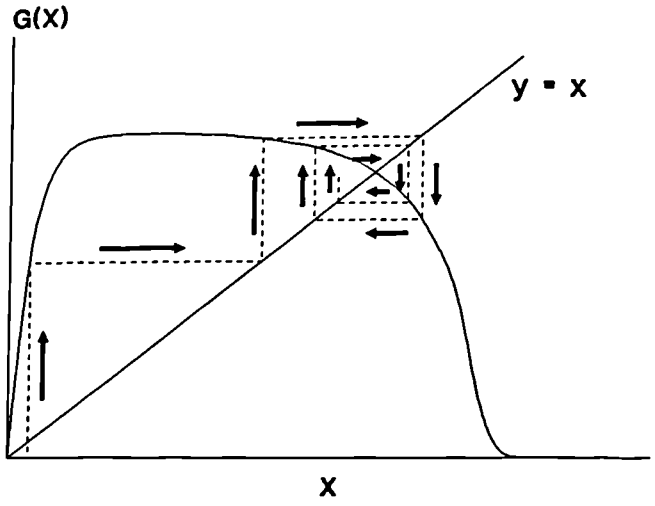

Figure 7. *The non-zero fixed point of $G(x)$ is stable.*

Alternatively the non-zero fixed point may be unstable causing the level of infection in the tick population to either cycle or fluctuate erratically (figure 8a), or to become extinct – if the amplitude of the function $G(x)$ is great enough to permit escape from the positive $x - y$ quadrant (figure 8b), and catastrophe of the system.

Unfortunately, due to the superinfection rules S3–S5, the order of the function $G(x)$ increases with x and so becomes extremely complex for values of x greater than 0.5. It is, therefore, difficult to find analytical conditions for each of these possibilities.

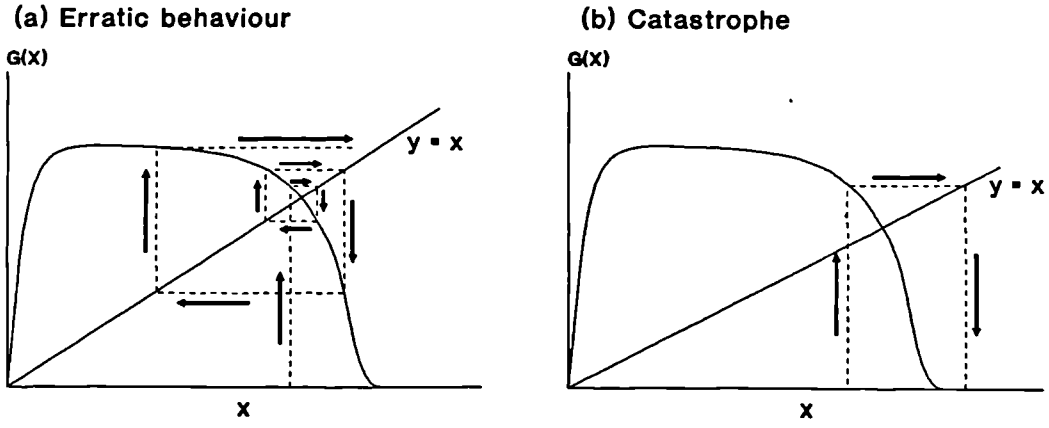

Figure 8. *The non-zero fixed point of $G(x)$ is unstable.*

The properties of the system can be established by performing repeated simulations of the process under increasing values of D, and plotting the results in the form of a bifurcation map. This bifurcation map is illustated in figure 9.

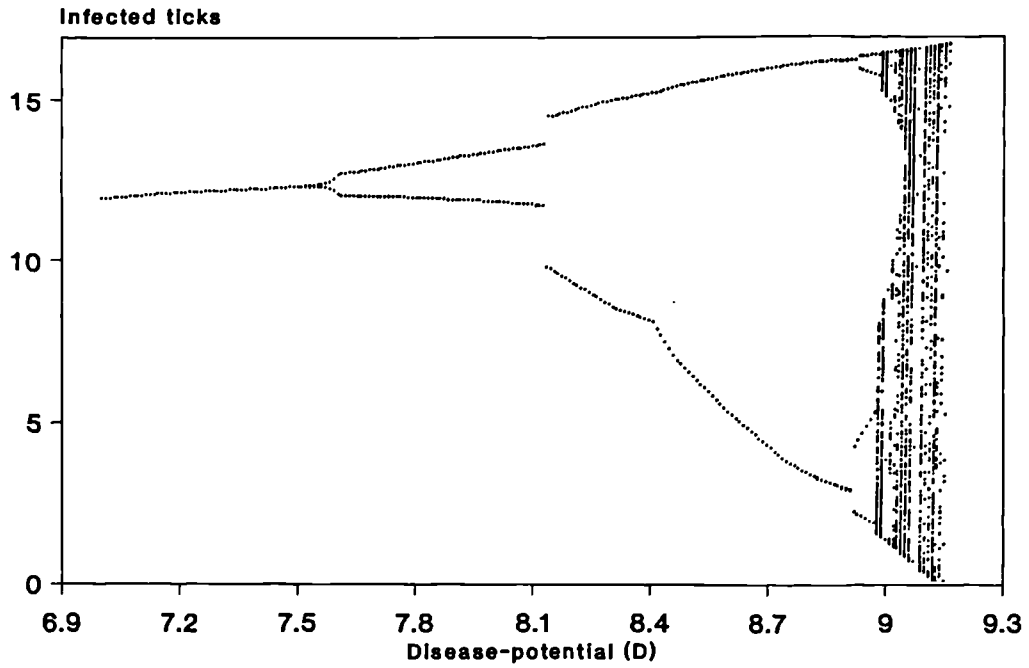

Figure 9. *Bifurcation map showing the behaviour of the level of infection in the tick population under increasing disease-potential, D.*

For $D < 7.48$ a single line appears on the diagram, showing that the process attains equilibrium at a single non-zero fixed point. For example, at $D = 7$ the number of infected ticks on each cycle converges to around 12. At $D = 7.48$, the line divides into two. This represents the point at which the non-zero fixed point of $G(x)$ becomes unstable, and the two non-zero fixed points of the function $G(G(x))$ become stable. Hence the process oscillates between the two equilibria. When D reaches 8.82, the fixed points of $G(G(x))$ become unstable, but the four fixed points of $G^4(x)$ become stable causing the level of infection to flip between four limits. These points become unstable at $D = 8.95$, and for $D > 8.95$ chaotic behaviour is observed at most values of D. There are, however, a number of regions for $D > 8.95$ where oscillations between a small number of points exist, such as the cycle between six points at $D = 8.98$; but, in general, chaos appears to dominate this region until at $D = 9.13$ catastrophe occurs. Catastrophe occurs at the point when the amplitude of the function $G(x)$ becomes great enough to permit extinction of the parasite because the disease reaction is so severe that the cattle are dying before producing piroplasms.

The behaviour is summarised in table 3.

Table 3. The behaviour of the level of infection in the tick population for various values of D.

Disease-potential (D)	**Limiting behaviour**
$D \leq 0.5$	Extinction.
$0.5 < D \leq 7.48$	Equilibrium level achieved.
$7.48 < D \leq 8.82$	Cycling behaviour between two limits.
$8.82 < D \leq 8.95$	Cycling behaviour between four limits.
$8.95 < D \leq 9.13$	Erratic behaviour.
$D > 9.13$	Escape from positive $x - y$ quadrant.
	Extinction of the infection.

It is interesting that these results have similarities to those reported for the simple difference equation systems described in chapter 2. Period doubling appears to commence at around a disease-potential of $D = 7.48$, chaotic behaviour at around $D = 8.95$, and catastrophe at around $D = 9.13$. However, one difference is apparent: in this case the bifurcation map is discontinuous, suddenly leaping to a different set of fixed points at D = 8.1135. In fact, two pairs of fixed points exist for $8.0365 < D < 8.1135$, but only one pair is attained, dependent on the choice of initial conditions. By observing the zeros of the function $H(x) = G(G(x)) - x$ for $8.0365 < D < 8.1135$ it becomes clear that a third pair of fixed points exists, but these fixed points are never attained. The values of this pair of unstable fixed points always lie between the values of the two stable pairs, and form an unstable branch to the bifurcation map which connects the two overlapping stable branches. This phenomonen is known as hysteresis, and is illustrated for the lower branch of the bifurcation map in figure 10. The two possible stable branches are drawn with a solid line, the connecting unstable branch with a broken line.

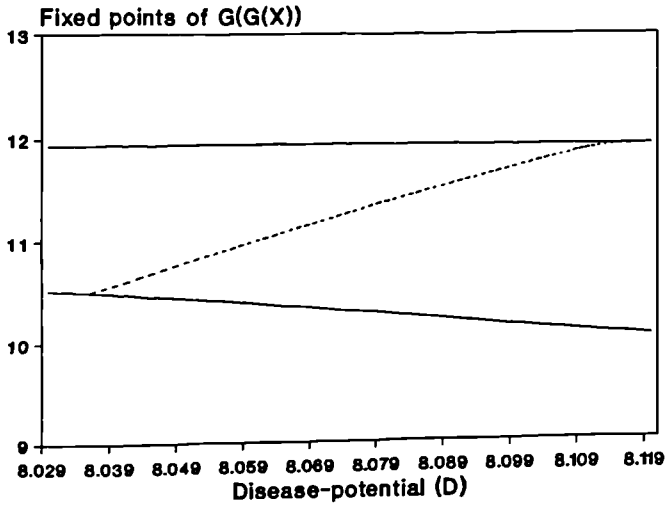

Figure 10. *Behaviour of the lower branch of the bifurcation map of figure 9 at the point of discontinuity.*

The results on the behaviour of the level of parasitisation in the tick population gives an indication as to how the infection affects the cattle population. The predicted behaviour of ECF under different disease potentials (D) are listed below:

(a) $D \leq 0.5$

Extinction of infection in the ticks, causing elimination of ECF in cattle after an initial outbreak.

(b) $0.5 < D \leq 7.48$

Equilibrium of the infection level in ticks, implying that cattle are always under a constant challenge. This could possibly represent an area where ECF is either enzootic or epizootic.

(c) $7.48 < D \leq 9.13$

Fluctuating levels of infection in the tick population, suggesting that sudden outbreaks of ECF may occur erratically. ECF is possibly epidemic.

(d) $D > 9.13$

Extinction of infection in the tick population due to death of cattle. ECF is absent due to the absence of the cattle population!

It is clear that the potential damage that ECF can inflict to a cattle population is controlled by the disease potential, which in turn depends on the number of ticks per beast (N), the chance of a tick becoming infected from an infective animal (a), and the

survival and attachment rates of ticks (p). Many external and environmental factors influence the value of these parameters, such as cattle density, tick density, tick control strategies, climatic conditions, vegetation type and state, cattle breed, and *T. parva* strain. Many of these factors are inter-linked. For example, it might be thought that increasing the cattle density would increase the attachment chances of ticks. However, due to increased grazing pressure, the vegetation length may be reduced sufficiently to make tick attachment more difficult.

Conclusions

The bifurcation map presented in figure 9 gives some clues to controlling the level of infection in a tick population. Where D is less than 8 it is seen that the equilibrium levels of infection achieved increase with D. Thus, for areas represented by disease potentials below 8, the best way of reducing the infection level in the ticks, and therefore controlling the disease, would be to reduce D. As $D = Nap$, reduction of D would involve reducing N, the number of ticks attaching per day, reducing a, the probability that a tick receives infection from an infective animal, or reducing p, the probability that an engorged tick survives to reattach next cycle. Reduction of these parameters could be achieved as follows:

(a) Dipping cattle would reduce p the survival probability, and also N, as ticks are less likely to attach to cattle recently treated with acaricide.

(b) Adopting herd management strategies:

  (i) Pasture switching reduces the numbers of ticks surviving and attaching (N and p),

  (ii) Quarantine of animals exhibiting clinical symptoms would reduce the probability of cattle transmitting infection to ticks (a).

(c) Treatment of animals showing clinical symptoms would reduce the infective periods of infective cattle and hence reduce a.

(d) Changing the vegetation type of pastures to grasses that support ticks less effectively would reduce survival and attachment chances (p and N).

It is interesting, however, that where $D > 8$, the bifurcation map shows two equilibria which the process cycles between. The higher equilibrium point increases slowly with D, but the lower branch is seen to decrease rapidly as D increases. This suggests that the average level of infection of the tick population over two cycles of ticks is decreasing as D increases. Thus, for values of D in this region, reduction of D would cause the

average infection level to rise, and therefore increase the danger of ECF. In fact, it appears that increasing the disease potential would provide the most beneficial results!

Where the process cycles between a small number of limits, if fresh susceptible cattle are to be introduced to pastures it would be most sensible to time their introduction with the predicted time of occurrence of the lowest tick infection level. This would provide an early low input of infection which may provide a level of resistance to subsequent higher infections.

When the process is in chaos, $D > 8.95$, two possibile methods are available to control the disease, either:

(a) Attempt to reduce N, a, or p to reduce D and hopefully throw the system into a stable cycle – so that times of high infection can be predicted and catered for,

or

(b) increase D in attempts to cause catastrophe of the system and thus extinction of the parasite. It should be noted, however, that heavy mortality of the herd is required to bring about such behaviour, and so this option may not be practical.

4.4 FURTHER MODELS

The infective period function $F(x)$ was based on the results of a mathematical model developed for cattle of a certain susceptibility to tick challenge, and a certain susceptibility to ECF. This function will change for cattle resistant to tick challenge, and cattle which produce an immune response to sporozoites. The previous model assumed a constant tick population and constant tick attachments over the herd, but the effects of seasonality amongst ticks and the randomness of tick attachments can also be taken into account. Finally, the effects of drug treatment of animals suffering from ECF can also be investigated by making modifications to the model. The remainder of this chapter considers each extension in turn.

4.4.1 Increased resistance to tick challenge

Ticks attaching to tick-resistant cattle do not feed as effectively as those attaching to fully susceptible cattle. This would suggest that, as ticks ingest less erythrocytes when feeding on resistant cattle, the degree of infection received by the tick would be reduced. Because the host's disease response is dose dependent, if ticks carry less sporozoites, then more infected ticks will be required to bring about a specific disease reaction. To take account of the increased numbers of ticks required, the function $F(x)$, the infective

period of an animal with an effective tick challenge of x ticks, is stretched along the x-axis.

Any transformation on $F(x)$ representing a stretch along the x-axis by a factor 'S', causes an identical transformation of the function $G(x)$ by the same factor. Therefore, the conditions on D for certain behaviour to exist are now conditions on D/S and should be modified accordingly.

So, for example, let $F1(x) = F(x/2)$

$$F1(x) = \begin{cases} x; & 0 \leq x \leq 8, \\ 8 - (4/13)(x-8); & 8 < x \leq 34, \\ 0; & \text{otherwise.} \end{cases}$$

The resulting behaviour exhibited by this system at different disease potentials is summarised in table 4.

Table 4. The behaviour of the level of infection in the tick population for various values of D, under function $F1(x)$.

Disease-potential (D)	**Limiting behaviour**
$D \leq 1.0$	Extinction.
$1.0 < D \leq 14.96$	Equilibrium level achieved.
$14.96 < D \leq 17.64$	Cycling behaviour between two limits.
$17.64 < D \leq 17.9$	Cycling behaviour between four limits.
$17.9 < D \leq 18.26$	Erratic behaviour.
$D > 18.26$	Escape from positive $x - y$ quadrant.
	Extinction of the infection.

Conclusions

Due to the similarity of this system to the earlier system, the inferences made from the bifurcation map are identical to those made earlier. However, by comparison of tables 3 and 4 it follows that increased resistance to ticks reduces the effect of the disease at a given disease potential.

4.4.2 Increased resistance to sporozoites

Sporozoites are only exposed to ECF antibodies for an extremely short time before they penetrate the lymphocytes. If cattle become more resistant to sporozoites, this might suggest that the animal's immune system could effectively deal with a certain level of infection received at any one time. Above this level, some sporozoites may avoid destruction and be successful in penetrating lymphocytes to become schizonts. This can be represented by transforming the function $F(x)$, the infective period of an animal under challenge, by a translation along the x-axis. The point at the origin being translated to a point on the positive x-axis corresponding to the threshold level of sporozoites required to bring about a disease reaction in the animal.

So, for example, consider a positive translation of $F(x)$ by 2 units along the x-axis. This represents a threshold level of 2 infected ticks, below which all sporozoites are destroyed by the animal's immune system. The infective period function can then be expressed as:

$$F2(x) = \begin{cases} 2(x-2); & 2 \leq x \leq 6, \\ 8-(8/13)(x-6); & 6 < x \leq 19, \\ 0; & \text{otherwise.} \end{cases}$$

This gives rise to an identical transformation of $G(x)$ to $G2(x)$, illustrated in figure 11.

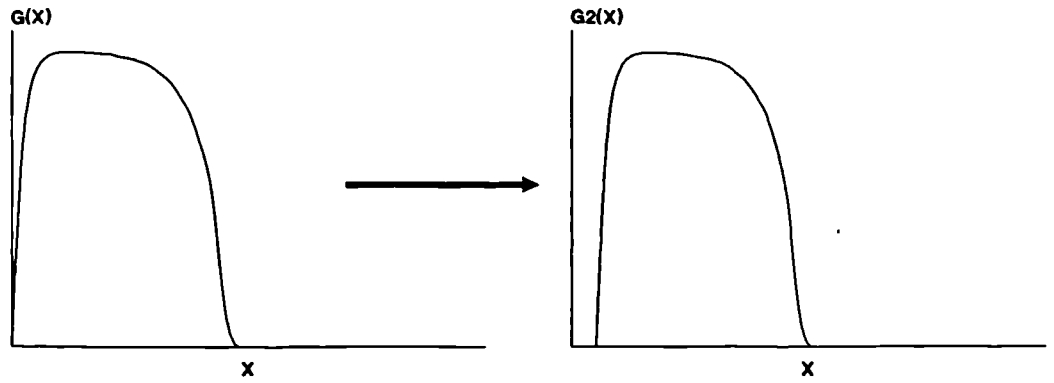

Figure 11. *Transformation of $G(x)$ to $G2(x)$ to account for increased resistance to sporozoites.*

Observation of the function $G2(x)$ shows that the line $y = x$ does not cross the curve $y = G2(x)$ at the origin, and so no fixed points need in fact exist. If there are no fixed points then extinction of the parasite from the tick population is immediate.

If fixed points exist, then the behaviour of the system is dependent on their sta-

bility. Plotting the bifurcation map, figure 12, reveals that a number of stable cycles do exist before the system becomes chaotic and eventually extinct. This behaviour is summarised in table 5.

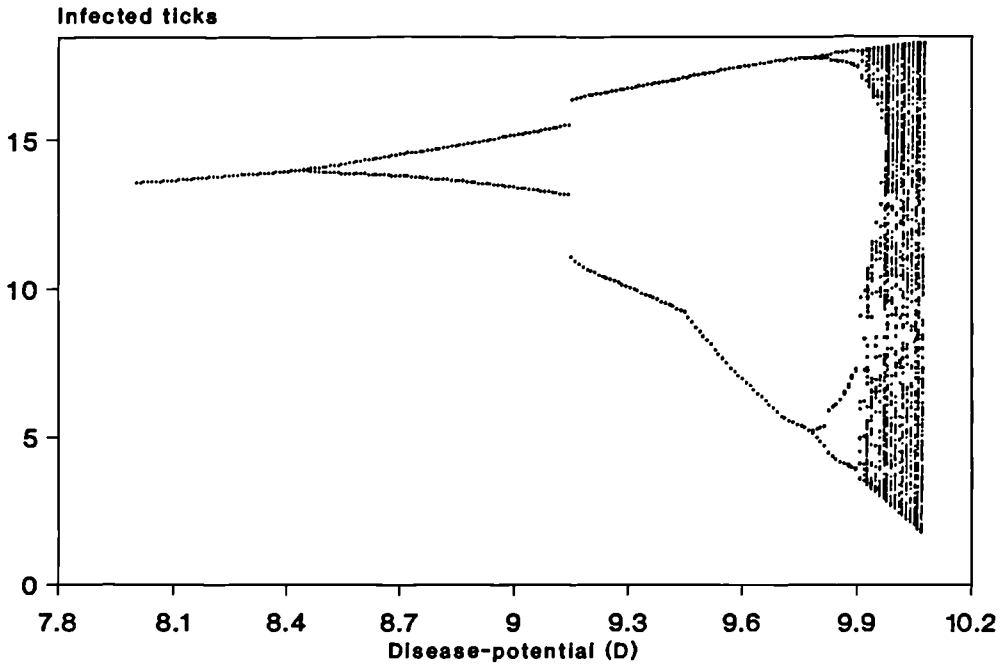

Figure 12. *Bifurcation map showing the behaviour of the level of infection in the tick population under increasing disease-potential (D), allowing for increased resistance to sporozoites.*

Table 5. The behaviour of the level of infection in the tick population for various values of D, under function $F2(x)$.

Disease-potential (D)	**Limiting behaviour**
$D \leq 2.0$	Extinction.
$2.0 < D \leq 8.42$	Equilibrium level achieved.
$8.42 < D \leq 9.73$	Cycling between two limits
$9.73 < D \leq 9.81$	Cycling between four limits
$9.81 < D \leq 10.03$	Erratic behaviour.
$D > 10.03$	Escape from positive $x - y$ quadrant.
	Extinction of the infection.

Conclusions

By comparison of tables 3 and 5, it follows that increased resistance to sporozoites reduces the effects of the disease at specific disease potentials, as might be expected. Other inferences are as for the earlier systems.

4.4.3 Seasonally fluctuating tick population

The assumption made in rule S9 that the tick population is constant is not consistent with field observations. Tick populations often follow distinct seasonal cycles dictated by climatic conditions.

First, consider the simplest case of a tick population alternating between two levels, causing the number of ticks to attach each cycle to alternate between two levels, N_1 and N_2 say. This can be represented by applying in turn two different functions for the effective tick challenge, $G_1(x)$ and $G_2(x)$; where $G_1(x)$ allows for an attachment rate of N_1 ticks per animal per day, and $G_2(x)$ for N_2 ticks. Letting A_0 be the initial number of infected ticks, and A_n be the effective tick challenge on the nth cycle of ticks, the dynamics of infection within the tick population can be described by the following difference equation scheme:

$$\begin{aligned} A_1 &= G_1(A_0), \\ A_2 &= G_2(A_1) = G_2(G_1(A_0)), \\ A_3 &= G_1(G_2(G_1(A_0))). \end{aligned}$$

etc..

As earlier, it is found that for an effective tick challenge, x, of less than a half, superinfection on the next cycle of ticks does not occur. In this case the effective tick challenge next cycle can be simply expressed as:

$$G_i(x) = N_i apF(x) = 2N_i apx; \qquad i = 1, 2.$$

The two subsequences $\{A_0, A_2, A_4, \ldots\}$ and $\{A_1, A_3, A_5, \ldots\}$ can be considered separately to establish whether or not the process A_n becomes absorbed at zero as n increases. Defining $Z_n = G_2(G_1(Z_{n-1}))$, and $Y_n = G_1(G_2(Y_{n-1}))$, each referring to one of the above subsequences, then for absorption we require both subsequences to tend to zero. That is, the fixed point at zero must be stable for both Z_n and Y_n.

Now,

$$G_1(G_2(x)) = 2N_1ap(2N_2apx)$$
$$= 4a^2p^2N_1N_2x$$
$$= G_2(G_1(x)),$$

which means that the stability condition is the same for both processes, as might be expected. By the fixed point theorem, the condition for stability of the fixed point at zero is:

$$\frac{d(G_1(G_2(x))}{dx}\Big|_{x=0} < 1,$$

Therefore,

$$4a^2p^2N_1N_2 < 1$$
$$\Rightarrow D_1D_2 < (0.5)^2,$$

where D_1 is the disease potential of the process under $G_1(x)$ alone, and D_2 is the disease potential under $G_2(x)$ alone.

$$\Rightarrow (D_1D_2)^{0.5} < 0.5.$$

This is the condition that the geometric mean of the disease potentials D_1 and D_2, $GM(D_1, D_2)$ is less than 0.5

Extending this result to the case of a tick population switching between N levels, the general condition for stability of the fixed point at zero becomes:

$$D_1D_2 \ldots D_N < (0.5)^N.$$
$$GM(D_1, D_2, \ldots D_N) < 0.5$$

Unfortunately, no similar results can be easily obtained concerning the stability of the non-zero fixed point, due to the complexity of $G(x)$ for $x > 0.5$. The properties of the system for $x > 0.5$ have been investigated by simulation.

It now remains to define a suitable sequence of functions $G_i(x)$ such that the seasonal fluctuations in the size of the tick population are accurately accounted for. The literature provides some general observations. Branagan (1973) showed that temperature is the strongest controlling factor in the time of development of ticks through their various stages. Tukahirwa (1976), stated that humidity has a strong influence on the survival chances of eggs. Short and Norval (1981), observed peak numbers of ticks in the field corresponding to the position and duration of the rainy seasons. If we assume

that tick numbers fluctuate sinusoidally over the year, and the period of this sine wave is one year, this might correspond to a location with one major rainy season.

The time between successive attachments is d days, which implies that the tick population can go through $n = 365/d$ cycles per year.

Defining N_i to be the number of ticks attaching on day 1 of the ith cycle, N_i is given by:

$$N_i = A + B\sin(\frac{2\pi i}{n}).$$

The behaviour of the level of infection in the tick population is dependent on the values taken by N_i, which itself depends on A, B, and n. Consider, as an example, the situation when ticks have a reattachment probability, $a = 0.5$; a probability of receiving infection from an infective cow, $p = 0.4$; and a period, $d = 45$ days, between cycles. This produces aproximately 8 cycles per year, causing the number of ticks to attach per cow each cycle to be described by:

$$N_i = A + B\sin(\frac{2\pi i}{8})$$

and so

$$N_0 = A,$$
$$N_1 = A + B/2^{0.5},$$
$$N_2 = A + B,$$
$$N_3 = A + B/2^{0.5},$$
$$N_4 = A,$$
$$N_5 = A - B/2^{0.5},$$
$$N_6 = A - B,$$
$$N_7 = A - B/2^{0.5},$$
$$N_8 = A = N_0,$$
$$N_9 = N_1,$$

etc..

The behaviour of the system is dependent on the choice of the parameters A and B, and by varying these, different properties can be observed. As shown earlier, the fixed point at zero is stable if GM is less than a half. In this case $N = 8$, and the mean disease potential is given by:

$$
\begin{aligned}
GM &= [D_0 D_1 D_2 D_3 D_4 D_5 D_6 D_7]^{1/8} \\
&= [(ap)^8 A(A + B^{0.5})(A + B)(A + B^{0.5}) \\
&\qquad \times A(A - B^{0.5})(A - B)(A - B^{0.5})]^{1/8} \\
&= [(ap)^8 A^2(A^2 - B^2)(\frac{A^2 - B^2}{2})^2]^{1/8}
\end{aligned}
$$

So the condition for stability of the fixed point at zero is:

$$
\begin{aligned}
&[(ap)^8 A^2(A^2 - B^2)(\frac{A^2 - B^2}{2})^2]^{1/8} < (0.5) \\
&\Rightarrow A^2(A^2 - B^2)(A^2 - B^2/2)^2 < (\frac{1}{2ap})^8
\end{aligned}
$$

If satisfied, the tick population will eventually become clean of the parasite; otherwise the fixed point will be unstable, and the only way for the tick population to become clean is by catastrophe of the system.

Simulation studies suggest that the behaviour of the system for values of GM greater than a half is dependent not only on the size of GM but also on the magnitude of the amplitude of the sine wave controlling the fluctuations of tick numbers, B. That is, for similar values of GM different behaviour of the system can be observed, due to the position and height of the sine wave. From the constant tick population model it was seen that certain bands of disease-potentials exist, each referring to a different type of behaviour exhibited by the system. In the fluctuating tick population case, we have a sinusoidally fluctuating disease potential, which traverses a number of these behavioural bands. The average level of the sine wave being Aap and the amplitude being Bap. This function for the disease potential is shown in figure 13.

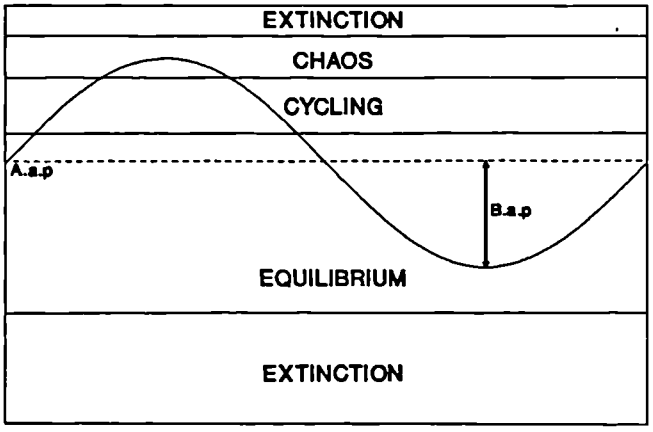

Figure 13. *Change in disease potential traversing various behavioural bands.*

The time spent in each zone has an influence on the resulting behaviour of the system. The results of a number of simulations are given below in table 6.

Table 6. The behaviour of the level of infection in a sinusoidally fluctuating tick population with 8 cycles per year, for different A and B.

A	*B*	*GM*	*Aap*	*Bap*	**Behaviour**
2	2	0	0.4	0.4	Extinction (rapid)
2	1	0.376	0.4	0.2	Extinction (rapid)
2.5	0.5	0.495	0.5	0.1	Extinction (slow)
2.5	0.25	0.498	0.5	0.05	Extinction (v. slow)
3	2.25	0.498	0.6	0.45	Extinction (v. slow)
10	5	1.866	2	1	Cycling between 8 points
10	10	0	2	2	Extinction (eventual)
20	5	3.940	4	1	Cycling between 8 points
30	5	5.958	6	1	Cycling between 8 points
40	5	7.969	8	1	Cycling between 8 points
43	2	8.595	8.6	0.4	Cycling between 8 points
43	2.5	8.593	8.6	0.5	Chaos
43	3	8.590	8.6	0.6	Catastrophe
44	0.6	8.800	8.8	0.12	Cycling between 8 points
44	1.5	8.797	8.8	0.3	Chaos
44	1.75	8.796	8.8	0.35	Catastrophe (extinction)
46	1	9.200	9.2	0.2	Catastrophe (extinction)

Discussion

Consider the two cases, $GM < 0.5$ and $GM \geq 0.5$, separately.

1. $GM < 0.5$

The mean disease potential over one period of the sine curve is less than 0.5, which means that the tick population will eventually become clean of the parasite. This behaviour is supported by the results presented in the first five lines of table 6, where extinction always occurs when GM is less than a half. As expected, the closer to a half GM becomes, the slower the absorption at zero is. An interesting result is the absorption at zero predicted for the case when $A = 10$, and $B = 10$. GM is zero, so absorption is certain. However, the level of infection in the tick population fluctuates for a long time before the inevitable extinction. This is because the vast majority of the disease-potential sine wave lies out of the zone referring to stability of the fixed point at zero and so absorption is achieved eventually. The speed of absorption depends very much on the choice of starting value.

2. $GM \geq 0.5$

When considering the remaining results presented in table 6 it is useful to recall that if the disease-potential of a system with a constant tick population becomes greater than 7.5, the non-zero fixed point also becomes unstable; if it becomes greater than 8.9 chaos is possible; and if it exceeds 9.1 catastrophe is possible. With reference to this, consider the following examples.

For $(A, B) = (10, 5), (20, 5)$, or $(30, 5)$ the disease potential of the system always lies between 0.5 and 7.5, suggesting that at each cycle of ticks there exists a non-zero attractive fixed point. Thus, the result of an equilibrium being attained where the level of infection cycles between $N = 8$ points, is not surprising. It should be noted, however, that these 8 fixed points are not the same as the 8 equilibrium points expected if the model was run separately for constant tick attachments of $N_0, N_1, \ldots, N_7$. This behaviour is illustrated in figure 14.

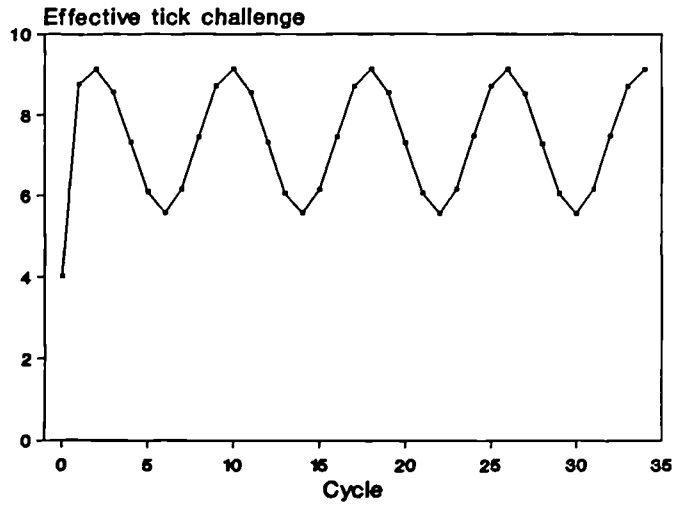

Figure 14. *The infection level achieves a stable cycle for seasonal ticks.*

For $(A, B) = (40, 5)$ the disease-potential of the system varies between 7.0 and 9.0. Most of the time, the disease-potential lies within the bifurcation zone $7.5 < D < 8.9$, but exists below 7.5 for a small amount of time. The resulting behaviour is, as before, a stable cycling between 8 points. It appears that the alternation of functions $G_i(x)$, has a stabilising effect on the system. This is further highlighted by the observed behaviour of the system for $(A, B) = (44, 0.6)$, where the disease-potential is always greater than 7.5. At each cycle there is no unique attracting fixed point, but a stable cycle between 8 points is still achieved.

The dependence of the system on the amplitude and position of the disease-potential sine wave is shown by the differing behaviours of the system under $(A, B) = (43, 2)$, $(43, 2.5)$, and $(43, 3)$. In each case the average position of the disease-potential sine wave is $Aap = 8.6$. Increasing the amplitude of this function (Bap) makes the system less stable, even though GM is reduced. For $B = 2$, a stable cycling between 8 points is observed; increasing B to 2.5 throws the system into chaos; and increasing B further to 3 causes catastrophe, producing a tick population clean of the parasite. This behaviour is illustrated by the bifurcation map of figure 15 where $A = 43$ and B is varied from 0 to 3.

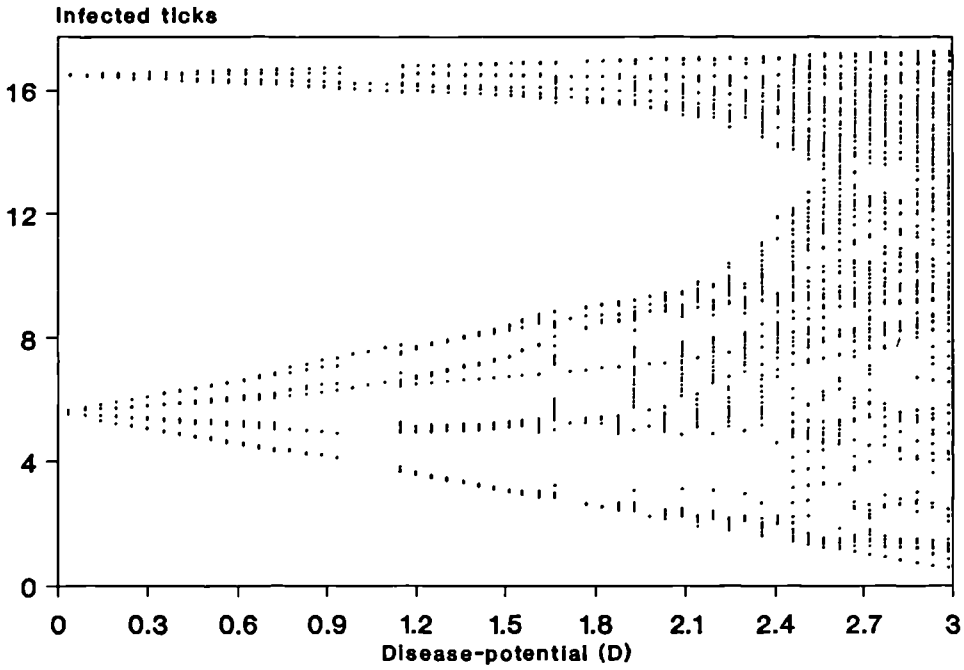

Figure 15. *Bifurcation map showing the behaviour of the level of infection in the seasonal tick population where* $Aap = 8.6$ *and* Bap *is varied from 0 to 3.*

At $B = 0$ the tick population is constant with $D = 8.6$, hence the oscillation between two points. As D increases the process oscillates between 8 points and becomes more and more noisier until chaos at around $B = 2.4$. Finally catastrophe occurs at around $B = 2.9$.

Similar results are observed for $(A, B) = (44, 0.6)$, $(44, 1.5)$, and $(44, 1.75)$. Clearly the stability of the system is very much dependent on the average level of disease-potential (Aap), and the degree of variation from this level (Bap) which brings the system temporarily into different behavioural zones.

For $(A, B) = (46, 1)$ the disease-potential of the system extends into the catastrophe region, and catastrophe can, and does, occur, as illustated in figure 16.

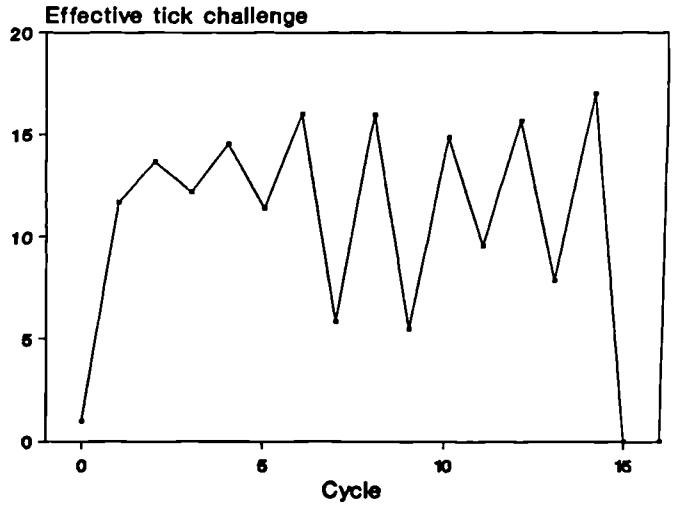

Figure 16. *The tick population becomes clean of infection due to catastrophe.*

Thus, the simulation study suggests that for a sinusoidally fluctuating tick population, where the number of ticks attaching per cycle is given by $N_i = A + B\sin(\frac{2\pi i}{8})$; the resulting behaviour of the level of infection in the tick population is dependent of the values of a, p, A, and B.

The behaviour observed could be a gradual cleaning of the tick population with eventual extinction of the parasite and ECF for small A and B; or, for larger A and B, a stable fluctuation of the number of infected ticks reflecting the seasonal changes in tick numbers, and possibly causing seasonal outbreaks of the disease. Alternatively, for even larger A and B, the level of infection in the tick population may fluctuate erratically producing sudden outbreaks of disease which are not seasonally controlled; or sudden disappearance of the parasite due to an extremely severe case of ECF when A and B are still larger.

Conclusions

Because the condition for extinction of the parasite is that GM is less than a half, the best way to control the parasite is to reduce GM. However, efforts can be optimised by looking at the position and form of the disease potential sine wave. If tick control strategies are to be used then it may be the case that reduction of GM is most effective when cattle are dipped at times when the tick population is at peak levels. It may, therefore, appear most conservative to dip only at these times. However, it should also be noted that the change in the level of infection in the tick population may bear no relationship to the rise and fall of the number of ticks, and so tick control strategies

may not always provide the desired results in disease control.

4.4.4 Random tick attachments

The assumption of rule S11 that daily tick attachments are constant over the herd is also inconsistent with observations. Challenge can vary considerably between members of the same herd. As the tick population is assumed constant (rule S9), it follows that the number of questing ticks per day is also constant. Letting the number of tick attachments over a herd of size N be X per day, we can assume that the number of ticks to attach to a specific animal follows a Poisson process of rate $\lambda = X/N$.

Thus, the expected infective period of an animal can be calculated as:

$$E[\text{infective period of animal}] = \sum_{X=0}^{\infty} \frac{\lambda^X e^{-\lambda} F(X)}{X!}$$

where $F(X)$ is the infective period function. The function $F(X)$ is zero for $X < 1$ and $X > 17$, and so this reduces to:

$$E[\text{infective period of animal}] = \sum_{X=1}^{17} \frac{\lambda^X e^{-\lambda} F(X)}{X!}$$

As the herd contains N animals, the expected infective period of the herd is given by:

$$E[\text{infective period of herd}] = N \times E[\text{infective period of animal}]$$

$$= N \sum_{X=1}^{17} \frac{\lambda^X e^{-\lambda} F(X)}{X!}$$

as opposed to the earlier deterministic estimate of $NF(X/N)$ for the herd under uniform tick challenge (rule S11). The functions for the deterministic and probabilistic infective period, $F(x)$ and $F4(x)$, and effective tick challenge, $G(x)$ and $G4(x)$, are contrasted below in figures 17 and 18.

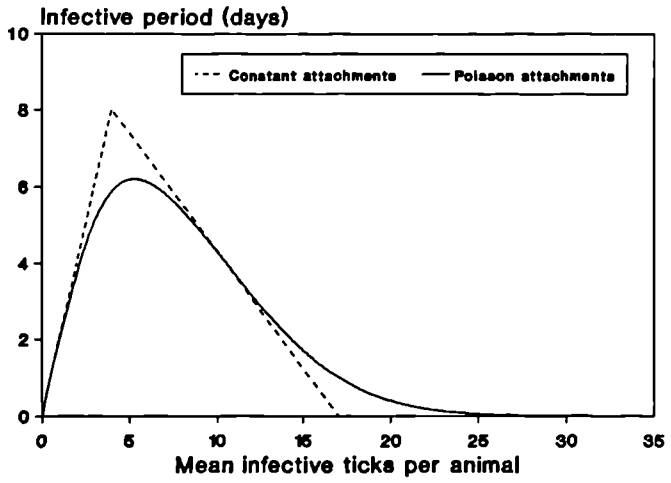

Figure 17. *Infective period of cattle under constant and Poisson attachments.*

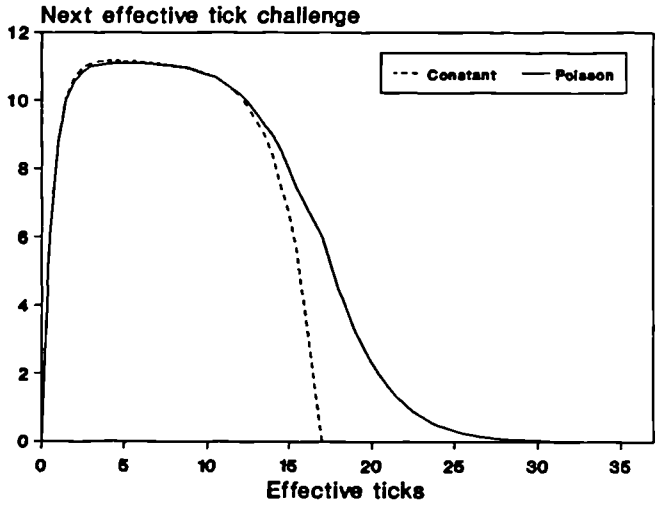

Figure 18. *Functions $G(x)$ and $G4(x)$ for effective tick challenge for constant and Poisson attachments.*

The main effect of Poisson attachments is to extend the right hand tail of each function. This heavier tail influences the behaviour of the system, which can be seen in the bifurcation map of figure 19 and is summarised in table 7 below.

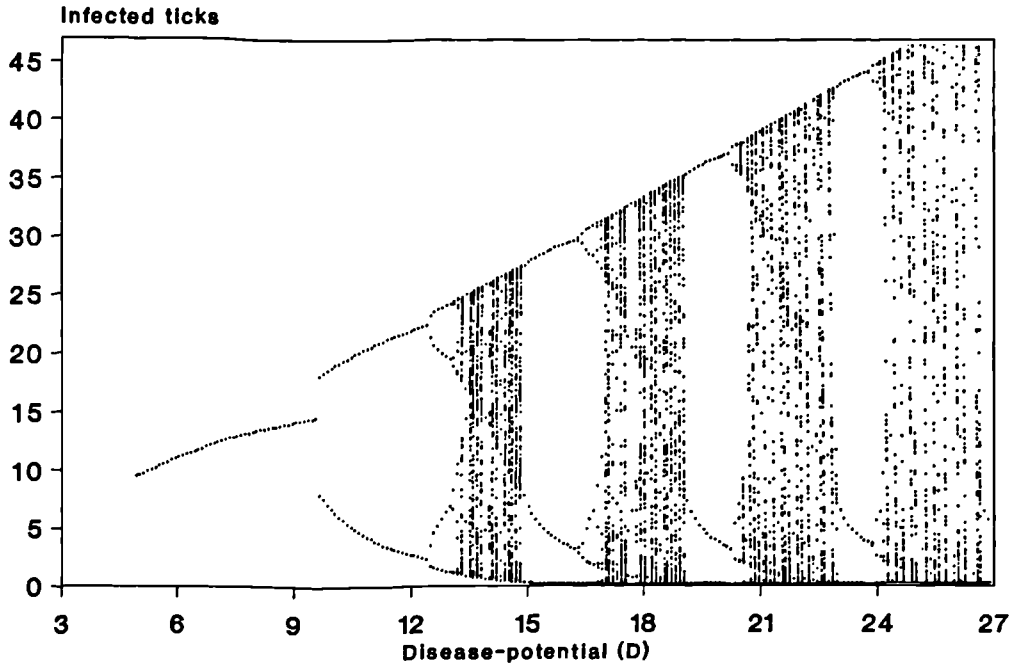

Figure 19. *Bifurcation map showing the behaviour of the level of infection in the tick population where attachments are Poisson, for increasing disease-potential (D).*

Table 7. The behaviour of the level of infection in the tick population for various values of D, under function $F4(x)$.

Disease-potential (D)	**Limiting behaviour**
$D \leq 0.5$	Extinction.
$0.5 < D \leq 9.65$	Equilibrium level achieved
$9.65 < D \leq 12.45$	Cycling between two limits
$12.45 < D \leq 13.05$	Cycling between four limits
$13.05 < D \leq 13.15$	Cycling between eight limits
$13.15 < D \leq 13.25$	Cycling between 16 limits
$13.25 < D \leq 14.85$	Chaos
	Note: 6-cycle at D = 13.4
	5-cycle at D = 13.9
$14.85 < D \leq 16.25$	Cycling between three limits
$16.25 < D \leq 16.75$	Cycling between six limits
$16.75 < D \leq 16.85$	Cycling between 12 limits
$16.85 < D \leq 19.05$	Chaos
	Note: 5-cycles at D = 18.1
	and $17.55 < D < 17.75$
$19.05 < D \leq 19.9$	Cycling between four limits
	(two close to zero)
⋮	⋮

Conclusions

In general the inferences made from this model are similar to those made earlier. It should be noted, however, that the system can never attain catastrophe. This is because the right hand tail of the function $G4(x)$ approaches zero asymptotically, and so there is no non-zero value of x for which $G4(x)$ equals zero. This is rather unrealistic, as there must come a point, L say, where for $x > L$, $G4(x)$ corresponds to an infection of less one infected acinus, or even less than one sporozoite.

4.4.5 Drug treatment of infected cattle

A small amount of data from clinical trials performed by Wellcome Research Laboratories was made available to investigate and quantify the effects of drug action on the disease response of treated cattle. This data is discussed in more detail in Chapter 5. However, the main effects of drug treatment are increased survival chances of cattle receiving normally lethal tick challenges; reduced probability of infected cattle being infective to feeding ticks; and longer infective period in recovering cattle that are infective.

In order to construct a model allowing for chemotherapy, the following rules are required in addition to those presented earlier:

T4. Cattle that would die if left untreated have a probability, f, of death following treatment.

T5. Those animals that would normally die on day x without treatment, will die on day Dx if the treatment is unsuccessful, and will be infectious to feeding ticks.

T6. Those animals that recover following treatment will be infective to feeding ticks with a probability i.

In the absence of chemotherapy, rule S6 dictated the relationship between challenge of infected ticks, x, and the resulting infectious period in the animal, $F(x)$:

$$F(x) = \begin{cases} 2x; & 0 \leq x \leq 4, \\ 8 - (8/13)(x-4); & 4 \leq x \leq 17, \\ 0; & \text{otherwise.} \end{cases}$$

where, cattle recover from challenges of $x \leq 4$, and die if the challenge exceeds this.

Taking account of the three new rules, the function $F(x)$ can be transformed into a function $F5(x)$, which describes the infectious period of cattle treated with an antitheilerial agent. This transformation can be brought about by performing three consecutive mappings on the function $F(x)$:

$$F(x) \xrightarrow{[1]} F1(x) \xrightarrow{[2]} F2(x) \xrightarrow{[3]} F5(x)$$

Mapping [1] takes account of the increase in the day of death in cattle that receive potentially fatal tick challenges; mapping [2] accounts for the reduced chances of recovering animals being infective to ticks; and mapping [3] allows for the reduced probability of animals dying from potentially fatal doses. These mappings are illustrated in figure 20, and are discussed below.

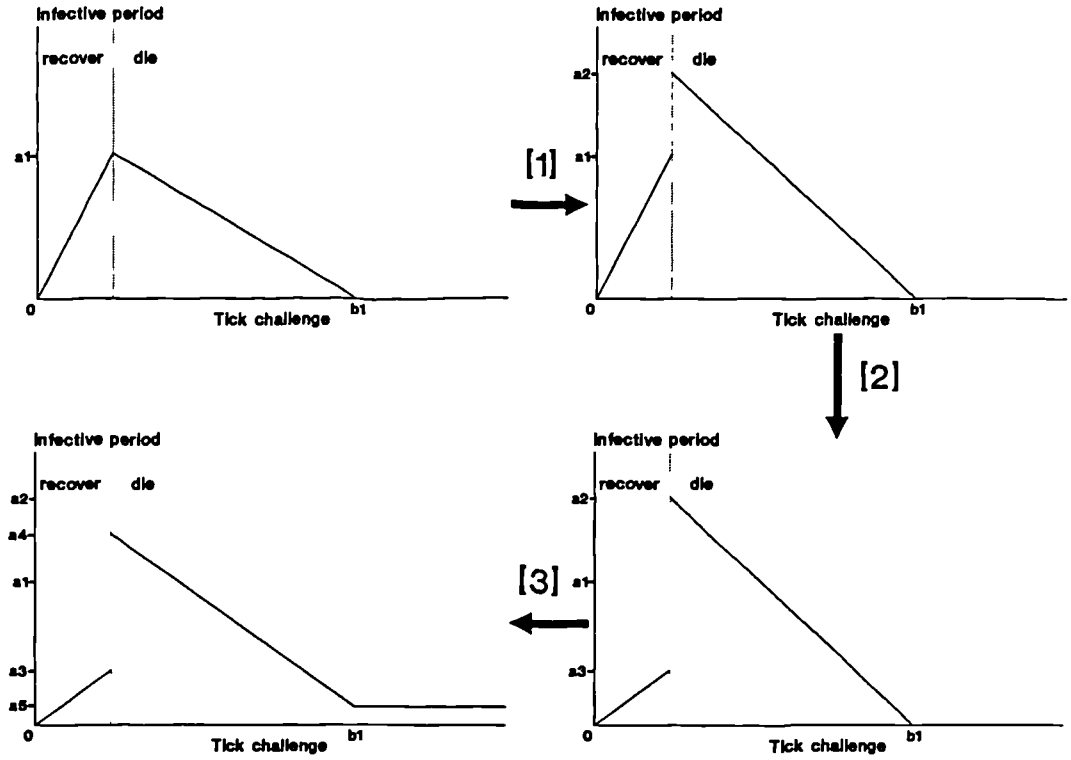

Figure 20. *Transformations on the infective period function $F(x)$ to account for chemotherapy.*

Mapping [1] – using rule (T5).

Animals receiving challenges which would normally be fatal if left untreated ($x > 4$) will now survive for a longer period before dying. Moreover, if their infective period is normally I days, it will now be dI days, where $d = (Dx - 13)/(x - 13)$, due to the prolonged disease response. Allowing for this, the infective period function becomes:

$$F1(x) = \begin{cases} 2x; & 0 \leq x \leq 4, \\ 8d - (8/13)d(x-4); & 4 \leq x \leq 17, \\ 0; & \text{otherwise}, \end{cases}$$

as illustrated in Figure 20, where $a2 = da1$.

Mapping [2] – using rule (T6).

In those animals that would normally recover from challenge without drug treatment ($x \leq 4$), chemotherapy may mean that piroplasms will not always be produced. Only a proportion, i, of these animals will be infectious to feeding ticks, having an infectious period of $2x$ days, the remainder will not transmit infection, being infectious for 0 days. Thus, for challenges of no more than four infected ticks, the expected infectious period is given by:

$$F(x) = i(2x) + (1-i)(0) = 2ix, \quad (x \leq 4).$$

So the infective period function $F1(x)$ is transformed to the function $F2(x)$, where:

$$F2(x) = \begin{cases} 2ix; & 0 \leq x \leq 4, \\ 8d - (8/13)d(x-4); & 4 \leq x \leq 17, \\ 0; & \text{otherwise.} \end{cases}$$

This is illustrated in Figure 20, where $a3 = ia1$.

Mapping [3] – using rule (T4).

Those cattle receiving potentially fatal doses ($x > 4$) have a probability f of dying with infective period $8d-(8/13)d(x-4)$, and a probability $(1-f)$ of recovering with infective period $8i$. Those cattle receiving very high doses ($x > 17$) still have a chance $(1-f)$ of recovery with infective period $8i$. Allowing for this, the final transformation yields the required infectious period function $F5(x)$ below:

$$F5(x) = \begin{cases} 2ix; & 0 \leq x \leq 4, \\ 8fd + 8i(1-f) - \dfrac{8fd(x-4)}{13}; & 4 \leq x \leq 17, \\ 8i(1-f); & \text{otherwise.} \end{cases}$$

This is illustrated in Figure 20, where $a4 = fda1 + (1-f)ia1$, and $a5 = (1-f)ia1$.

Analysis of the model

As before, the height of this function $G(x)$ is dependent on the size of the disease-potential $D = Nap$,

where

N = the number of ticks attaching to each cow per day.

a = the probability that a tick receives infection from an infective animal.

p = the probability that a tick survives to reattach.

The higher the parameter Nap, the greater the amplitude of $G(x)$. This effects the gradient of $G(x)$ at the intersection of the curve $y = G(x)$ with the line $y = x$, and hence the behaviour of the system: $X_n = G(X_{n-1})$, through time (fixed point theorem). However, in this case the shape of the curve $G(x)$ is also influenced by the choice of parameters d, i, and f. The size of $i(1-f)$ controls the steepness and extent that the function $G(x)$ decreases from its maximum value. The parameter d has an influence on the size of the maximum. This can be seen clearly in Figure 21.

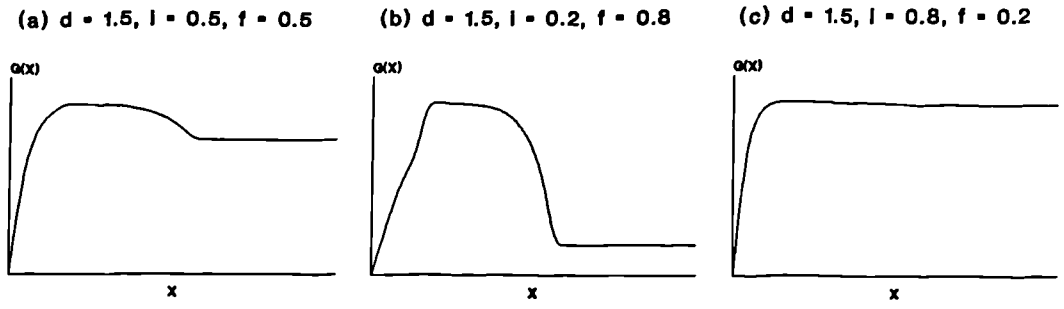

Figure 21. *Forms of the function $G(x)$ for the chemotherapy model under different values of the parameters i and f, when $d = 1.5$.*

In each case (a), (b), and (c), the parameter d takes a value of 1.5. In case (a), i and f are both 0.5, and the function $G(x)$ is seen to steeply rise to its maximum at $x = 4+$, then descend gradually to become a straight line at $x = 17$. Case (c), when $i = 0.8$ and $f = 0.2$, is similar but the peak caused by the maximum is smoothed out due to the large value of $i(1 - f)$. In case (b), $i = 0.2$ and $f = 0.8$, however, the maximum of the function is very well pronounced due to the steep descent to a small global minimum value at $x = 17$. The behaviour of the system with chemotherapy is therefore going to be very dependent on the choice of parameters d, i and f.

The systems described by cases (a) and (c) will achieve stable equilibria at all disease-potentials, due to the gradient of the functions $G(x)$ never exceeding 1 in absolute value at the point of intersection of the line $y = x$ (fixed point theorem).

However, case (b) is of greater interest. Clearly, due to the function $G(x)$ becoming a straight line for $x \geq 17$, the system $X_n = G(X_{n-1})$, will eventually acheive a stable equilibrium for Nap large enough. Before that point some interesting behaviour is observed, as illustrated by figures 22 and 23.

Figure 23 shows the behaviour of the system for disease-potentials from 7.0 to 57.0. The predicted eventual stable equilibrium occurs at around $D = 55$. Figure 22 shows the behaviour at disease-potentials of 7.0 to 13.0 in more detail. Clearly the discontinuities in the function $G(x)$ produce some irregular changes in the behaviour of the system.

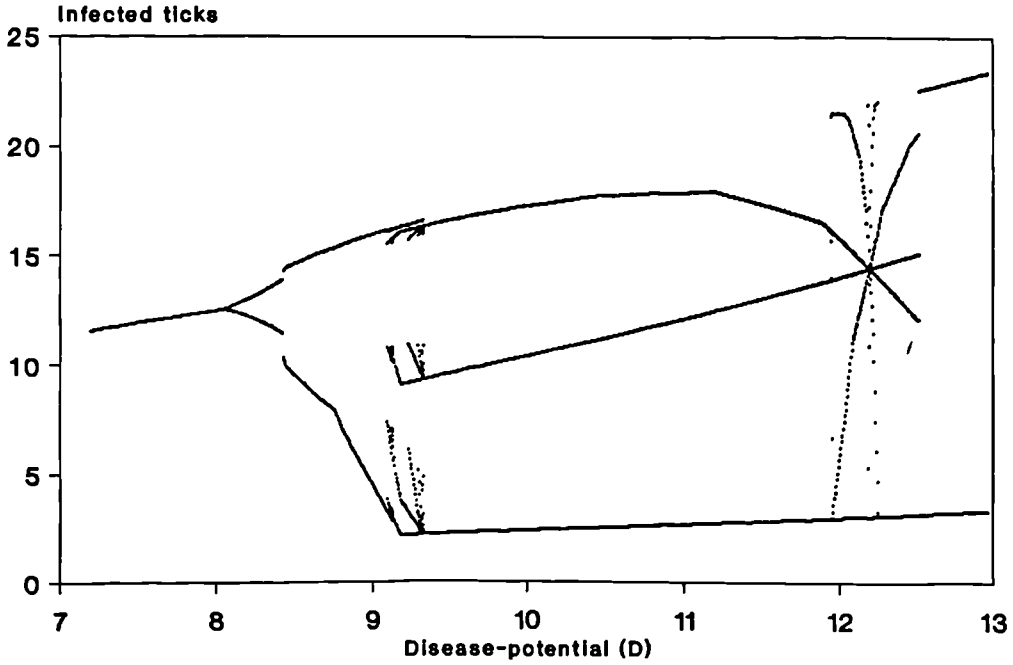

Figure 22. *Bifurcation map showing the behaviour of the level of infection in the tick population for the chemotherapy model with* $d = 1.5$, $i = 0.2$ *and* $f = 0.8$, *and disease-potentials (D) increasing from 7 to 13.*

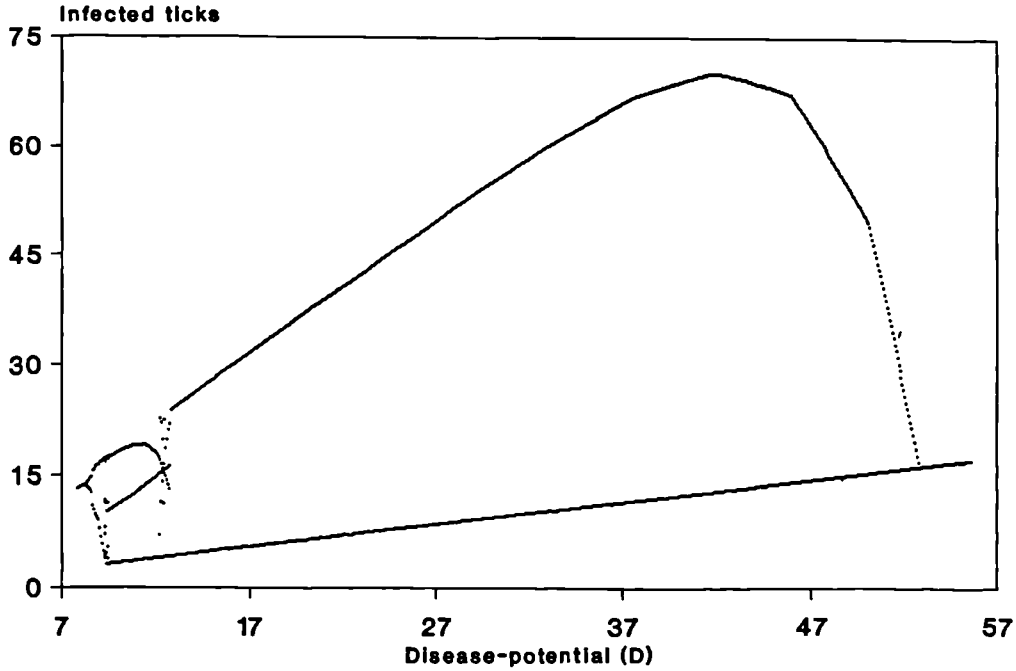

Figure 23. *Bifurcation map showing the behaviour of the level of infection in the tick population for the chemotherapy model with* $d = 1.5$, $i = 0.2$ *and* $f = 0.8$, *and disease-potentials (D) increasing from 7 to 57.*

Conclusions

The administration of chemotherapy on a herd appears to be a stabilising influence on

the resulting infection level in the tick population. Certainly, little complex behaviour is observed for most drug regimes, making ECF outbreaks more predictable. There is clearly a balance of effects to be allowed for when considering the application of a new drug. A drug that extends the life-expectancy of a suffering animal, also extends its infectious period, and so has a bad influence on the level of infection amongst the ticks, allowing infection to increase. However, a drug that reduces the chance of a recovering animal being infective has the opposite effect. These two factors, which are both side-effects of most drugs, have to balance themselves out to prevent the infection level in the tick population increasing and producing problems in the future. In the field, most chemotherapy regimes are administered alongside acaricidal dipping strategies, which would certainly prevent the tick population receiving high infection due to the prolonged disease reactions of suffering cattle.

The functions $G(x)$ estimated from clinical trials data for single and double doses of Parvaquone totalling 10mg/kg and 20mg/kg are shown below in figures 24 and 25. The higher doses clearly result in less infection in the tick population. Single and double doses do not appear to effect the resulting transmission of infection to ticks, although double doses are significantly more effective as a cure of the disease, and are those recommended by the manufacturer.

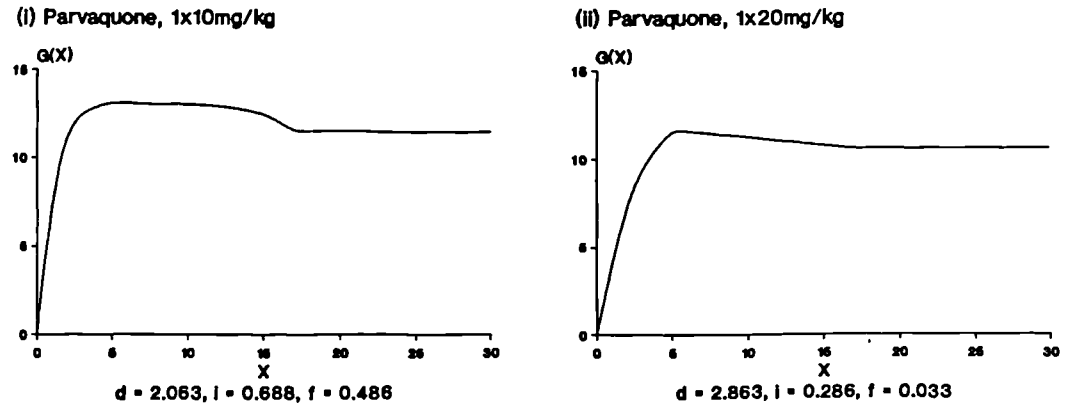

Figure 24. *Forms of the functions $G(x)$ estimated for single treatments with Parvaquone at doses of 10 and 20mg/kg.*

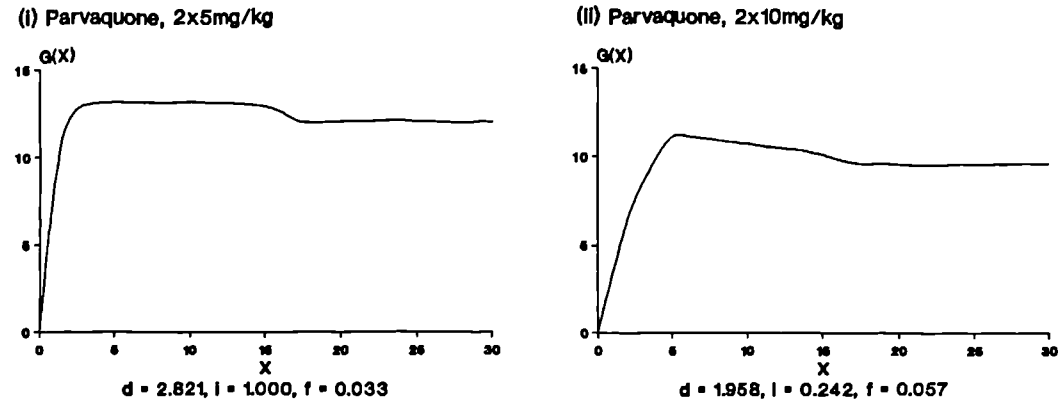

Figure 25. *Forms of the functions $G(x)$ estimated for double treatments with Parvaquone at doses of 10 and 20mg/kg.*

4.5 DISCUSSION

One of Africa's possible answers to disease control is to breed cattle for resistance. The indigenous African cattle are genetically more tolerant than exotic breeds to the important African diseases such as trypanosomiasis and ECF. Previously, exotic cattle were introduced and crossed with indigenous animals in attempts to increase milk and liveweight productivity. This, however, resulted in increased disease prevalence. Due to the severe effects of disease, thoughts are now returning to support the theory that natural disease resistance outweighs the benefits of increased productivity.

Tick resistance is a property that is thought to be partly innate and partly acquired. Resistance to ECF is also seen to vary with different breeds of cattle. Therefore, both these traits are properties that can be developed by the careful management of breeding programs. The models presented in sections 4.4.1 and 4.4.2 illustrate the benefits of the tick and sporozoite resistant traits respectively.

Results from the earlier model of section 4.3 and the model for increased resistance to ticks of section 4.4.1 are given in tables 3 and 4 respectively. It is clear that under each model the level of infection amongst the tick population exhibits the same behavioural characteristics. However, equivalent behaviour occurs at much higher disease-potentials under the model allowing for the effects of tick resistance. For example, at a disease-potential of $D = 7$ a single equilibrium level of infection is obtained with both models. For the no tick resistance case, this level represents an effective tick challenge of around 12 infected ticks per cycle. When $S = 2$, as for the example in section 4.4.1, the model for increased tick resistance predicts an equilibrium level of around effectively 9

infected ticks per cycle. Tick resistance is clearly a property of great value in lowering the number of infected ticks present, and therefore lowering the number of fatalities caused by ECF.

The benefits of breeding for sporozoite resistance are not so straight forward. Comparison of tables 3 and 5 shows that similar behaviour occurs under each model, and equivalent behaviour occurs at higher disease-potentials with the model assuming sporozoite resistance. However, in the example considered in section 4.4.2, the threshold level required for a disease reaction was represented by an effective tick challenge of 2 infected ticks. Comparing figures 9 and 12 shows that this causes the equilibrium level(s) predicted by this model to be at higher values than those predicted by the earlier model. This is because more ticks are now required to bring about a similar disease reaction. For the parasite to survive, it must cause a disease reaction in the host it infects. If no disease reaction occurs, no piroplasms will be produced in the host, and the parasite will not be passed on to future feeding ticks as the life cycle has been broken. Thus, if the parasite is to exist, it needs to be able to adapt to the more hostile environment by infecting more ticks. This illustrates an important warning. Although at similar disease-potentials the number of fatalities amongst a sporozoite resistant herd are likely to be lower than amongst a fully susceptible herd, the corresponding infection level in the tick population is likely to be higher. Great care, therefore, must be taken when introducing fully susceptible stock into areas colonised by ECF resistant cattle.

The final disease control method considered was chemotherapy, where infected cattle are treated with an antitheilerial drug to increase their chances of survival. Comparison of figures 9 and 23 shows that not only can a drug have the effect of reducing fatalities amongst a herd of cattle, but it may also stabilise the behaviour of the level of infection in the tick population, making disease challenge more regular and more predictable. Chemotherapy depends on rapid diagnosis of disease, which is often difficult in the African situation. It is also greatly limited by expense. It could well be, therefore, that the answers to the problems of disease in the African cattle industry lie in the pool of genetic information contained in the cattle population of Africa.

5. SIMULATION MODELS OF TICK AND CATTLE POPULATIONS AND DISEASE TRANSMISSION

"The rule is, jam tommorrow and jam yesterday
– but never jam today."

Lewis Carroll, *Alice Through The Looking-Glass.*

The models described earlier in chapters 2 and 4 illustrate the difficulties involved in extracting analytical solutions from even very simple mathematical models. Modelling using computer simulation provides a way of obtaining specific solutions to models of complex mathematical structure. This chapter discusses the formulation of computer simulation models to investigate East Coast fever and its control. Certain mathematical techniques are discussed, but the models themselves are not presented in mathematical form as analytical results are not sought. Four models were developed: a tick model, an ECF model, a dipping model, and a chemotherapy model. The tick model is a population model which describes the day-to-day changes in the numbers of eggs, larvae, nymphae and adults in relation to site-specific environmental factors. The ECF model simulates the transmission of the East Coast fever infection between such a tick population and a herd of cattle. The number of cattle dying from the disease under different circumstances can be investigated. The dipping model introduces acaricidal tick control strategies to consider the effects of dipping both on the tick population and on the disease, and the chemotherapy model investigates the effects of drug treatment on disease prevalence.

In the following sections, each model is presented in turn, along with the expert knowledge important in their composition. The tick model is described first, as each of the other models are centred around its basic structure.

5.1 THE TICK MODEL

The initial stage in the formulation of any life cycle model is to divide the cycle into a sequence of distinct stages, and to define properties associated with each stage. The life cycle of the *R. appendiculatus* tick was discussed in detail in chapter 3. It was observed that ticks develop through four successive stages: egg, larva, nymph and

adult. For the purposes of modelling, these stages can be further subdivided into periods of development, questing, and feeding which takes place during attachment. These twelve distinct stages are illustrated in figure 1.

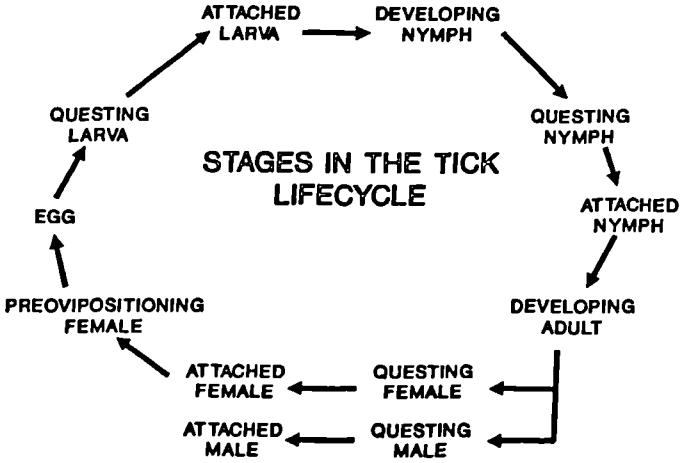

Figure 1. *Important stages in the life cycle of R. appendiculatus*

The life cycle can be translated into a mathematically concise form, using a network representation (Lewis, 1976) as displayed below in figure 2.

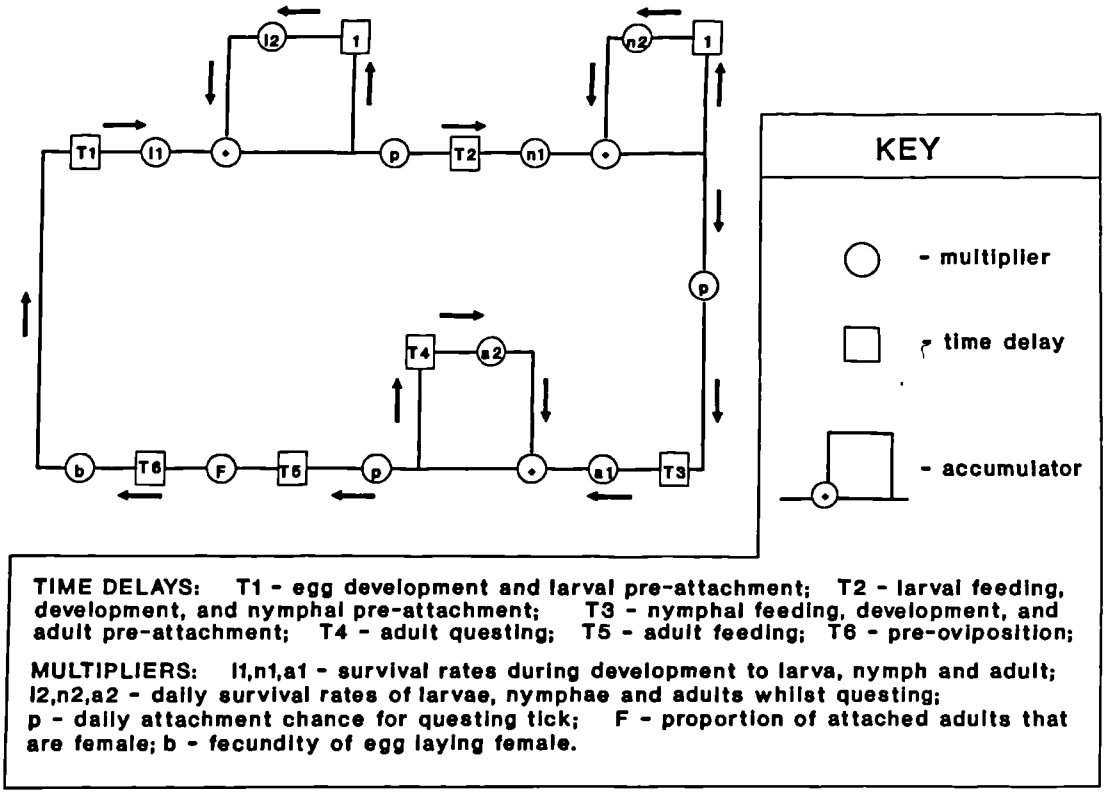

Figure 2. *Network representation of the life cycle of R. appendiculatus*

In this representation, square boxes represent time delays, corresponding to the times spent developing, feeding, or questing. The length of each delay, in days, is given by the parameter in the box. A cohort of ticks arriving at a time delay cannot proceed until the appropriate number of days has elapsed. Circles represent multipliers and contain mortality rates ($l1$, $n1$, $a1$, $l2$, $n2$, $a2$), attachment probabilities (p), the proportion of female to male adult ticks (F), and the number of eggs laid by an egg-laying female (b). When a cohort of ticks arrives at a multiplier, a number of ticks are added or removed from the cohort, depending on the value of the multiplier. Questing is represented by a feedback loop or accumulator. Ticks entering the loop are added to the pool of ticks already questing. An individual tick has a probability p of attaching to a host on a given day. Those ticks that are successful in attaching that day go on to feed, but the remaining ticks encounter a time delay, normally of one day, before they again have an opportunity to attach.

The network description of the life cycle is as follows. A cohort of newly laid eggs commence by entering the time delay box containing the variable $T1$. All the development time delays are variable, and are driven by field temperatures (Branagan, 1978). $T1$ days later the eggs emerge as questing larvae. However, only a proportion, $l1$, of the initial cohort of eggs will survive to commence questing as larvae. Each day, questing larvae have a probability p of attaching to a host, and a survival rate of $l2$. Larvae that find a host spend a length of time, $T2$, feeding then returning to the vegetation to eventually emerge as questing nymphae. Attached larvae have a probability, $n1$, of feeding successfully and surviving to join the pool of questing nymphae. Nymphal ticks have a daily survival rate of $n2$ whilst questing.

Successful questing nymphs are delayed by a time, $T3$, corresponding to the time spent attached to the host, and the time spent moulting into an adult tick. The probability of a nymph surviving to become a questing adult is given by $a1$. The activity of adult ticks is controlled by climate (Short and Norval, 1981), and so an adult tick that is unable to attach to a host on a given day will have to wait for a variable length of time, $T4$, before it can quest again. The probability that a given adult tick survives the $T4$ days of inactivity is given by $a2$.

Attached adult ticks spend $T5$ days feeding and mating whilst on the host. A proportion, F, of these ticks are female and go on to the egg laying stage, which consists of a pre-oviposition time-delay, $T6$, followed by the production of b eggs.

The network representation effectively identifies the minimal set of parameters

required for modelling the tick life cycle. These parameters must be estimated, where possible, from published findings. In the absence of published results, they should at least be based on expert opinion. The model allows certain parameters to remain variable, and allows the user the facility to alter their value. Such parameters may be those that are important in accurately describing the site being studied. Alternatively, these may be parameters which have not been measured in the literature, and the value of these can be investigated by computer experimentation. Once these parameters have been estimated, the network structure can be taken and transformed into programming code, to create a working model of the life cycle. The programming language used was Prospero Pascal, and details of the computer programs are discussed later in chapter 7.

The remainder of this section concentrates on the data available for estimation of these fundamental model parameters, and, where appropriate, looks at methods of incorporating this data into the model.

5.1.1 Time delays

The time delays in the tick life cycle are attributable to times spent developing, such as the nymph to adult moult; pre-questing times, when the tick cuticle hardens following the moult; attachment times, when the tick feeds and adult ticks mate; and the periods of inactivity of adult ticks. For example, the time delay $T2$ is composed of the time spent feeding in the larval stage, the duration of the larva to nymph moult, and the pre-questing time of the nymphal tick. Consider each attribute separately.

(1) Development times

The development stages of ticks have been studied extensively. Branagan (1973a,b) investigated the climatic factors controlling tick development both in the laboratory (Branagan, 1973b) and in the field (Branagan, 1973a). All four development phases: pre-eclosion, larva to nymph moult, nymph to adult moult, and pre-oviposition, were studied. A similar study was later reported by Punyua (1984).

The work of Branagan (1973a,b) provides the basis for a model of tick development driven by climate. The laboratory data provides the detailed information required for constructing a model, and the field data provides a source by which to validate the model.

In laboratory studies, Branagan (1973b) concluded that temperature was the major factor controlling the speed of tick development. When tick populations were kept

at constant temperature, it was observed that higher temperatures increased the development rate whereas at lower temperatures development was retarded. Temperatures below $4°C$ were observed to be lethal to developing ticks. Between $4°C$ and $9°C$ ticks did not develop, and between $9°C$ and $15°C$ development was very slow. Development times were seen to reduce rapidly as the temperature was raised from $18°C$ to $29°C$. Above $29°C$ no apparent reduction in the development times was observed.

Branagan (1973b) presented data on the experimental duration of tick development phases at each of the constant temperature regimes: 15, 18, 21, 25 and $29°C$. The data were presented in the form of the mean, modal, maximum and minimum development times observed for each tick stage at each temperature. Due to the skewed nature of the development times, we can assume the mode to be the most appropriate statistic to consider at each temperature. The modal development times for each of the four stages at each of the temperature regimes are presented below in table 1.

Table 1. Modal development periods for ticks in different stages at various constant temperature regimes. (Branagan, 1973).

	Days to develop at constant temperatures (° C)		
	18	21	25
Development stage:			
Pre-oviposition	13	9	8
Pre-eclosion	76	52	30
Larva to nymph moult	33	18	12
Nymph to adult moult	56	28	17

For each development phase it is possible to fit curves to these data in order to estimate development times at temperatures other than those observed in the experiments. Given that development does not occur below $9°C$, and the rate does not significantly increase at temperatures above $29°C$, it is possible to estimate the development time for ticks at any constant temperature.

The literature presents two possible methods for estimation of development times at constant temperature regimes, and then applying these estimates to the field situation where temperatures fluctuate daily and within each day. The two methods are degree-days (H. Chao-Kuang and H.D. Levine, 1977), and development fractions (Gettinby *et al.*, 1974, 1979).

(a) Degree-days

The degree-day method assumes that the relationship between the development rate, $1/D(T)$, and temperature, T, is linear crossing the x-axis at the threshold temperature for development, $9°C$.

On a specific day, the number of degree-days accumulated is calculated as the days average temperature minus the threshold temperature. Denoting the number of degree-days associated with day i as D_i, then development in a phase is considered complete after n days when the sum of successive degree-days exceeds a certain total. The total degree-days required for development can be calculated from the development rate to temperature graph. Figure 3, for example, shows the fitted line for development rate against temperature for the nymph to adult moult data.

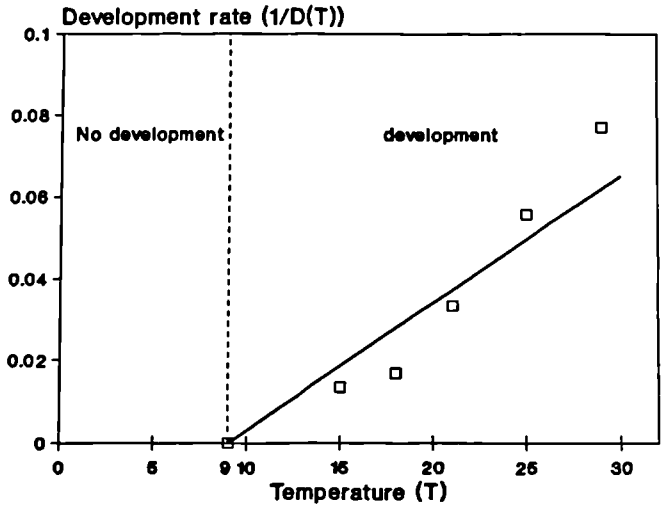

Figure 3. *Relationship between development rate and temperature for the nymph to adult moult phase.*

Using this graph it can be seen that at $20°C$ the development rate for the nymph to adult moult is approximately 0.035 days. This represents a development time of 28.6 days at a constant $20°C$. With a threshold for development of $9°C$, a tick requires $28.6 \times (20 - 9) = 314.6$ degree-days to complete the nymph to adult moult. Thus, for the nymph to adult moult, the rule for completion of development becomes:

If

$$\sum_{i=1}^{n}(D_i) \geq 314.6,$$

Then development complete on day n

where D_i = average temperature (day i) - 9.

To apply the degree-day method to the fluctuating conditions in the field, a measure of each days average temperature is required. This can be estimated as (maximum + minimum temperature)/2.

It should be noted at this stage, however, that the data presented in figure 3 may throw into question the assumption of a linear relationship between development rate and temperature. Using figure 3 to estimate the development time of ticks kept at $15°C$, yields an estimate of 52.4 days for completion of the nymph to adult moult. The observed development time at $15°C$ is 75 days. Estimation inaccuracies arise due to the development rate of these ticks increasing exponentially with temperature. This may affect the accuracy of the method when applied to fluctuating field temperatures.

(b) Development fractions

Data for the development times, D, for ticks in each stage kept at various constant temperatures, T, (Branagan, 1973b) provide relationships of the form:

$$D = f(T).$$

Maximum and minimum daily temperatures can be used to estimate the relationship between temperature, T, and time of day, t $(0 \leq t \leq 1)$. Numerical integration of

$$F = \int_0^1 \frac{1}{f(T)} dt$$

yields an estimate of the fraction of development, F_i, completed by a tick in a given stage on a given day, i. Development within a stage is considered complete when the sum of the development fractions on successive days exceeds one:

If

$$\sum_{i=1}^{n} (F_i) \geq, 1$$

Then development complete on day n.

This approach was satisfactorily accomplished by King *et al.* (1988). Using the data of Branagan (1973b), King *et al.* (1988) suggested that the development time, $D(T)$, reduced exponentially with increasing temperature, T, for each of the four development stages in the tick life cycle. Development times data were, therefore, interpolated using curves of the form $1/(aX+b)$ or $exp\{1/(aX+b)\}$ for temperatures at the lower end of the scale where the development time appears to decrease very sharply with increasing temperature. Linear interpolation was employed at higher temperatures, where development times appeared more stable. A summary of the

development curves fitted relating development time $D(T)$ to temperature T is given below in table 2.

Table 2. Summary of development curves relating constant temperature T to development time $D(T)$. (King *et al.*, 1988).

Development stage	**Temperature**	$D(T)$
Pre-oviposition	T < 15	$exp\{1/(0.00149 + 0.0193T)\}$
	$15 \leq T < 18$	$121 - 6T$
	$18 \leq T < 21$	$37 - 1.33T$
	$21 \leq T < 29$	$24.75 - 0.75T$
Pre-eclosion	$T < 15$	$1/(0.00109T - 0.00738)$
	$15 \leq T < 18$	$280 - 11.33T$
	$18 \leq T < 21$	$220 - 8T$
	$21 \leq T < 29$	$115 - 3T$
Larva to nymph moult	$T < 15$	$1/(0.00236T - 0.01458)$
	$15 \leq T < 18$	$1/(0.00258T - 0.01786)$
	$18 \leq T < 21$	$1/(0.00899T - 0.13333)$
	$21 \leq T < 25$	$47.5 - 1.5T$
	$25 \leq T < 29$	$37 - T$
Nymph to adult moult	$T < 15$	$1/(0.00139T - 0.00750)$
	$15 \leq T < 18$	$1/(0.00111T - 0.00333)$
	$18 \leq T < 21$	$1/(0.00555T - 0.08333)$
	$21 \leq T < 25$	$93.3 - 3T$
	$25 \leq T < 29$	$49.25 - 1.25T$

These curves appear to describe the data satisfactorily. For example, the curves fitted to the modal development times for the nymph to adult moult are illustrated in figure 4.

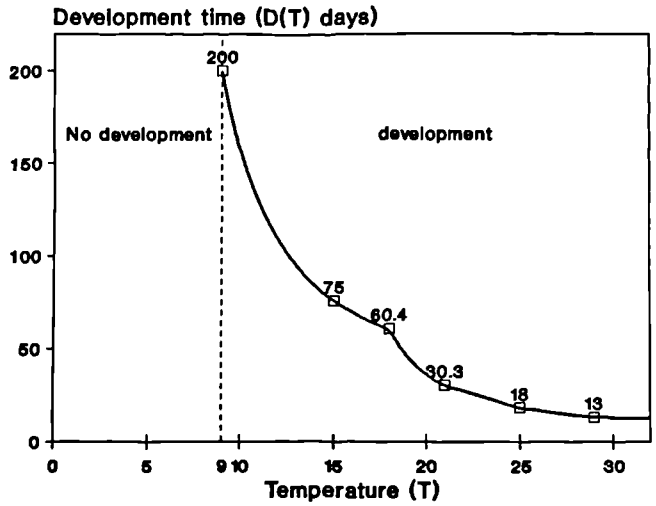

Figure 4. *Relationship between development time and temperature for the nymph to adult moult phase.*

In this figure, the observed development time at each of the five experimental temperatures is presented as a blank square accompanied by the appropriate numerical value. Due to discrepancies in the data, the curves fitted are not perfectly smooth, as each curve is knotted between two observed values. This, however, has the advantage of describing the data accurately which is of greater importance to the model, as an approximation to the true data may disregard information important in characterising the system it describes.

These curves provide the means of estimating the length of tick development periods at any constant temperature regime. In the field, however, temperatures are far from constant. Typical daily temperatures at an African site might range from around $10°C$ at 6.00 a.m., to around $35°C$ at noon.

In their paper, King *et al.* (1988) fitted a mixed sinusoidal function to each days temperature profile. It was assumed that the minimum temperature of the day occurs at around 6 a.m., and the maximum temperature at noon. At near equatorial locations this assumption is likely to hold fairly rigidly throughout the year. Denote the times 06.00, 12.00, and 18.00 hrs. as $t = 0$, $t = 0.5$ and $t = 1$ respectively. Letting the current days minimum and maximum temperatures be denoted as $T1$ and $T2$ respectively, and the subsequent days minimum temperature as $T3$, the daily temperature profile can be approximated by a mixture of sine functions:

$$T = A1 + B1 \sin(2\pi t - \pi/2)$$

where,

$$A1 = \begin{cases} \frac{(T1+T2)}{2}; & 0 \leq t \leq 0.5 \\ \frac{(T2+T3)}{2}; & 0.5 < t \leq 1 \end{cases}$$

and

$$B1 = \begin{cases} \frac{(T2-T1)}{2}; & 0 \leq t \leq 0.5 \\ \frac{(T2-T3)}{2}; & 0.5 < t \leq 1 \end{cases}$$

The days development fraction, F_i, can then be given by:

$$F_i = \int_{t1}^{0.5} \frac{1}{D(T)} dt + \int_{0.5}^{t2} \frac{1}{D(T)} dt$$

where the times $t1$ and $t2$ represent the lower and upper endpoints of the period of the day when the temperature exceeds the threshold for development, $9°C$.

This method has two clear advantages over the degree-day method. Firstly, development fractions take more account of the true development time to temperature relationship by more elaborate curve fitting, and secondly, development fractions take more account of the way temperatures fluctuate during a given day.

(c) Comparison of predictions from degree-day and development fractions methods.

Between 1967 and 1968, Branagan (1973a) performed an extensive experiment at Muguga in Kenya, in an attempt to quantify the effect of temperature on development times of ticks under field conditions. In each month of the test period, batches of new eggs or freshly engorged larvae, nymphae or adults were deposited in transparent plastic tubes in the vegetation. Observations on the development of ticks in each tube were made daily, and the range of development times for tick batches deposited during each month was presented. King *et al.* (1988) estimated modal development times from these ranges. These observed development times provide a way to compare the two proposed prediction methods.

Each model was executed using climatic data from Muguga in 1968. Temperature data were obtained in the form of maximum and minimum temperatures for each day of the year. For each method, development times for each phase, pre-oviposition, pre-eclosion, larva to nymph moult and nymph to adult moult, were predicted. Tick batches were assumed to be deposited on the first day of each month. The resulting development time predictions under each method for ticks deposited each month are displayed in table 3.

Table 3. Predicted and observed development times for ticks deposited each month at Muguga, Kenya (1968).

	Pre-oviposition			Pre-eclosion			larva-nymph			nymph-adult		
	obs	dd	df	obs	dd	df	obs	dd	df	obs	dd	df
Jan :	15	22	13	92	70	74	33	22	23	55	40	40
Feb :	14	19	14	91	75	80	34	19	26	48	41	45
Mar :	14	25	17	96	86	88	35	25	31	52	47	53
Apr :	23	25	18	108	100	99	37	25	34	58	50	59
May :	30	28	21	102	126	114	36	28	41	58	59	71
Jun :	34	35	26	105	126	117	42	35	48	65	79	83
Jul :	42	46	34	98	116	107	43	46	55	64	82	78
Aug :	21	41	32	99	100	97	36	41	45	56	67	66
Sep :	15	30	20	99	88	88	27	30	33	46	51	52
Oct :	18	22	16	86	83	85	26	22	27	49	45	52
Nov :	17	27	20	84	84	82	29	27	36	48	51	56
Dec :	14	25	17	80	75	76	25	25	30	43	47	46

obs – observed value, dd – degree-day prediction,

df – development fraction prediction.

The observed development times and the predicted times using the development fractions method were taken from King *et al.* (1988). The predicted development times for the degree-day method were calculated by using (maximum + minimum temperature)/2 as an estimate of each days average temperature. The number of degree-days required for complete development in each phase was taken to be 108.0 for pre-oviposition, 550.0 for pre-eclosion, 161.8 for the larva to nymph moult, and 314.6 for the nymph to adult moult.

Inspection of the results shows that both methods perform fairly well, although a number of bad estimates do occur – such as for the nymph to adult moult in July. The development fraction method appears to provide more accurate estimates in well over 50% of the total predictions. However, the degree-day method predictions are extremely good considering the simplicity of the model.

Because the development fractions method appears to perform slightly better, and because the method appears to take more account of the physical process, it is this method that is used in the tick model. It should be noted that the development fractions method assumes all members of a cohort of ticks entering a development phase on the same day will complete development in the same period of time. This has many programming advantages, as treating large numbers of ticks as cohorts conserves both computer time and memory, allowing large tick populations to be efficiently simulated. However, the assumption will not always hold. Development times within batches of ticks can vary considerably, especially at lower temperatures. This has consequences for the model, as non-constant developments will smooth out the profiles of ticks in each stage throughout the year. At present, large numbers of eggs and larvae developing at the same time cause large jumps in the egg and larval frequency curves. This may effect the predicted spread of disease.

The experimental results of Branagan (1973b) provide the mean, mode, maximum, minimum and standard deviation of development times of ticks in pre-oviposition, pre-eclosion, larva to nymph moult, and nymph to adult moult phases. In the absence of the observed probability distributions, it is possible that this data could be used to estimate the probability distribution for the development time of ticks in each phase.

Assuming that theoretical probability distributions could be estimated for the constant temperature regimes reported by Branagan (1973b), then it should be possible to infer the probability distributions of other constant temperatures by interpolation over a surface. In a similar way to the development fractions method it should then be possible to make some inferences about the range of probable development times of ticks under fluctuating temperatures. Section (d), below, highlights the difficulties in estimating the distribution of tick development times from very limited data, and illustrates the problems associated with such a method.

(d) The distribution of tick development times

Developments at constant temperature

At a constant temperature T, the time taken by a tick to develop through a specific phase, $D(T)$, is given by

$$D(T) = \mu_T + \epsilon_T,$$

where μ_T is the mean development time of ticks at temperature T, and ϵ_T is the error associated with that estimate such that $E[\epsilon_T] = 0$ and $\mathrm{Var}[\epsilon_T] \approx \sigma_T^2$. σ_T^2 is the

variance of the development times at temperature T.

Thus $E[D(T)] = \mu_T$, and $\mathrm{Var}[D(T)] = \sigma_T^2$, which can both be estimated from the experimental results of Branagan (1973b) for a number of different values of T.

Development fractions at constant temperature

Letting F_T be the development fraction associated with constant temperature T, then

$$F_T = \frac{1}{D(T)} = \frac{1}{(\mu_T + \epsilon_T)}$$
$$= (\frac{1}{\mu_T})(1 + \frac{\epsilon_T}{\mu_T})^{-1}.$$

By Taylors theorem this becomes

$$= (\frac{1}{\mu_T})(1 - \frac{\epsilon_T}{\mu_T} + \frac{\epsilon_T^2}{\mu_T^2} - \frac{\epsilon_T^3}{\mu_T^3} + \ldots)$$

Second order approximations to the mean and variance of the development fraction at constant temperature T are

$$E[F_T] = E[(\frac{1}{\mu_T})(1 - \frac{\epsilon_T}{\mu_T} + \frac{\epsilon_T^2}{\mu_T^2} - \frac{\epsilon_T^3}{\mu_T^3} + \ldots)]$$
$$\simeq E[(\frac{1}{\mu_T})(1 - \frac{\epsilon_T}{\mu_T} + \frac{\epsilon_T^2}{\mu_T^2})]$$
$$= (\frac{1}{\mu_T})(1 + \frac{\sigma_T^2}{\mu_T^2})$$
$$Var[F_T] = E[F_T^2] - E^2[F_T]$$
$$\simeq E[(\frac{1}{\mu_T^2})(1 - \frac{2\epsilon_T}{\mu_T} + \frac{3\epsilon_T^2}{\mu_T^2} - \ldots)]$$
$$- (\frac{1}{\mu_T^2})(1 + \frac{\sigma_T^2}{\mu_T^2})^2$$
$$\simeq (\frac{1}{\mu_T^2})(1 + \frac{3\sigma_T^2}{\mu_T^2}) - (\frac{1}{\mu_T^2})(1 + \frac{\sigma_T^2}{\mu_T^2})^2$$
$$= (\frac{1}{\mu_T^2})(\frac{\sigma_T^2}{\mu_T^2} - \frac{\sigma_T^4}{\mu_T^4})$$

At each temperature, the mean development time is seen to be much greater than the variance of development times. Hence, disregarding terms of order $(\epsilon_T/\mu_T)^3$ and above, should not result in a great loss of accuracy in these estimates. However, given the mean and variance of F_T, it still remains to find the probability distribution of F_T if we wish to randomly generate development fractions. Remembering that the development fraction is the inverse of the development time, development fractions can be randomly generated if we know the distribution of the development time $D(T)$.

Distribution of the sum of development fractions

Development was defined complete when the sum of each days development fractions first exceeds one. Letting S_n be the sum of development fractions for the first n days of development, then

$$S_n = \sum_{i=1}^{n} \{F_{Ti}\}$$

where F_{Ti} is the development fraction associated with day i, at constant temperature T. As T is constant, the F_{Ti} are identically distributed having the same mean and variance as estimated earlier. It would also appear fair to assume that for a given tick the development fractions for each day will be independent of each other.

By the central limit theorem, as S_n is the sum of n independent identically distributed random variables, S_n will tend towards a Normal distribution with mean and variance:

$$\begin{aligned} E[S_n] = E[\sum_{i=1}^{n} \{F_{Ti}\}] &= \sum_{i=1}^{n} \{E[F_{Ti}]\} \\ &= n(\frac{1}{\mu_T})(1 + \frac{\sigma_T^2}{\mu_T^2}) \\ Var[S_n] = Var[\sum_{i=1}^{n} \{F_{Ti}\}] &= \sum_{i=1}^{n} \{Var[F_{Ti}]\} \\ &= n(\frac{1}{\mu_T^2})(\frac{\sigma_T^2}{\mu_T^2} - \frac{\sigma_T^4}{\mu_T^4}) \end{aligned}$$

Thus, $S_n \sim N(n(\frac{1}{\mu_T})(1 + \frac{\sigma_T^2}{\mu_T^2}), n(\frac{1}{\mu_T^2})(\frac{\sigma_T^2}{\mu_T^2} - \frac{\sigma_T^4}{\mu_T^4}))$

Distribution of the number of days to develop

Denote the number of days required for a tick to complete development as N. The probability that a tick has developed by day N is equal to the probability that the sum of development fractions is greater than one by day N. That is

$$P(N \leq n) = P(S_n \geq 1)$$

Thus,

$$\begin{aligned} P(N = n) &= P(N \leq n) - P(N \leq n-1) \\ &= P(S_n \geq 1) - P(S_{n-1} \geq 1) \\ &= \{1 - P(S_n < 1)\} - \{1 - P(S_{n-1} < 1)\} \\ &= P(S_{n-1} < 1) - P(S_n < 1) \end{aligned}$$

Standardising S_{n-1} and S_n this becomes

$$= P(Z < \frac{1-(n-1)(1/\mu_T)(1+\sigma_T^2/\mu_T^2)}{\sqrt{(n-1)(1/\mu_{T^2})(\sigma_T^2/\mu_T^2-\sigma_T^4/\mu_T^4)}})$$
$$- P(Z < \frac{1-n(1/\mu_T)(1+\sigma_T^2/\mu_T^2)}{\sqrt{n(1/\mu_T^2)(\sigma_T^2/\mu_T^2-\sigma_T^4/\mu_T^4)}})$$

where $Z \sim N(0,1)$.

Thus, the probabilities of the value of N, the time to develop, can be estimated from standard Normal tables.

Results

Consider the data on development times presented in the experiments of Branagan (1973b) for the larva to nymph moult phase. The range, mean, mode and standard deviation of development times observed for batches of 2749 to 2840 ticks kept under constant temperature regimes of $18°C$, $21°C$ and $25°C$ are presented below in table 4.

Table 4. Distribution of development times of ticks moulting from larva to nymph. (Branagan, 1973b).

	Development (days)				
Temperature($°C$)	Minimum	Maximum	Mode	Mean	Standard deviation
18	31	41	33	34.30	2.117
21	16	22	18	18.12	1.066
25	10	15	12	11.89	1.049

The data suggest that the distribution of development times of ticks at constant temperature is skewed.

Using the above theory, the distribution of the larva to nymph development time can be predicted and compared to the observed data. Consider first development at $25°C$.

At $25°C$ the sum of development fractions, $S_n(25)$ is assumed to follow a $N(0.0848n, (0.00739)^2n)$ distribution. Thus, $P(S_n < 1) = \Phi((1-0.0848n)/0.00739\sqrt{n})$.

$P(S_n < 1)$ is calculated as 1, 1, 0.9971, 0.2530, 0.000066 and 0 for n taking values of 9, 10, 11, 12, 13 and 14 days respectively. Hence, $P(N = n)$ is calculated as

0, 0.0029, 0.7441, 0.2529, 0.000066 and 0 for n equal to 10, 11, 12, 13, 14 and 15 days respectively.

This expected distribution of development times is certainly skewed, although its range is smaller than that observed. The expected range is from 11 days to 14 days, whereas the observed development times vary from 10 days to 15 days. This inadequacy is further highlighted by the results of the expected development times at $18°C$.

At $18°C$ the sum of development fractions, $S_n(18)$ is assumed to follow a Normal distribution with mean and variance $0.02927n$ and $(0.0017960)^2n$ respectively. This gives rise to the following probability density function for N, the number of days to develop.

n	≤ 32	33	34	35	36	≥ 37
$P(N=n)$	0	0.0046	0.3169	0.6715	0.0111	0

The expected range in development times is from 33 to 36 days, whereas the observed range was from 31 to 41 days.

In both cases, the expected range in development times is smaller than that observed. The most likely reason for this is that the assumption that development fractions from day to day are independent is not valid. A tick developing slowly on one day may be morphologically different to other ticks, and so may be likely to develop slowly on other days. Without allowing for this dependence structure, the expected variation in development times is likely to be smaller than that observed, which is consistent with the results generated. In the absence of hard data it is difficult to establish the true distribution of $D(T)$.

Without a well fitting theoretical probability distribution, or an accurate observed distribution, it is difficult to progress further with this method. As described earlier, if obtained, such a method would be difficult to implement efficiently into a working model due to limited memory and user-time (see chapter 7). In the absence of a suitable alternative, the model employs deterministic development time prediction.

(2) Pre-questing times

The pre-questing time is the minimum time that a newly emerged larva, nymph or adult spends in the vegetation preparing to commence questing. Minimum durations proposed by Branagan (1973b) were 13 days for unattached larvae, 17 days for unattached nymphae, and 21 days for unattached adults. These are treated as constant time delays as it is uncertain what, if any, factors control the length of these periods.

(3) Attachment times

The length of time that a tick spends attached to a host is fairly constant within each stage, larva, nymph, adult male and adult female. For attached larvae and nymphae, Branagan (1973b) estimates feeding periods of 5 and 6 days respectively. For attached male and female ticks, Gettinby (1987) quotes estimated durations of 18 and 9 days respectively. These estimates were obtained from personal communication with Dr. R. M. Newson.

(4) Adult activity periods

The seasonal occurrence of *R. appendiculatus* has been well documented at a number of different locations. MacLeod and Colbo (1976) and MacLeod *et al.* (1977) report observations on ticks in Zambia; Yeomann (1966), Tatchell and Easton (1986), and McCulloch *et al.* (1968) studied ticks in Tanzania; and Branagan (1973a,b), Rechav (1982) and Short and Norval (1981) report the seasonal occurrence of ticks at sites in Kenya, South Africa and Zimbabwe respectively. This is not an exhaustive list. Studies of many other locations have also been reported.

Seasonality appears to become most marked at locations furthest away from the equator. Equatorial locations do not experience large climatic changes from month to month, and so tick populations remain fairly constant throughout the year.

The life cycles of some species of Ioxdid ticks, such as *R. appendiculatus*, are interrupted by periods of diapause induced by seasonal climatic change (Balashov, 1968). Diapause occurs either as a pause in the development of fed ticks, or as a period of inactivity in unfed ticks. Such inactivity in unfed ticks is known as quiescence.

Based on his extensive laboratory studies, Branagan (1973a) observed no evidence to suggest that periods of diapause occur during the development of the engorged tick stages. Short and Norval (1980) showed, however, that unfed adults may enter a period of quiescence before feeding. In a later study on the seasonality of ticks at eight different African sites, Short and Norval (1981) inferred that daylength, rainfall and temperature are the major climatic factors responsible for controlling quiescence in unfed adult ticks. They also suggested that it is quiescence in adult ticks that is solely responsible for the observed seasonality in tick populations.

The precise conditions suggested by Short and Norval (1981) for monthly activity of unfed adults are as follows:

If rainfall per month > 10mm

and mean monthly minimum temperature > 15^oC

and (mean monthly maximum temperature < 30^oC

or > 30^oC and monthly rainfall > $20mm$)

and hours of daylight > 11hrs

Then adult tick active

Otherwise adult tick inactive.

By reviewing the climatic data of each month, a decision can be made as to whether unfed adult ticks are active or quiescent. In the absence of daylength data for most sites, only the rules for rainfall and temperature are used by the model to determine periods of inactivity.

The seasonal patterns of ticks observed in simulations can be compared to those presented in the literature to validate the model (see chapter 8).

5.1.2 Survival rates

Many studies on tick survival have been reported. In Kenya, Branagan (1973a) provided the first quantitative data on the survival of *R. appendiculatus* ticks under quasi-natural conditions at two sites, Muguga and Kedong. More recently, also in Kenya, Newson *et al.* (1984) produced lifetables for tick survival based on the observed survival of ticks kept in paddocks at Muguga.

Tukahirwa (1976) investigated the longevity of ticks under laboratory conditions. Different combinations of relative humidity and temperature were seen to affect survival. His study suggested that eggs and larvae were especially sensitive to low humidity, and that as temperatures increased longevity decreased. Tukahirwa found that in the micro-environment of a long grass habitat, temperature and humidity fluctuations were much less pronounced than in a similar short grass habitat, suggesting that eggs and larvae are especially vulnerable in short grass habitats. Tukahirwa also performed a number of experiments on tick survival under changing temperature regimes. No simple temperature dependent relationship was established.

More recently, Pegram and Banda (in press) investigated the survival of ticks under quasi-natural conditions in Zambia. Over a two year period, ticks of each stage were placed in pastures at times coinciding with their natural life cycle. Data was recorded in the form of 95% mortality periods. Short (1984) also performed field experiments on

the survival of ticks in Harare, Zimbabwe. Between 1980 and 1981 batches of eggs or unfed ticks were deposited in both short and long grass pastures in the three distinct climatic seasons: warm wet (February), cool dry (June), and hot dry (September). The survival of all tick stages was seen to be not significantly affected by season in the long grass habitat. However, in short grass the survival of eggs and larvae was significantly reduced during the hot dry season.

Daily survival probabilities estimated from the 95% survival periods quoted by Pegram and Banda (in press) are given below in table 5.

Table 5. Estimated daily survival probabilities of ticks in various stages of development.

Tick stage	**Daily survival probability**
Pre-eclosion development	0.988
Larva to nymph moult	0.997
Nymph to adult moult	0.995
Pre-oviposition development	1.000
Questing larva	0.950
Questing nymph	0.975
Questing adult	0.991

These survival rates appeared to produce the closest to a steady state tick population in most simulation experiments when the fecundity of ticks was 4000.

The daily survival probabilities of eggs and larvae in dry seasons in short grass habitats were estimated as 0.700 and 0.841 respectively, from the work of Short (1984). A month was defined dry when the monthly rainfall total fell below 5mm (Dr. A. Norval, personal communication).

Norval (personal communication) suggested that the daily survival rates of unfed adult ticks increase, perhaps as much as tenfold, during periods of quiescence. This is due to the tick remaining inactive in a suitable niche where the micro-environmental conditions are stable and favourable. In the model, daily survivals of unfed adult ticks are increased to 0.998 and 0.997 for females and males respectively during periods of quiescence, estimated from the results of Newson *et al.* (1984).

Fivaz (1984) investigated the feeding stages of the tick and estimated the percent-

age of attached larval, nymphal and adult ticks that feed successfully to be 20%, 35% and 20% respectively. If a tick is unable to feed successfully, it is unlikely to be capable of attaching to another host, and so these feeding rates can be regarded as survival rates.

The use of random numbers in model decisions

Random numbers can be used to decide whether or not a tick survives a particular day, based on the daily survival probabilities presented above. Most modern programming languages are supplied with library routines including random number generators. Such a generator produces a stream of pseudo random numbers. These numbers are not truly random as each number is calculated from the value of the last. However, most random number generators are sophisticated enough to provide a sequence of numbers that certainly appears random. Commonly used algorithms for generation of Uniform random numbers are discussed by Ripley (1988).

Thus, letting the daily survival rate of a certain tick be P, a typical decision can be made by simulating a Bernoulli trial as follows:

1. Generate a Uniform random variate, U, in the interval [0,1)
2. *If* $U < P$ *then* the tick survives that day

   Otherwise the tick dies.

More generally, for n ticks in a particular stage with daily survival rate P, the binomial distribution can be used as the sampling distribution to simulate the number of ticks, X, that go forward:

1. Let $X = 0$
2. Generate a Uniform random variate, U, in the interval [0,1)
3. *If* $U < P$ *then* $X = X + 1$
4. Repeat steps 2 and 3 n times
5. Return X.

The speed of the simulation model greatly depends on the efficiency of the programming. Procedures and functions should be executed as little as possible. Performing one Bernoulli trial for each tick in each stage will be slow and inefficient. However, when n is large and P is small, the Poisson approximation to the binomial distribution can be used. An algorithm for the generation of random variables from a Poisson process of rate nP is as follows (multiplicative method):

1. Let $X = -1$, $M = 1$
2. Generate a Uniform random variate, U, in the interval [0,1)
3. Let $M = M \times U$ and $X = X + 1$
4. If $M > e^{-nP}$ then go to step 2
5. Return X

Alternatively, when n is large and nP or $n(1-P) > 5$, the Normal approximation to the binomial distribution can be used. The polar-marsaglia algorithm for the generation of random variables from a Normal distribution with mean nP and variance $nP(1-P)$ is as follows:

1. Generate Uniform[-1,1) random variates $U1$ and $U2$
2. Let $W = U1^2 + U2^2$
3. If $W > 1$ then go to step 1
4. Let $C = \sqrt{-2W^{-1}lnW} \times U1$
5. Return $X = C\sqrt{nP(1-P)} + nP$

Derivations of the algorithms for Poisson and Normal random variable generation are based on the theoretical properties of sums and products of independent random variables. These can be found in Devroye, L. (1986) and Ripley, B.D. (1987) respectively.

5.1.3 Attachment rates

No accurate measurements of the attachment rates of ticks in the field have been published. An attachment probability of 0.04 is chosen as default, but can be adjusted by the user. The effect of changing this parameter is discussed with other results in chapter 8.

5.1.4 Ratio of sexes of adult ticks

The ratio of female to male ticks has been observed to follow the usual Mendelian law for sexual reproduction, being 1:1 (Branagan, 1973b). This makes the probability of an individual adult tick being female, F, to be 0.5.

5.1.5 Fecundity

Engorged female ticks are seen to produce between 4000 and 6000 eggs. The fecundity of ticks is chosen to be 4000, but can be adjusted to a more appropriate value by the user.

5.2 THE ECF MODEL

The model for ECF follows the rules composing the tick model along with a number of additional rules concerned with modelling the disease and the cattle population. The tick model assumes a constant herd, whereas in this model a herd is defined where natural births and deaths can occur on a random basis. The growth of the parasite within infected cattle is modelled using similar rules to those described in chapter 4. Questing ticks attach randomly to herd members, and may become infected depending on the disease status of their host. Ticks that are infected contain a random quantity of the parasite, which is transferred to cattle during the next blood meal. This section concentrates on the model for the herd, and for the disease dynamics.

5.2.1 Modelling the herd

The state vector $\underline{x}_y$ describes the age structure of the herd in year y. The elements of this state vector consist of the number of cattle in each age group: 0–1 yrs, 1–2 yrs, ..., 9–10 yrs. Cattle are assumed to be removed from the herd if they exceed the age of 10 yrs. Along with each age group is a yearly natural mortality rate p_i, and a yearly calving rate f_i $(i = 0, 1, \ldots, 9)$. A deterministic model for the change in herd structure from year y to year $y+1$ would use the recurrence equation

$$\underline{x}_{y+1} = \underline{L}\underline{x}_y$$

where $\underline{L}$ is a Leslie transition matrix (Leslie, 1945) containing the annual mortality and calving rates of cattle in each of the age groupings:

$$\underline{L} = \begin{bmatrix} f_0 & f_1 & f_2 & \cdots & f_9 \\ p_0 & & & & \\ & p_1 & & 0 & \\ & & p_2 & & \\ & 0 & \cdots & & \\ & & & p_8 & 0 \end{bmatrix}$$

Theory presented on such matrix models (Leslie, 1945) shows that the dominant eigenvalue of the matrix $\underline{L}$ is equivalent to the growth rate of the population it describes. This provides a numerical check for the calving and natural mortality rates before commencing a simulation. The herd growth rate must be at least one, or the herd would eventually die out even in the absence of ECF.

The deterministic model provides a description of the expected behaviour of the herd in the absence of disease. However, a stochastic model is more appropriate as

the tick population is modelled stochastically. It is also appropriate to adjust the herd parameters to allow for day-to-day changes in the herd, as the tick population is modelled using a daily time-step. Transforming the yearly mortality rates into daily mortality rates, an animal in age group i–$i+1$ yrs will have a daily survival rate of $d_i = (1 - p_i)^{1/365}$. On a given day, the decision as to whether or not a specific animal dies can be made by using Uniform random numbers. Decisions are made in an identical way to the method described earlier for tick survivals in section 5.1.2.

Births occur at random times throughout each year. A female member of the herd in age group i–$i+1$ yrs will be expected to give birth to f_i offspring once during a year, the timing of the birth being equally likely to occur on any day of the year. Assuming equal proportions of male and female animals, a selected herd member has a probability of 0.5 of being female. In this manner, random day-to-day changes in the herd are taken into account.

5.2.2 Tick attachments

As discussed in the previous section, there are no published data giving estimates of the attachment rate of ticks. This parameter is under the control of the user. However, those ticks that do attach each day are assigned randomly to specific members of the herd. Each herd member is equally likely to become the host for a specific tick. In practice, however, it is unknown whether or not this assumption reflects the true field situation. Younger animals, due to their naivety, might not avoid large clusters of questing ticks and so become heavily burdened. Older, more wary animals, may positively avoid such areas of high tick density, and thus avoid heavy infestation. In the absence of data concerning the relationship between host age and tick burden, the assumption of Uniform tick attachments appears reasonable.

5.2.3 The disease

Much of the model for the disease dynamics has been presented in chapter 4. For simplicity, consider the disease within the tick population and the herd separately.

(a) Infection within the tick population

From the experiments of Purnell *et al.* (1974), ticks feeding on cattle with a parasitaemia exceeding 1% appear to have a probability of 0.4 of subsequently becoming infected with the parasite. Parasitaemia was defined earlier to be the percentage of red blood cells that were infected with the parasite per 1000 red cells examined. Ticks feeding on cattle with lower levels of parasitaemia do not become infected. A measure

of the size of infection received by feeding ticks can be obtained by dissection of the ticks salivary glands. The number of acini cells containing the parasite in sporozoite form reflects the size of infection the tick is capable of transmitting on its next blood meal. From the data published by Purnell *et al.* (1974), the number of infected acini contained in each parasitised tick appeared to follow a Normal$(6.2, 1.6^2)$ distribution. Thus the algorithm for randomly assigning infection to ticks feeding on infective cattle consists of two parts: performing a Bernoulli trial to establish whether or not the tick is to be infected; then, if infected, sampling from a Normal distribution to assign an appropriate amount of infection.

(b) Infection within the herd

In areas where ECF is prevalent, cattle can be assigned to five distinct groups reflecting their status with respect to the disease. These five distinct disease status groups are: *healthy*, *infected*, *infective*, *immune* and *dead*. Cattle can move between specific groups, as the disease spreads amongst the herd. A *healthy* cow that is bitten by an infected tick immediately becomes *infected* with the parasite. Thirteen days later, piroplasms begin to appear in the bloodstream, and when the parasitaemia reaches 1% the animal becomes *infective* to feeding ticks. A number of days later the animal either *dies* or recovers and returns to the *healthy* group. Alternatively, a recovered animal could become *immune* to the disease. Immune cattle may or may not be infective to feeding ticks. The passage of disease amongst a population of cattle can, therefore, be represented in compartmental form as shown in figure 5.

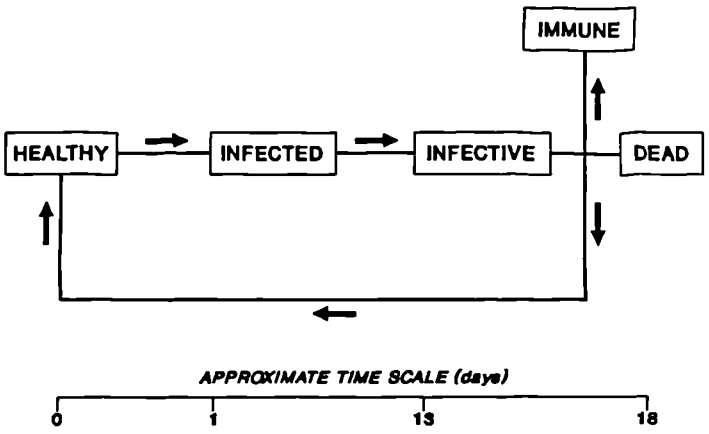

Figure 5. *Compartmental representation of the disease in cattle.*

The development of the parasite within the bovine host is modelled using rules P1–P12 contained in section 4.1 of chapter 4, and rules P6, P7 and S1–S7 of section

4.3, with the following alterations.

(i) Rule S6, *Infectious period function*

In this rule, the infectious period of a recovering cow was assumed to be 5 days, due to lack of data. This infectious period has been adjusted to 20 days in line with expert opinion. The effects of changing this parameter are discussed with the model results in chapter 8.

(ii) Rule S5, *Superinfection rule*

In the previous model, the superinfection rule was as follows:

The disease reaction following superinfection is calculated by adding the proportion of the new dose of sporozoites that infect unparasitised lymphocytes to the level of schizonts estimated for that day. Backward extrapolating the schizont growth curve to day 0 will yield the number of sporozoites required to be transmitted on day 0 to bring about this new level of infection. From this new dose specific disease responses, such as death or recovery, are predicted.

This rule appeared to reduce the effects of the parasite too severely, as few animals were seen to die from ECF in most simulations. The rule was abandoned in favour of the following rule:

S5. If an infected animal receives a further infection then only a proportion of this new infection, equal to the proportion of lymphocytes that are uninfected that day, is assumed active. This fraction of the new dose is added to the initial infective dose to calculate specific disease responses such as death or recovery.

(iii) Rule P10, *Probability of death*

From the titration experiments of Dolan *et al.* (1984), a probability density function can be constructed for the probability of death over a range of infective doses. The data presented (Dolan *et al.*, 1984) yields the following probabilities of death, at certain doses, presented in table 6 below.

Table 6. Predicted probabilities of death at various sporozoite doses (Dolan *et al.*, 1984)

Infected acinus dose	Probability of death
40	8/10
40/32	2/9
40/64	1/9
40/128	1/10
40/256	0/9

Linear interpolation can be employed to estimate probabilities at doses not listed below 40 infected acini. Above this dose, cattle are assumed to die from ECF with probability 1. The sporozoite dose can be simply calculated from the number of infected acini by assuming each infected acinus contains 17.5×10^4 sporozoites (rule S2). The decision as to whether an animal dies after receiving a certain dose of sporozoites can be made by generating Uniform random numbers to perform Bernoulli trials with the appropriate probability of death.

5.3 THE DIPPING MODEL

The dipping model contains the ECF model along with a number rules describing the treatment of cattle with acaricides. Ticks attached to cattle being dipped, or that have been dipped recently, will have a reduced survival chance due to the presence of the chemical. The following rules specify a particular dipping strategy:

T1. The number of days between dips, the dipping interval, is D.

T2. The probability of the acaricide killing an attached tick, the acaricidal efficacy, is p.

T3. The number of days the chemical remains active on the coat of treated cattle after the day of dipping, the residual effect, is d.

Therefore on a specific day, n, the acaricide will be active if

$$\text{Remainder } (n/D) \leq d$$

If the chemical is active then the chance of a freshly attached tick dying is p, otherwise this probability is zero.

The dipping interval of tick control strategies employed in most African countries is once or twice a month. Dipping is generally limited by the cost it entails. Acaricidal

efficacy and residual effect depend on the choice of chemical, but normally acaricides do not remain active for much longer than a week following dipping, and are unlikely to destroy all attached ticks.

5.4 THE CHEMOTHERAPY MODEL

As mentioned earlier in chapter 4, a small amount of data from clinical trials performed by Wellcome research laboratories was made available to investigate and quantify the effects of drug action on the disease response of treated cattle. This data was kindly offered by Dr. N. McHardy at Cooper Pitmann-Moore Animal Health Ltd., Berkhamsted, who was responsible for many of the trials.

The Wellcome clinical trials data suggested that there are a number of factors that have an influence on the success of any antitheilerial drug. Of these, there appeared to be five major factors that strongly attributed to the success or failure of a drug during a clinical trial. These were, firstly, the source of the parasite used, either from parasite stabilates extracted from infected ticks at Kiambu, Muguga or other sites, or from natural tick challenge at various sites. Secondly, different drugs were seen to behave differently. Most data concerned the use of four drugs – Menoctone, Halofuginone, Parvaquone and Buparvaqoune. Finally, the quantity of drug administered, whether infected cattle received the drug in a single or a double treatment, and the timing of the commencement of treatment were all seen to influence the resulting disease reaction.

In most trials the time of treatment was similar: three or four days after the appearance of schizonts and a febrile response (TS3, or TS4) for a single treatment, or on the fifth and seventh day of schizont detection (S5 and S7) if two doses were administered.

In most experiments, cattle were given a potentially lethal dose of sporozoites, and in the majority of trials all control cattle died. The effect of any drug could, therefore, be seen both in the increased survival probability of treated cattle, and in the more prolonged death of those cattle that were treated but did not survive. The relationship between drug regime and day of death in treated cattle that die is important in calculating the increased length of time these cattle are infective to feeding ticks.

Drug action also appeared to have an effect on the piroplasm levels of recovering cattle. Many recovering cattle were seen to have only a slight parasitaemia. This observation is supported by Dolan *et al.* (1984) who state that in some infected cattle that were treated, only very low levels of parasitaemia were observed. If cattle are

assumed to be infectious to ticks only when parasitaemia reaches at least 1% (Rule P4, Purnell *et al.*, 1974), then for each drug regime the probability that a recovering treated animal becomes infectious to feeding ticks can be established.

Thus, the clinical trials data yields estimates of three important chemotherapy responses: the probability of recovery following treatment, the timing of death for treated animals that die and the probability of parasitaemia above 1% for treated animals that recover. These parameters can be estimated for various combinations of stabilate, drug, number of doses, and size of dose. It is then possible to adjust the ECF model to take account of drug action on the parasite by employing the following additional rules:

T1. Cattle that would die if left untreated have a probability f of death following treatment.

T2. Those animals that would normally die on day x without treatment, will die on day dx if the treatment is unsuccessful.

T3. Those animals that recover following treatment will be infective to feeding ticks with a probability i.

By performing Bernoulli trials with Uniform random numbers these rules can be administered.

The clinical trials data was sparse, but a number of parameter estimates were made for common drug regimes on cattle infected with the *T. parva* (Muguga) stabilate. These estimates are given below in table 7. Only the results of drug action using the Muguga stabilate were used for consistency, as this stabilate was also employed in much of the experimental work that comprises other rules in the ECF model.

Table 7. Estimates of the action of various chemotherapy regimes on the resulting disease reaction in infected cattle.

Regime	f	d	i
Parvaquone, 1 x 10mg/kg	0.486	2.063	0.688
Parvaquone, 1 x 20mg/kg*	0.033	2.863	0.286
Buparvaquone, 1 x 1.25mg/kg	0.250	1.305	0.000 (!)
Buparvaquone, 1 x 2.50mg/kg*	0.208	2.472	0.552

* manufacturers recommended dosage.

It should be noted that the infective probability, i, for Buparvaquone at 1 x 1.25mg/kg is estimated to be zero, and is lower than the estimate obtained for Buparvaquone at a higher dose. Only a small quantity of data was available to make this estimate, and it should be treated with caution.

The effect of using Parvaquone and Buparvaquone in a field situation are investigated, along with other computer investigations, in chapter 8.

5.5 CONCLUSIONS

This chapter has demonstrated that it is possible to pull together enough detailed information about a very complex process, and to produce a sufficiently complicated model to mimic its behaviour under different conditions. The process of modelling illuminates areas where knowledge is lacking, such as the rate of tick attachments and the role of carrier status, and encourages the formulation of hypotheses to bridge gaps in the knowledge. Such hypotheses can be based on observations on other similar systems, or purely on speculation, and a model can be instrumental in assessing the practicability of different hypotheses. This aids future research.

Different hypotheses concerning tick attachment rates and carrier status are considered in the results sections of chapter 8.

6. GENERATION OF WEATHER SEQUENCE DATA

"I shall never believe that God plays dice with the world".

Albert Einstein.

6.1 INTRODUCTION

Climate is one of the crucial factors that distinguishes disease patterns from area to area. The use of climatic data as a controlling factor within ECFXPERT leads to a site-specific model of disease. The relationships between ticks and climate have been well documented. Branagan (1978) showed that temperature is the major factor controlling the speed of tick development in each of the four developmental phases: pre-eclosion, larva to nymph moult, nymph to adult moult, and pre-oviposition. Branagan (1978) also published data characterising the relationship between temperature and the time taken to complete development in each phase. Short (1986) reported that the monthly rainfall total had an influence on tick survival, especially on the survival of eggs and larvae in short grass habitats. From a study of a number of sites, Short and Norval (1981) inferred that the monthly average for daily maximum and minimum temperatures, the monthly rainfall total, and the daylength, influenced the activity of adult ticks. Thus it is climate that dictates the suitability of ticks to different sites, and that creates the seasonality of tick populations by affecting adult activity. This in turn has an influence on the timing of disease outbreaks.

This section briefly explores some existing models for randomly generated climatic data. The results of one method are explored in detail and an alternative method proposed which involves time series analysis of a number of climatic datasets from sites in Africa.

6.2 EXISTING MODELS FOR RAINFALL AND TEMPERATURE

Weather patterns are typically represented by models to predict rainfall and temperature. Most models attempt to predict the daily level of rainfall. Then, depending on the wet or dry status of a day, and preceding days, the daily maximum and minimum temperatures are predicted. In some cases solar radiation and evaporation are also

predicted, which are of special importance to models predicting plant growth.

Due to problems caused by the high proportion of zero observations in daily rainfall data, most models for rainfall consist of two parts, modelling the occurrence of wet days and modelling the amount of rainfall on wet days.

Gabriel and Neumann (1962) proposed a first order Markov chain model to predict the occurrence of wet or dry days. The probability of rainfall on any day depended on whether the previous day was wet or dry. The two parameters used by the model were therefore

$$P_1 = P(\text{wet day} \mid \text{previous day wet})$$

$$P_0 = P(\text{wet day} \mid \text{previous day dry})$$

The model was fitted to data from Tel Aviv on 27 rainy seasons. This period spanned a total of 2437 days, and the empirical data:

		Day	
		Dry	Wet
Previous day	Dry	1049	350
	Wet	351	687

yielded estimates of 0.250 for P_0 and 0.662 for P_1.

A wet spell of length W was defined as W successive wet days followed by a dry day. Thus, given day 1 is wet, and W is the length of time up to, and not including, the next dry day

$$\begin{aligned} P(W = n) &= P(X_1 = 1 = X_2 = X_3 = \ldots = X_n, X_{n+1} = 0 | X_1 = 1) \\ &= P_1^{n-1}(1 - P_1) \\ &= (0.662)^{n-1}(0.338) \end{aligned}$$

Similarly, the probability of a dry spell, D, of length m is given by

$$P(D = m) = (1 - P_0)^{m-1} P_0 = (0.750)^{m-1}(0.250)$$

A weather cycle is defined as a wet spell followed by a dry spell. The distribution of the length C of a weather cycle is therefore

$$\begin{aligned} P(C = n) &= \sum_{i=1}^{n-1} \{P(i \text{ wet days, followed by } (n - i) \text{ dry days})\} \\ &= \sum_{i=1}^{n-1} \{P_1^i (1 - P_0)^{n-i}, \end{aligned}$$

as successive spells were assumed to be independent, following evidence presented in earlier work (Gabriel and Neumann, 1957)

$$= \frac{P_0(1-P_1)((1-P_0)^{n-1} - P_1^{n-1})}{1-P_0-P_1}$$

Gabriel and Neumann (1962) used the theoretical distributions for the lengths of wet and dry spells, and of weather cycles, to test the fit of the model. They stated that significance tests show these computations to give a satisfactory fit to the observed distributions.

The distribution of the number of wet days, S, among n successive days was also obtained. The computation of these formulae presented a difficult and complex problem in combinatorics. Once obtained, the theoretical and observed distributions of the number of wet days in a week were calculated and compared. These distributions are presented below in table 1.

Table 1. Theoretical and observed distributions of the number of wet days in a week using data for Tel Aviv (Gabriel and Neumann, 1962)

Number of wet days in the week	Theoretical frequency frequency	Observed frequency
0	36	39
1	51	38
2	63	73
3	65	65
4	57	69
5	42	45
6	25	18
7	12	13
	total: 351	total: 351

The Chi Squared test was used to assess the fit of the model based on the number of wet days occurring in each week, which was concluded satisfactory (p = 0.1–0.2).

The time unit of seven day intervals was chosen for ease of calculating the theoretical frequencies. For larger time units, accurate computation becomes increasingly difficult, and approximations to the formulae have to be made. This proves to be a disadvantage. Clearly the idea of using the observed and predicted lengths of wet and

dry spells to validate the model is well founded. It would not be difficult to produce a model that accurately conserves the mean or variance of the number of wet or dry days. Accurately mimicing extreme events, such as long periods of dry or wet weather, however, is more difficult but of absolute importance. A model predicting the suitability of a species of crop to an area that does not allow for the possibility of longer than average periods of dryness, must be treated cautiously. It is these extreme events that govern the long-term success or failure of a species in a habitat.

The theoretical properties of the Markov chain model are certainly of interest, but cannot be repeated when the model is extended to second or higher orders. A new approach is required to bridge mathematical thought with reality. Previously, models have been developed by mathematicians, with an interest in mathematics. Models, such as the one described above, had to be kept simple, to allow the extraction of theoretical properties. Simulation provides a way forward. Instead of obtaining the theoretical frequencies of certain events to validate a model, the model can be programmed and estimates of these theoretical frequencies obtained by simulation. Ensuring the random number generator provides numbers that are close enough to uniform (Ripley, 1988), and that the number of simulations is great enough, these estimates should be very close to the true theoretical frequencies. The advantages of this approach are twofold. First, the model can be made as complex as required, and second, any observed property of the system can be used to validate the model. In the case of the Markov chain model, perhaps the number of wet or dry days in a month rather than a week would have provided a more satisfactory test of validation, but the theoretical formulae proved too complex to accurately deal with this case.

The Markov chain model is a model for simulating the sequence of rain or no-rain days, and does not consider the amount of rainfall falling on wet days. Woolhiser and Pegram (1979) adapted the Markov chain model to describe daily rainfall totals:

Letting $Z_t = X_t Y_t$

where Z_t = amount of rain on day t,

$$X_t = \begin{cases} 0, & \text{if day } t \text{ is dry,} \\ 1, & \text{if day } t \text{ is wet,} \end{cases}$$

and Y_t = amount of rain falling on day t when $X_t = 1$.

$\{X_t\}$ was in the form of the first order Markov chain of Gabriel and Neumann (1962). $\{Y_t\}$ was assumed to be described by a mixture of two exponential distributions. Not

surprisingly, they found that the mixed exponential distribution fitted significantly better than the simple exponential distribution.

Given data covering a period of years, the parameters of each process $\{X_t\}$ and $\{Y_t\}$ were estimated separately for each day of the year, then the seasonal change in estimates described with a finite number of terms from a Fourier series. Maximum likelihood estimates of these Fourier coefficients were calculated numerically. Woolhiser and Pegram (1979) concluded that, with careful selection of the method for estimating the Fourier coefficients for each parameter, the model yielded "acceptable results" at each of the four sites considered.

Other distributions for $\{Y_t\}$ have also been proposed, such as a gamma distribution by Bruhn, Fry and Fick (1980). Bruhn, Fry and Fick (1980) had access to 30 years of daily rainfall data at the two sites they considered, from which to estimate the parameters of the gamma probability density function for $\{Y_t\}$. Fitting a function to such a vast quantity of data appears to be totally unnecessary. Thirty years of daily data is likely to represent the exact probability density of $\{Y_t\}$. Approximating the data by a curve only has the effect of discarding information, some of which might be critical in describing the true process.

Their model, however, also included temperature generation. The temperature component was described by a trivariate Normal distribution. Maximum temperature was correlated with maximum temperature on the previous day, minimum temperature was correlated with the current days maximum temperature. The parameters of the probability distribution depended on whether the previous day was wet or dry. The parameters were estimated separately for each month to take some account of seasonality, using 30 years of climatic data at two sites, Geneva and Fort Collins.

The results of the rainfall model were good, the actual and simulated distributions of the amount of rainfall being very similar. There were no significant differences between the distributions of simulated and observed temperatures for either Geneva or Fort Collins using the Kolmogorov-Smirnov non-parametric test.

Nicks and Harp (1980) fitted a first order Markov chain model to climatic data from each month to predict the occurrence of rainfall. They claimed that "to generate representative air temperature data, simulated temperatures must be related to the sequence of rain or no-rain days". The model for maximum temperature they presented was

$$T_i(k,m) = \overline{T}(k,m) + r_T(k,m)[T_{i-1}(k,m) - \overline{T}(k,m)] + \text{error}$$

where,

$$\text{error} = ts_T(k,m)[1 - r_T^2(k,m)]^{1/2}$$

$$k = \text{the wet/dry sequence} = \begin{cases} 1, & \text{for D-D,} \\ 2, & \text{for D-W,} \\ 3, & \text{for W-D,} \\ 4, & \text{for W-W,} \end{cases}$$

m = month,

$\overline{T}$ = mean daily maximum temperature,

r_T = lag 1 correlation,

T_i = current days maximum temperature,

T_{i-1} = previous days maximum temperature,

s_T = standard deviation of daily maximum temperatures,

and $t = N(0,1)$ random variable.

The derivation of the error term is given later in this chapter.

A similar model was used for minimum temperatures.

Nicks and Harp (1980) used the Kolmogorov-Smirnov statistic to confirm the goodness of fit of the theoretical to the observed distribution of maximum and minimum temperatures. Richardson (1981) produced a more complex model, whereby maximum temperature and minimum temperature were considered to have different means and standard deviations for each day of the year, conditioned on the wet or dry status of the day. A number of years data were used to estimate the means and standard deviations for wet days and dry days for each of the 365 days in the year. These parameters were plotted, and the seasonal fluctuations of each were smoothed by fitting a finite Fourier series to each sequence. The observed daily sequences were then standardised by subtracting the expected mean and dividing by the expected standard deviation, resulting in a series of standardised residuals. These residuals were claimed to follow a Normal(0,1) distribution with an auto-correlation structure, and cross-correlations between maximum and minimum temperatures. This supported Richardson's claim that maximum temperatures should be serially correlated from one day to the next, and maximum and minimum temperatures on a given day should be related, due to heat storage of the soil and surrounding atmosphere. An appropriate first order Markov chain model was proposed to generate the standardised residuals. The predicted temperatures could then be obtained by multiplying by the appropriate estimated standard deviation and adding the appropriate estimated mean.

Richardson (1984) estimated that twenty years of precipitation records, and ten years of temperature records are sufficient for accurate parameter estimation at most sites.

6.3 SIMULATION MODEL REQUIREMENTS

For accurate parameter estimation a vast supply of daily meteorological data is required, up to 20 years of rainfall and temperature records in most cases. A user interested in the simultion models discussed in chapter 5 is unlikely to have access to such information, and is unlikely to have the resources to enter all the data, especially if a number of sites are being compared. Weather records for African sites are rarely accessible in daily form, and if so are unlikely to span more than a few years, rendering parameter estimation difficult. Most climatic data that are readily accessible are in the form of monthly averages of the daily maximum and minimum temperatures, and monthly rainfall totals. This data is usually averaged over a number of years (often twentyfour), and is presented with standard deviations. Such data can be found in the F.A.O. handbook (1984a,b), and, because of its accessibility, operational models are constrained to utilise data of this form. As rainfall data are only presented as monthly totals, then the conditioning of maximum and minimum temperatures on the sequence of rain or no-rain days is impossible. Thus, a method is required to generate weather sequences using minimal datasets, and in particular monthly averaged data, that is representative enough to provide reliable estimates at different sites.

The models discussed paid special attention to the accurate generation of rainfall sequences. Accurate rainfall sequences are certainly of major importance to agricultural models comparing crop growth and yield for different sites. In modelling tick development, rainfall is less critical. Tick growth and development are temperature-driven, and, although rainfall does affect tick survival, monthly rainfall levels are likely to be sufficient for the prediction of survival rates.

6.4 MATERIALS AND METHODS

Five detailed datasets of one years daily maximum and minimum temperatures were available for examining different simulation methods. These datasets were obtained from meteorological records at a number of sites in Kenya, Tanzania and Zambia. ECF is endemic in these areas, and it is hoped that a model appropriate for generating accurate climate sequences at these sites would be also suitable at other sites where ECF is a threat. The data were collected from the following sites in East Africa:

Muguga, Kenya for 1968; Kizimbani, Kenya for 1984; Zanzibar Airport, Tanzania for 1986; and Chipata, Zambia for 1986 and 1987.

Missing values were few and usually due to failure of equipment. The appropriate monthly mean value was inserted in place of the missing data to preserve the monthly mean.

When comparing various proposed methods for climate data simulation, an appropriate statistic is required to keep the comparisons within the context of being useful to the tick model rather than providing a more accurate climatic data sequence. The statistic chosen was the expected time spent developing through all the four developmental stages: egg, larva, nymph and adult. This statistic, E, can be calculated as follows

$$E = \sum_{i=1}^{4}(E_i) = \sum_{i=1}^{4}(365/S_i)$$

where E_i is the expected time spent by a tick developing in stage i and S_i is the sum of each days development fraction over the year, for ticks in stage i.

The value of E does not represent the expected length of the ticks life cycle, as the complete life cycle also involves periods of questing and feeding in addition to the periods of growth and development.

The performance of a model can be assessed by comparing the expected development times calculated from the observed climatic datasets, with the expected development times estimated using the predicted sequences of climatic data obtained from model predictions. In testing stochastic models, the results of a number of simulations will have to be considered. In such cases, the minimum number of simulations thought appropriate was ten.

6.5 SIMULATION MODELS

6.5.1 Extreme value distribution

The approach adopted by Gumbel (1952) was to consider the theoretical properties of largest and smallest values within samples of a known size, then extend this theory to obtain asymptotic results for the distribution of extreme values. Consider a random variate X described by cumulative density function $F(x)$ and probability density function $f(x)$. The probability that n independent observations are at most as large as some value, x, is given by $F^n(x)$. This is the probability that the largest value out of

a sample of size n does not exceed x.

Denoting the largest out of n observations by x_n and the cumulative density function of the largest value by $\Phi_n(x_n)$,

$$P(x_n \leq x) = \Phi_n(x_n) = F^n(x_n),$$

and differentiating,

$$P(x_n = x) = \phi_n(x_n) = nF^{n-1}(x_n)f(x_n) \tag{1}$$

If the initial distributions are known, this provides the formulae required for calculation of extreme large values from samples of size n. Similar results can be found for extreme small values. However, given very large samples, such formulae make calculations difficult, and asymptotic results are required.

Return period

The return period is the number of observations expected to be required before an event is repeated. For example, if the event $(X \leq x)$ is seen to occur m times out of n then

$$P(X > x) = 1 - F(x) = 1 - \frac{m}{n} = \frac{1}{n/(n-m)}$$

where $T = n/(n-m)$ is the return period for the event $(X > x)$. In general, $T(x) = 1/(1-F(x))$, where $T(x)$ is the expected number of observations required to yield one observation of at least x in size.

Expected extremes

To obtain the expected extreme, T is treated as a fixed number of trials, n. Then a certain large value, u_n, can be uniquely defined by the probability

$$F(u_n) = 1 - \frac{1}{n} \tag{2}$$

as $F(x)$ is monotonic increasing.

The expected number of values at least u_n from a sample of n is $n(1-F(u_n)) = 1$. Hence u_n is the expected largest value. Define $\alpha_n = nf(u_n)$. By multiplying both sides of equation (2) by $f(u_n)du_n$ the following is obtained:

$$\alpha_n du_n = \frac{f(u_n)}{1 - F(u_n)} du_n$$

The right hand side of this equation being simply the conditional probability of a value lying in the interval $(u_n, u_n + du_n)$ given that this value exceeds u_n.

Differentiation of equation (2) gives

$$f(u_n)\frac{du_n}{dn} = \frac{1}{n^2}$$

which leads to

$$\frac{du_n}{dlogn} = \frac{1}{\alpha_n}.$$

So $1/\alpha_n$ is a measure of the increase of the expected largest value with the log of the sample size. Probability functions $F(x)$ which converge towards unity with increasing x at least as quickly as an exponential function are said to be of exponential type. The formal property of exponential type distributions (Von Mises, 1936) is

$$\lim_{x\to\infty}\{\frac{d}{dx}\frac{1-F(x)}{f(x)}\} = 0$$

Such distributions include the exponential, normal, F-distributions and logistic distributions, and investigations will be limited to these.

The asymptotic distribution of the extreme largest value

The mode of the largest value, $\tilde{x}_n$, is obtained by finding the maximum of the probability density function of the largest value given in equation (1). Setting the derivative of this equation to zero yields

$$\frac{(n-1)f(x)}{F(x)} = -\frac{f'(x)}{f(x)} \tag{3}$$

Because distributions of exponential type are being considered, the right hand side of this equation can be approximated by $f(x)/(1-F(x))$ for x large enough (L'Hopitals rule), so equation (3) becomes

$$\frac{(n-1)f(x)}{F(x)} \simeq \frac{f(x)}{1-F(x)}$$

which leads to $F(x) \simeq 1 - 1/n$, where x is the solution for the mode of the largest value, which also satisfies equation (2), the definition of the expected largest value. Hence, $\tilde{x}_n \longrightarrow u_n$.

By writing $x = u_n + x - u_n$, and expanding as a Taylor series, the equation for the cumulative density function of x becomes

$$\begin{aligned} F(x) &= F(u_n + x - u_n) \\ &= F(u_n) + (x-u_n)F'(u_n) + \frac{(x-u_n)^2}{2!}F''(u_n) + \cdots \end{aligned}$$

It is easily shown that $F'(u_n) = \alpha_n/n$, using the chain rule

$$\frac{dF}{du_n} = \frac{dF}{dn}\frac{dn}{du_n}$$

and for subsequent terms, L'Hopitals rule is employed as before

$$\frac{F''(u_n)}{F'(u_n)} = \frac{F'''(u_n)}{F''(u_n)} = \ldots = -\frac{f(u_n)}{1 - F(u_n)} = -\alpha_n$$

Thus, the equation for $F(x)$ can be reduced to

$$F(x) = 1 - (1/n)exp\{-\alpha_n(x - u_n)\}$$

Letting the asymptotic cumulative density function for the largest value be $\Phi(x)$, then

$$\begin{aligned}\Phi(x) &= \lim_{n\to\infty}\{\Phi_n(x)\} = \lim_{n\to\infty}\{F^n(x)\} \\ &= \lim_{n\to\infty}\{[1 - (1/n)exp\{-\alpha_n(x - u_n)\}]^n\} \\ &= exp\{-exp\{-y_n\}\},\end{aligned}$$

where $y_n = \alpha_n(x - u_n)$, the reduced largest value, u_n is the mode of the largest value and $1/\alpha_n$ is a measure of dispersion.

Similar working yeilds the asymptotic cumulative density function for the extreme smallest value

$$_1\Phi(x) = 1 - exp\{-exp\{-y_1\}\},$$

where $y_1 = \alpha_1(x - u_1)$, the reduced smallest value, u_1 is the mode of the smallest value and $\alpha_1 = nf(u_1)$.

Parameter estimation

In the case of climatic data, the distribution of temperature within a day is unknown, although maximum and minimum daily temperatures can easily be measured. The parameters of the asymptotic distribution, therefore, have to be estimated from observed data.

Let the moment generating function of the largest reduced value, y_n, be $G_n(t)$. This has been shown to be (Fisher and Tippett, 1928, Gumbel, 1944)

$$G_n(t) = \Gamma(1 - t),$$

where

$$\Gamma(t) = \int_{x=0}^{\infty}\{x^{t-1}e^{-x}dx\}.$$

Hence population means and standard deviations of the reduced extreme largest values are

$$\bar{y}_n = \gamma = 0.577215665, \text{ Euler's constant}$$

and $$\sigma(y_n) = \frac{\pi}{\sqrt{6}} \text{ respectively.}$$

As $y_n = \alpha_n(x - u_n)$, then the theoretical mean and standard deviation of the extreme largest daily temperatures, $x_{(n)}$, are

$$\bar{x}_{(n)} = u_n + \frac{\gamma}{\alpha_n}, \qquad \text{and} \qquad \sigma(x_{(n)}) = \frac{\pi}{\sqrt{6}}\frac{1}{\alpha_n}$$

By estimating the population mean and standard deviation of the extreme largest daily temperature, $\bar{x}_{(n)}$ and $\sigma(x_{(n)})$, by the observed quantities, $\bar{x}_n$ and $s(x_n)$

$$\hat{u}_n = \bar{x}_n - \frac{\gamma}{\hat{\alpha}_n}, \quad \text{and} \quad \frac{1}{\hat{\alpha}_n} = \frac{\sqrt{6}}{\pi}s(x_n)$$

and so $$\hat{u}_n = \bar{x}_n - \frac{\gamma\sqrt{6}}{\pi}s(x_n).$$

Similarly, for the extreme smallest daily temperature

$$\hat{u}_1 = \bar{x}_1 - \frac{\gamma}{\hat{\alpha}_1}, \quad \text{and} \quad \frac{1}{\hat{\alpha}_1} = \frac{\sqrt{6}}{\pi}s(x_1)$$

Random number generation from extreme value distribution

Using the inversion method, the algorithm for generating daily maximum temperatures from observed mean m and standard deviation s is simply obtained (Morgan, 1984), and is as follows:

1. Let $c_1 = \frac{\pi}{\sqrt{6}}s$
2. Let $c_2 = m - \frac{\gamma}{c_1}$
3. Generate a uniform random variate U in the interval (0,1)
4. Return maximum temperature $= c_2 - ln(-ln(U))/c_1$

The algorithm for generation of minimum temperatures is similarly constructed.

Results

Using the mean and standard deviations of the monthly maximum and minimum temperatures for each of the five datasets, daily maximum and minimum temperatures are simulated by sampling from the appropriate extreme value distribution. Values for the expected development time of ticks, E, are obtained and compared with the true E value obtained from the genuine daily temperature sequences at each site. The results of ten simulations at each site are displayed below in table 2.

Table 2. Expected developmental times, E, for ticks at each site using climatic data generated from extreme value distributions and using the true climatic data for five East African sites.

	Dataset				
	Muguga	Chipata	Chipata	Kizimbani	Zanzibar
	1968	1986	1987	1984	1986
	238.53	79.67	67.06	66.19	59.54
	238.17	73.08	68.08	65.87	66.00
	237.94	79.88	67.76	65.92	64.48
	237.55	71.50	60.28	67.92	67.30
	240.33	82.34	63.63	63.52	66.69
	237.48	78.51	58.12	66.33	62.48
	236.26	81.07	58.51	67.17	65.31
	238.47	84.82	63.11	67.63	65.78
	236.27	74.72	64.62	65.67	66.33
	238.80	81.35	65.07	65.18	66.90
mean	237.98	78.69	63.62	66.11	65.10
st. dev.	1.20	4.28	3.65	1.23	2.40
95% C.I.	(237.12, 238.84)*		(61.01, 66.23)*		(63.37, 66.80)*
		(75.63, 81.76)*		(65.23, 66.99)*	
true value	277.39	99.73	90.42	76.63	74.40

The 95% confidence intervals for the mean expected development time were con-

structed using the t-statistic. Those confidence intervals marked with an asterisk are those which correspond to sequences of climate data that are unsatisfactory as the true expected development time is very unlikely to represent the mean time from simulations. It is clear that the extreme value distribution method is not satisfactory, as the development time for ticks is consistently underestimated. The consequence of this underestimate can be seen by considering the predictions for Chipata 1987. From the ten simulations the minimum, maximum, and mean of expected development times, E, were 58.12 days, 68.08 days and 63.62 days respectively. The true expected development time is 90.4 days, so prediction estimates represent an error as large as one month per year. The extreme value distribution was used as the sampling distribution for generating climatic data by King *et al.* (1988) in their study of tick development times at five sites in Kenya. The suitability of this distribution was not considered, and the above results must throw considerable doubt over the conclusions they made.

6.5.2 Time series analysis

A time series is a collection of observations made sequentially in time, such as temperature, share prices or population size. The analysis of a time series is an attempt to describe and explain the underlying process that produces these observations, and often to provide the means of predicting a sequence of future observations. The five sets of one years daily maximum and minimum temperatures result from extremely complex physical processes which are both highly periodic and highly correlated. To describe such a process it is neccesary to transform the data into a sequence of observations that are stationary. Such a sequence is one in which there is no systematic change in the mean and variance of the observations through time, and no periodic influences. It is then possible to fit a model to the transformed data. Statistics thought useful in identifying appropriate models for stationary data are autocorrelations and partial autocorrelations (Box and Jenkins, 1976). This approach describes a suitable transformation on the sequences of extreme temperature measurements, and then considers a number of models to describe the transformed data.

Observation of the monthly means of daily maximum or minimum temperatures for each site reveals seasonal temperature changes, suggesting that each sequence is non-stationary. This is further illustrated by Figures 1 and 2, which show the autocorrelation functions (ACFs) for maximum and minimum temperatures at Chipata in 1987.

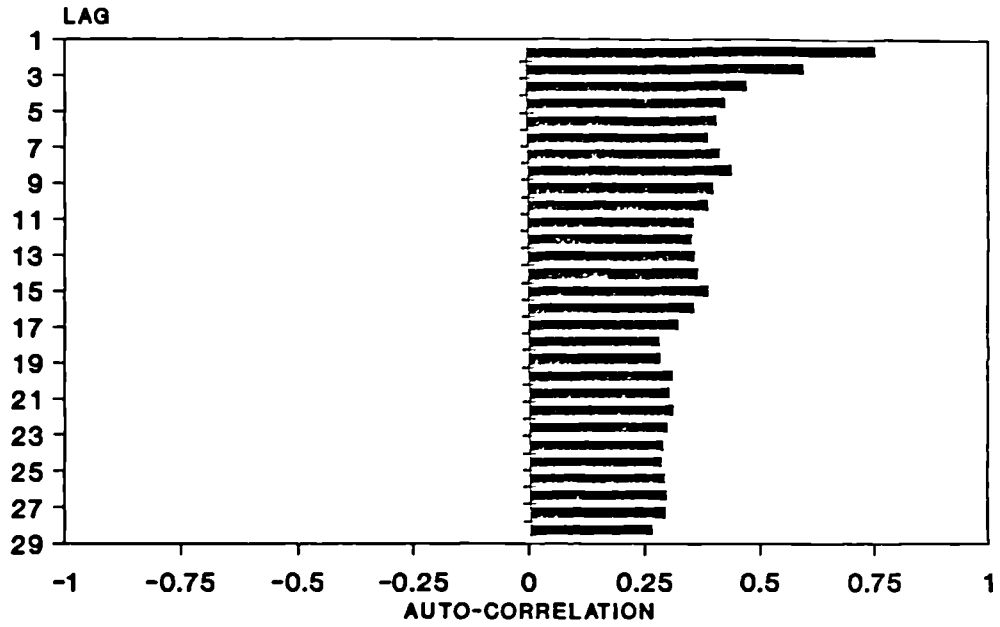

Figure 1. *Autocorrelation function of the maximum temperature sequence for Chipata, 1987.*

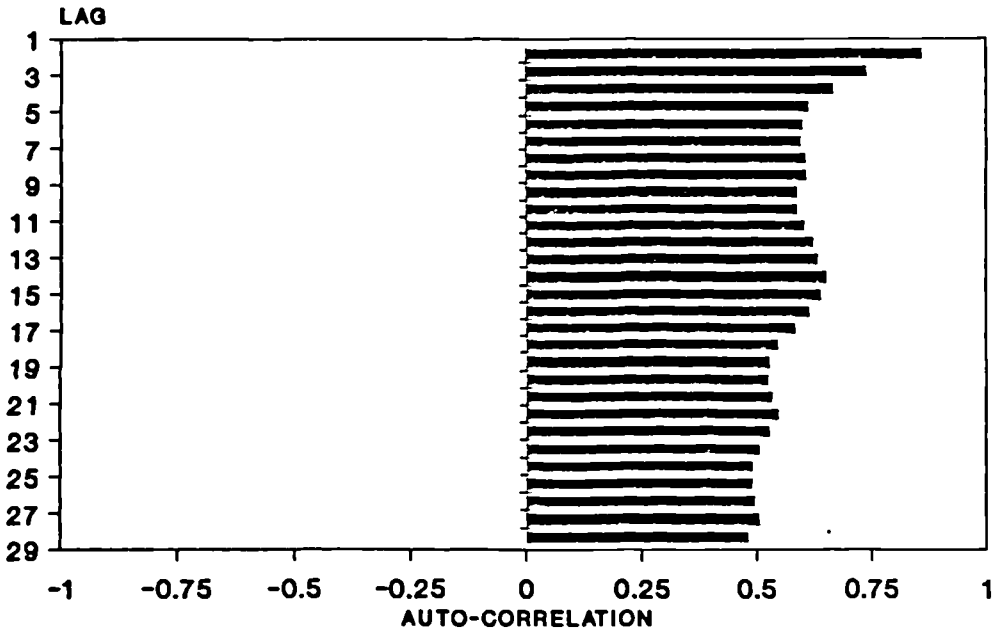

Figure 2. *Autocorrelation function of the minimum temperature sequence for Chipata, 1987.*

Each function is very slowly decaying, which suggests non-stationarity. Non-stationarity of a time series, however, can be due to either fluctuating mean or fluctuating variance. The variances within each month do not appear to change substantially between months, and when the years data for each site is boxplotted by month, the

monthly change in mean appears to be the most significant variable. One might expect the variance of maximum temperatures, for example, to be perhaps greatest during months exhibiting the highest daily maximum temperatures, and lowest when this statistic is at lower values. However, possibly due to the proximity to the equator of most of these sites, the variance does not change greatly from month to month, as in fact the mean temperature measurements do no differ between successive months by more than 2 or 3 degrees. At more seasonal locations, changes in the variance are likely to play a more important role. The month to month changes in mean daily maximum and minimum temperature can be observed from the graph of the data for Chipata in 1987 in Figure 3.

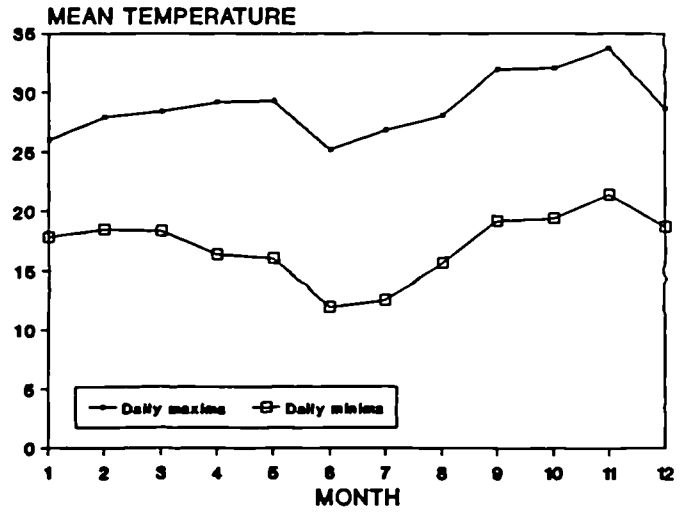

Figure 3. *Changes in the mean monthly maximum and minimum temperatures for Chipata in 1987.*

Given the constraint of modelling from monthly averaged data, it is important to find a suitable transformation on the daily data that utilises the monthly summary statistics. If a curve is fitted to the monthly means it is possible to obtain estimates of the mean maximum and minimum temperature for each day of the year. These estimates could be subtracted from the observed values to remove the effect of daily fluctuations in the means. On inspection of the monthly means at the various sites it was concluded that linear interpolation between monthly means would be adequate, each monthly mean being positioned at the midpoint of each month. When the appropriate estimated mean maximum and minimum temperatures were subtracted from each observed value, the new time series appeared stationary for each site. More-over,

the resulting process

$$W_t = X_t - M_t \tag{4}$$

where

W_t = adjusted maximum or minimum value for day t,

X_t = observed maximum or minimum temperature on day t,

M_t = expected maximum or minimum temperature on day t,

appeared to follow an autoregressive process of order 1 (an AR(1) process) for both maximum and minimum temperature. That is, the value of the adjusted temperature, W_t, is partially dependent on the value of the previous day, W_{t-1}. This is illustrated by the autocorrelation and partial autocorrelation functions (PACFs) for the adjusted maximum and minimum temperature time series at Chipata in 1987 shown in Figures 4, 5, 6 and 7. At a specific lag, the sample autocorrelation or partial autocorrelation can be assumed significantly greater than zero if its absolute value exceeds $2/\sqrt{365}$, where 365 is the sample size of one years daily data (Box and Jenkins, 1976).

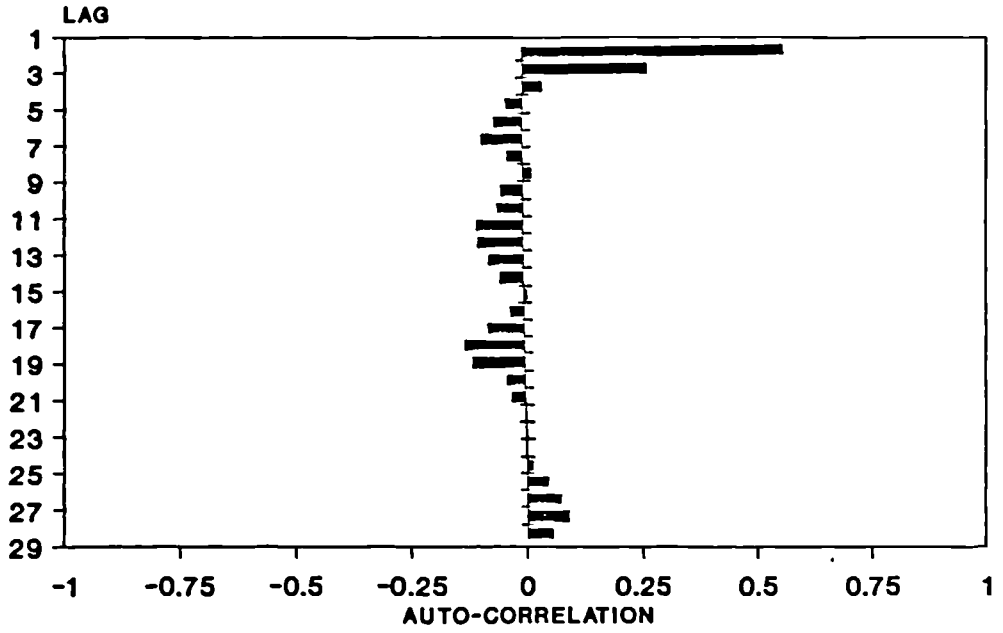

Figure 4. *Autocorrelation function of the adjusted maximum temperature sequence for Chipata, 1987.*

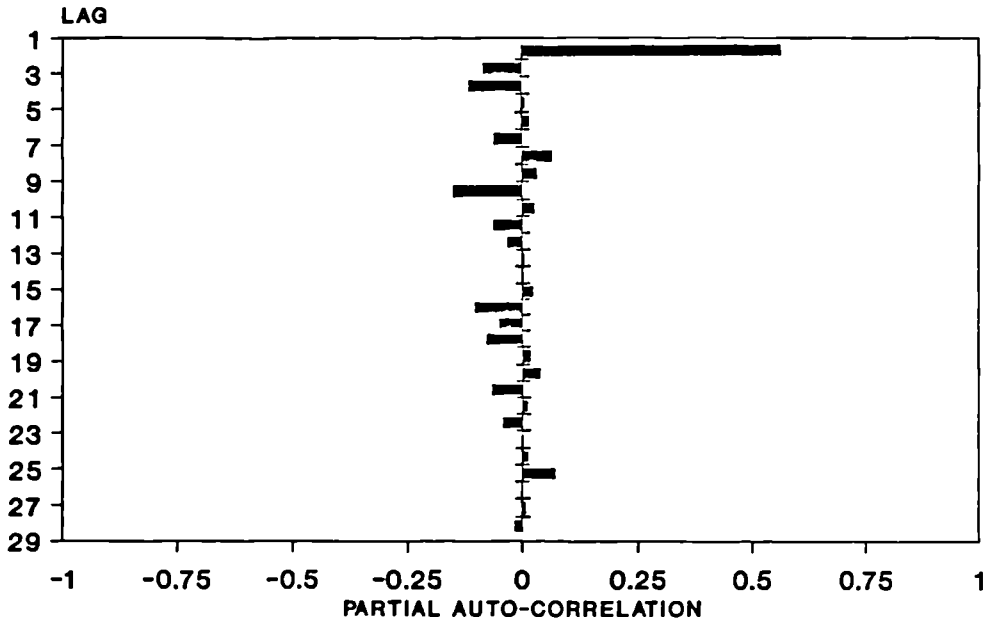

Figure 5. *Partial autocorrelation function of the adjusted maximum temperature sequence for Chipata, 1987.*

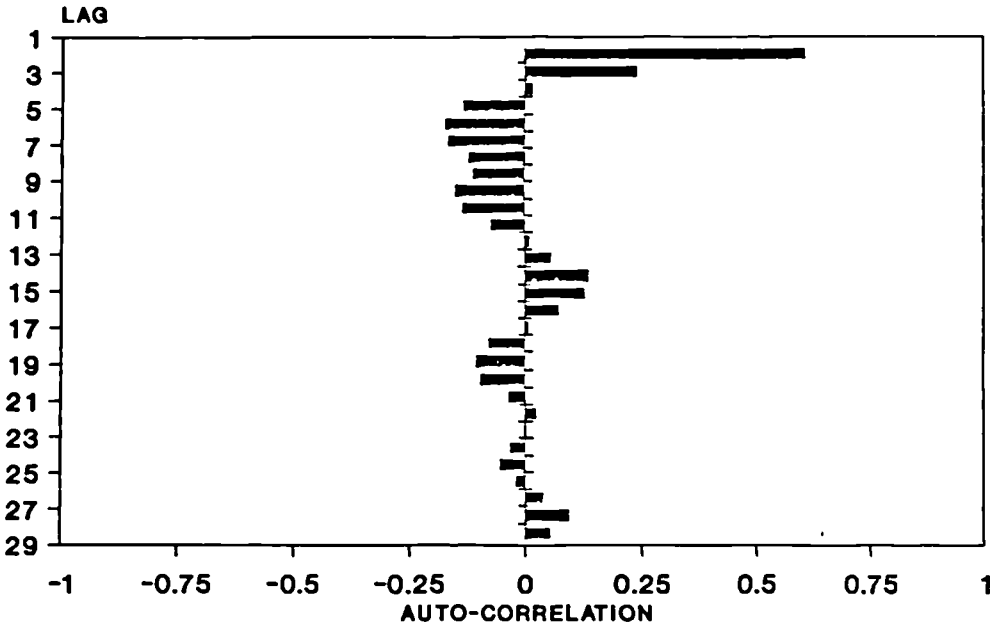

Figure 6. *Autocorrelation function of the adjusted minimum temperature sequence for Chipata, 1987.*

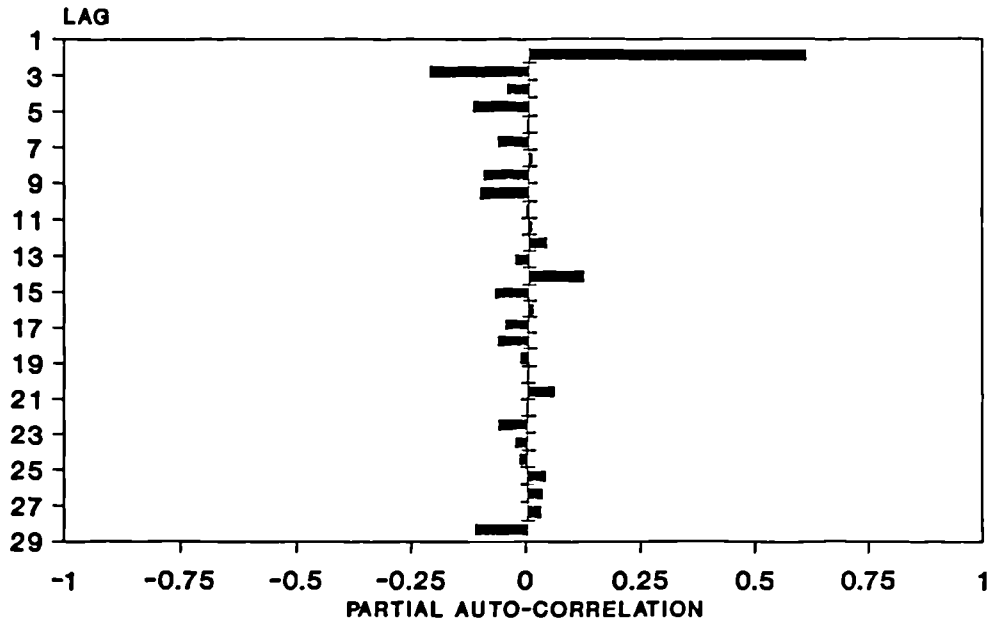

Figure 7. *Partial autocorrelation function of the adjusted minimum temperature sequence for Chipata, 1987.*

The AR(1) process is characterised by a quickly decaying ACF, and a PACF with a spike at lag 1 only (Box and Jenkins, 1976).

The correlations between the daily maximum and minimum temperatures at each site were generally low and could be ignored. The importance of the random element to the model can be investigated by considering two possibilities. Firstly by ignoring the noise element completely and modelling daily temperatures by their interpolated values using the formula $\hat{X}_t = M_t$. Or, secondly, by allowing for randomness by simulating the noise using an AR(1) process.

Interpolated means

Taking the monthly mean maximum and minimum temperatures to be the temperatures for the middle day of each month, and fitting a straight line between points provides estimates for each day of the year. Using these estimates, the expected development time for ticks, E, can be calculated and compared to the value obtained with the true climatic data. True and predicted values of E are presented in table 3.

Table 3. Expected developmental times, E, for ticks at each site using climatic data from interpolated monthly mean temperatures and using the true climatic data for five East African sites.

	Dataset				
	Muguga	Chipata	Chipata	Kizimbani	Zanzibar
Year:	1968	1986	1987	1984	1986
Interpolated data	273.77	109.10	99.05	78.79	75.74
True data	277.39	99.73	90.42	76.63	74.40

The differences between true and predicted values are within the order of ten days in each case. However, although these estimates are fairly good, the non-randomness of the simulation method means that climate data generated for each year will be identical. This is unrealistic, and does not allow for extreme occurrences in climate which could render certain sites unfavourable to ticks. More detailed examination of the sum of development fractions over the year for each stage, S_i, showed that prediction was unsatisfactory for certain stages. Predicted values of S_i for each stage at each site are displayed below in table 4.

Table 4. Development fractions sums, S_i, for ticks in each stage at each site using climatic data from interpolated monthly mean temperatures and using the true climatic data for five East African sites.

		Dataset				
		Muguga	Chipata	Chipata	Kizimbani	Zanzibar
Tick stage:		1968	1986	1987	1984	1986
Pre-oviposition	true:	16.48	122.16	222.86	151.85	167.83
	pred:	16.15	56.95*	106.14*	94.02*	125.74*
Pre-eclosion	true:	3.61	8.37	9.04	10.73	10.99
	pred:	3.80	7.92	8.46	10.64	10.90
Larva to nymph	true:	9.36	29.66	33.28	36.70	37.83
moult	pred:	9.13	25.96	28.16	36.19	37.36
Nymph to adult	true:	3.17	8.94	9.75	12.06	12.43
moult	pred:	3.17	8.58	9.24	11.96	12.34

In the table, those S_i values marked with an asterisk correspond to values that are largely under-estimated when compared with the true values. Other values appear to be well approximated. The reasons for the inaccuracy stem from the absence of noise in the model. The relationship between temperature and time to development of a tick is non-linear. A small difference above the mean temperature advances tick development. A small difference below the mean temperature slows down tick development, although the magnitude of this is less great due to the exponential nature of the development curve. Thus, the noise element is critical to the model for climate.

Interpolated means with AR(1) noise

Given that the adjusted process, $\{W_t\}$, in equation (4) follows a stationary AR(1) process, then the complete model for the system would be characterised by

$$\hat{W}_t = r\hat{W}_{t-1} + Z_t$$

where, $\{Z_t\}$ is white noise with mean zero and variance σ^2, and r is the lag 1 correlation of $\{W_t\}$.

A model was fitted to each adjusted maximum and minimum temperature sequence, and estimates of the lag 1 correlation and error variance were obtained for each.

The residuals of each fitted model were analysed by inspection of their dot plots, normal scores plots, ACFs and PACFs. The dot plots of $\{Z_t\}$ *appeared symmetrical* and centered on zero in most cases, although slightly skewed towards the right in two of the cases. The normal scores plots were generally linear but, however, in a number of cases these plots were slightly curved. Observation of the ACF and PACF of each adjusted sequence sugested that there was little remaining significant autocorrelation structure. This is illustrated by the ACF and PACF of $\{Z_t\}$ from the adjusted maximum temperature sequence of the Chipata 1987 data, shown in Figures 8 and 9 respectively.

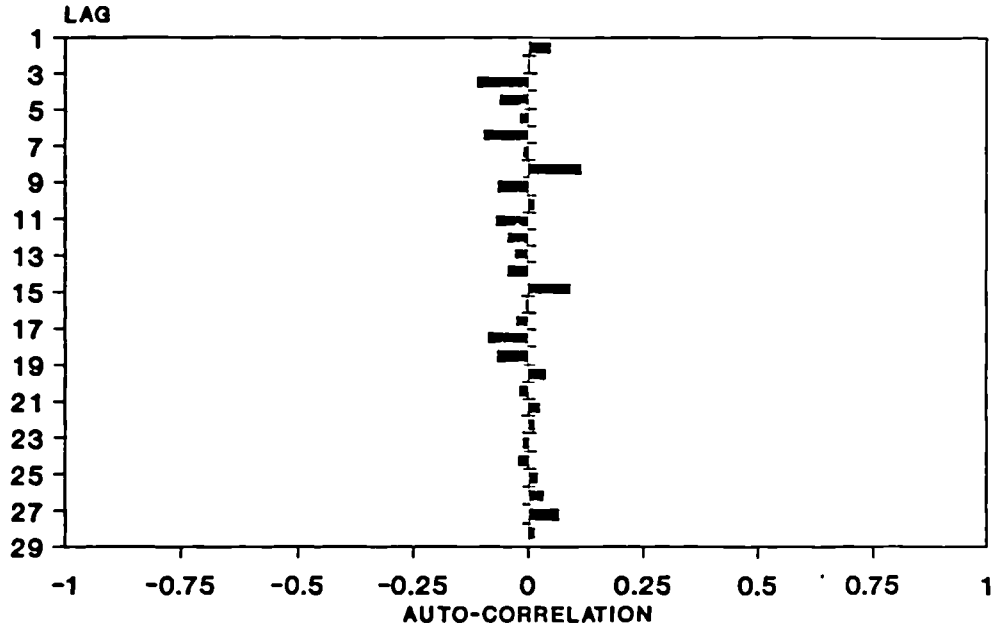

Figure 8. ***Autocorrelation function of the noise from the fitted AR(1) process for adjusted maximum temperatures at Chipata, 1987.***

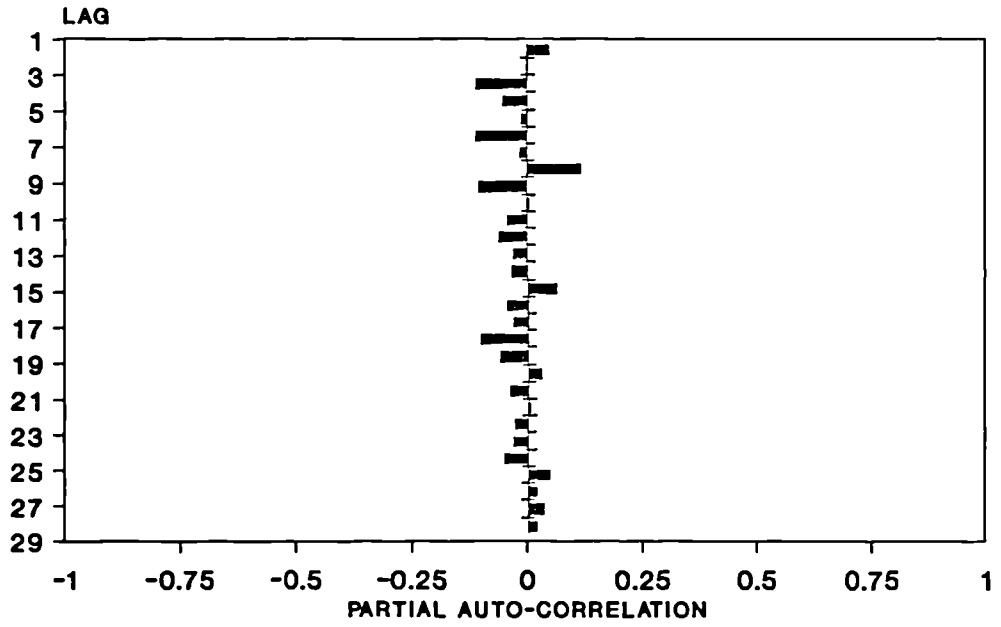

Figure 9. *Partial autocorrelation function of the noise from the fitted AR(1) process for adjusted maximum temperatures at Chipata, 1987.*

It was concluded that a normal distribution would be an adequate first approximation of $\{Z_t\}$, based on the limited data.

Hence the process $\hat{W}_t = r\hat{W}_{t-1} + Z_t$, can be easily simulated. The polar Marsaglia algorithm is used to generate the normal random variables constituting the process $\{Z_t\}$, as described earlier in Chapter 5. The predicted temperatures $\{\hat{X}_t\}$ can then be retrieved by adding the appropriate days mean

$$\hat{X}_t = \hat{W}_t + M_t.$$

The estimates of lag 1 correlation and error standard deviation for the adjusted AR(1) model when fitted to the daily maximum and minimum temperature sequences for each site are shown in table 5.

Table 5. Estimated lag 1 correlations and error standard deviations for adjusted maximum and minimum temperature sequences from five East African sites.

	Adj. max. temp.		Adj. min. temp.	
Dataset:	lag 1 corr	Error s.d.	Lag 1 corr	Error s.d.
Muguga 1968	0.48	1.45	0.20	1.08
Chipata 1986	0.62	2.03	0.67	1.37
Chipata 1987	0.59	2.13	0.62	1.51
Kizimbani 1984	0.38	1.02	0.32	0.90
Zanzibar 1986	0.25	1.17	0.34	1.25

Results

Using the mean and standard deviations of the monthly maximum and minimum temperatures for each of the five datasets, daily maximum and minimum temperatures are simulated using the fitted AR(1) models. Values for the expected development time of ticks, E, are obtained and compared with the true E value obtained from the genuine daily temperature sequences at each site. The results of ten simulations at each site are displayed below in table 6.

Table 6. Expected developmental times, E, for ticks at each site using climatic data generated from AR(1) models fitted to adjusted climatic data and using the true climatic data for five East African sites.

	Dataset				
	Muguga 1968	Chipata 1986	Chipata 1987	Kizimbani 1984	Zanzibar 1986
	279.14	95.32	82.77	75.21	75.28
	279.35	102.91	95.58	76.77	75.78
	277.03	97.80	87.83	76.86	76.14
	279.25	99.08	94.73	72.32	75.71
	283.93	99.33	81.29	77.17	75.24
	280.51	101.79	92.09	76.86	76.23
	279.38	104.87	91.67	76.17	75.83
	278.57	100.45	83.58	76.63	75.37
	279.81	99.32	86.50	76.88	75.82
	279.43	113.10	96.72	78.99	75.25
mean	279.64	101.39	89.28	76.39	75.66
st. dev.	1.76	4.90	5.65	1.71	0.36
95% C.I.	(278.38, 280.90)	(97.89, 104.90)	(85.24, 93.32)	(75.16, 77.61)	(75.40, 75.92)*
true value	277.39	99.73	90.42	76.63	74.40

The 95% confidence intervals for the mean expected development time were constructed using the t-statistic. Only one of these confidence intervals does not contain the true expected development time. This confidence interval was obtained from the model predictions using climatic data from Zanzibar airport, and is marked with an asterisk. However, the magnitude of this error is in the order of only one day, which is negligible. The adjusted AR(1) model therefore appears to produce very satisfactory results.

When using the interpolated means model, it was observed that the sum of the years development fractions for a specific stage in the tick life cycle, S_i, was grossly under-predicted for large values of the sum. The highest values of this sum were observed for the pre-oviposition phase which is the most rapid, and when employing the adjusted AR(1) model the development fractions sums in table 7 were obtained for pre-oviposition at each site.

Table 7. Development fractions sums, S_i, for ticks in pre-oviposition at each site using climatic data generated from AR(1) models fitted to adjusted temperatures and using the true climatic data for five East African sites.

	Dataset				
	Muguga	Chipata	Chipata	Kizimbani	Zanzibar
	1968	1986	1987	1984	1986
	16.36	143.93	209.76	148.27	163.16
	16.39	105.96	128.03	148.32	155.41
	16.54	148.00	199.60	127.40	148.23
	16.41	121.04	182.72	148.19	160.74
	16.02	117.74	219.10	128.51	169.34
	16.27	107.81	196.44	128.22	157.85
	16.31	116.29	173.86	135.90	160.90
	16.48	122.54	204.68	140.53	158.24
	16.38	149.17	257.60	139.80	153.46
	16.39	75.80	164.40	111.74	152.89
mean	16.36	120.83	193.62	135.69	158.02
st. dev.	0.14	22.40	34.70	11.90	5.96
true value:	16.48	122.16	222.86	151.85	167.83

It is clear that the sums of development fractions for the pre-oviposition stage for each year simulated are fairly accurately predicted at each site. The predicted sums for the development fractions of the other three stages were also close to the true values.

Thus the model appears adequate in predicting the expected development times for ticks. If more data on sequential years of daily temperatures were available, the

variance of the predictions could also be investigated for accuracy. However, there is no reason to assume that the method is not satisfactory with the data given.

Discussion

A number of questions now arise. Firstly, how much data is required to accurately estimate the lag 1 correlation of each adjusted process $\{W_t\}$, and how sensitive is the model to poor estimation of the lag 1 correlation? Secondly, is it possible to obtain theoretical estimates of any of the model parameters so that predictions can be obtained for sites where only monthly averaged climatic data is available?

Estimation of the lag 1 correlation of $\{W_t\}$

For each site, the lag 1 correlation for $\{W_t\}$ was calculated for the first $5, 15, 25, 35, \ldots,$ 365 days of the year. For each data set, the values of the estimate fluctuate erratically at first, but eventually stabilise. Given that one years data are the maximum available for some sites, then the number of daily data required for estimating the parameter to within the order of accuracy obtained from a full years data would be around 200 days for both the maximum and minimum temperature sequences. This is illustrated in Figures 10 and 11 showing the change in the estimated lag 1 correlation with sample size for the Chipata 1987 data. The estimates seem fairly stable after 180 days for the maximum temperature sequence, Figure 10, and after 150 days for minimum temperatures, Figure 11.

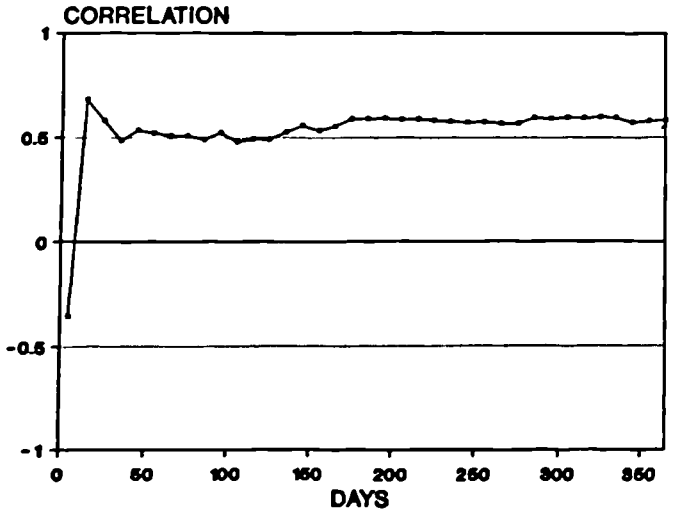

Figure 10. ***Estimated lag 1 correlation against increasing sample size of the adjusted maximum temperature sequence for Chipata, 1987.***

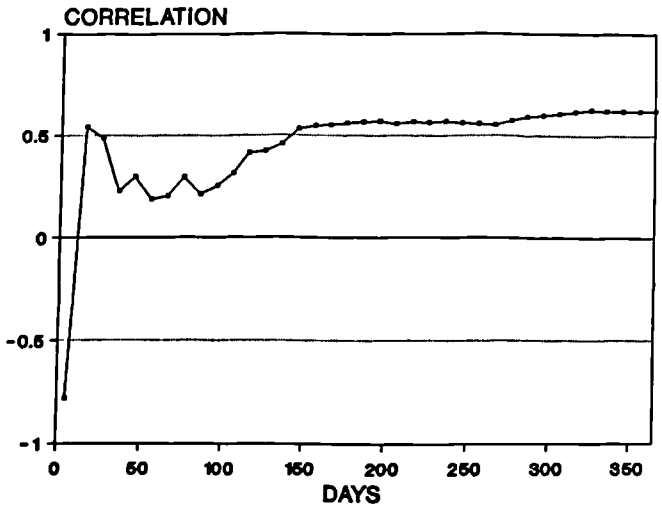

Figure 11. *Estimated lag 1 correlation against increasing sample size of the adjusted minimum temperature sequence for Chipata, 1987.*

Sensitivity of the model to changes in the lag 1 correlation

Examination of the Chipata 1987 climate sequence indicates the importance of the lag 1 correlation both in the prediction of the expected sum of development fractions, E_i, for each tick stage i, and in the variance of these estimates. The estimates of lag 1 correlation for the adjusted maximum and minimum temperature sequences at Chipata 1987 are both around 0.6. Assuming that the two lag 1 correlations are equal, the effects of changing the lag 1 correlations on the resulting development fractions sum can be investigated by varying their values over the range 0 to 1.

The graph of a 95% confidence interval for the expected development fractions sum for the oviposition stage, Figure 12, illustrates typical results. The confidence intervals were obtained from ten simulations at lag 1 correlation values of $0, 0.1, 0.2, \ldots, 0.9$.

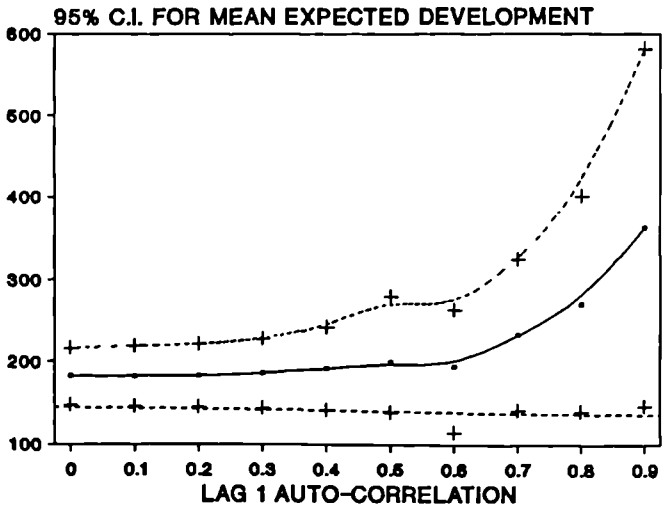

Figure 12. *95% confidence intervals for the expected sum of development fractions for ticks in preoviposition for Chipata 1987 under various values of lag 1 correlation.*

As the lag 1 correlation increases so does the variance of the development time statistic estimated. This is due to the exponential nature of the temperature to development time relationship. When the lag 1 correlation is zero, the adjusted temperatures for adjacent days are independent. In this case, it is likely that close to a half of the generated temperatures, $\hat{X}_t$, will be greater than their corresponding expected values, M_t; and around a half of the generated temperatures will be less than this value. Increasing the lag 1 correlation reduces the likelihood that half of the generated temperatures are greater than expected, and half are less than expected, as long series of values greater than or less than the mean become more probable. Because of the exponential relationship between temperature and the speed of tick development, this has the effect of producing a more variable estimate of the development time.

Similarly the expected value of the estimate seems to increase beyond a certain point. It would appear that for lag 1 correlations less than around 0.65 there is not much difference in the average prediction of the sum of development fractions; and for lag 1 correlations less than 0.4 there is little difference in the variance of the predicted development fractions sums.

It is clear, therefore, that the autoregressive nature of the model is important, but that some flexibility in the accuracy of the lag 1 correlation estimate is permissible without greatly affecting the resulting tick development predictions. This observation is consistent with the results following similar analyses of the temperature sequence models fitted to the other climatic datasets. This suggests that a default lag 1 corre-

lation estimate may provide reliable results for sites where daily temperature records are unavailable.

Theoretical estimates of the error variance for the AR(1) model

The AR(1) model for daily maximum or minimum temperature can be written in the form

$$X_t - M_t = r(X_{t-1} - M_{t-1}) + Z_t \tag{5}$$

The M_t are estimated from the monthly mean maximum and minimum temperatures by linear interpolation. Most climatic datasets also include the variance of the daily maximum and minimum temperatures for each month. It is possible to use these sample variances to estimate the variance of the noise process $\{Z_t\}$.

Rearranging equation (5) gives

$$X_t = M_t + r(X_{t-1} - M_{t-1}) + Z_t$$

and so

$$\begin{aligned} Var(X_t) &= Var(M_t + r(X_{t-1} - M_{t-1}) + Z_t) \\ &= Var(rX_{t-1} + Z_t) \\ &= r^2 Var(X_{t-1}) + Var(Z_t). \end{aligned}$$

That is,

$$Var(Z_t) = Var(X_t) - r^2 Var(X_{t-1})$$

Assuming that $Var(X_t) = Var(X_{t-1}) = \sigma^2$ for all t, then

$$Var(Z_t) = \sigma^2(1 - r^2). \tag{6}$$

Var(X_t) is not the variance of daily maximum or minimum temperatures within a month. The variance of the daily extreme temperatures within a month is a measure of spread about the months average maximum or minimum temperature. Var(X_t) is a measure of the dispersion of the maximum or minimum temperature for a specific day, t, about the expected maximum or minimum temperature for that day, M_t. The expected temperature, M_t, changes for each day of the month, and so the months variance is not a valid measure of the variation in daily extreme temperatures.

The daily maximum temperatures for one month consists of the sequence $X_1, X_2, \ldots, X_n$, where each X_t is a random variable from a distribution with mean M_t and variance σ^2. The monthly summary statistics consist of the mean, $\overline{X}$, and variance, s_X^2, of the X_t values, where

$$\overline{X} = \sum_{t=1}^{n} \frac{X_t}{n}$$

and $$s_X^2 = \sum_{t=1}^{n} \frac{(X_t - \overline{X})^2}{n}$$

Now, X_t can be expressed in the form

$$X_t = M_t + \epsilon_t$$

where $E[\epsilon_t] = 0$ and $\text{Var}(\epsilon_t) = \sigma^2$, and so the mean and variance of daily maximum temperatures for the month can be approximated as follows:

$$\begin{aligned}\overline{X} &= \sum_{t=1}^{n} \frac{M_t + \epsilon_t}{n} \\ &= \sum_{t=1}^{n} \frac{M_t}{n} + \sum_{t=1}^{n} \frac{\epsilon_t}{n} \\ &\simeq \sum_{t=1}^{n} \frac{M_t}{n}\end{aligned}$$

as

$$\sum_{t=1}^{n} \frac{\epsilon_t}{n} \simeq 0.$$

$$\begin{aligned}s_X^2 &= E[(M_t + \epsilon_t)^2] - E^2[(M_t + \epsilon_t)] \\ &\simeq E[(M_t + \epsilon_t)^2] - \{\sum_{t=1}^{n} \frac{M_t}{n}\}^2\end{aligned}$$

Now,

$$E[(M_t + \epsilon_t)^2] = \sum_{t=1}^{n} \frac{M_t^2}{n} + \sum_{t=1}^{n} \frac{\epsilon_t^2}{n} + \sum_{t=1}^{n} \frac{2M_t\epsilon_t}{n}.$$

The degree of change in the mean daily maximum or minimum temperatures between successive months is usually within two degrees, and so it is likely that

$$\sum_{t=1}^{n} \frac{2M_t\epsilon_t}{n} \simeq 2M \sum_{t=1}^{n} \frac{\epsilon_t}{n} \simeq 0$$

where M is the mean of the M_t.

Hence, the variance of the months daily maximum temperatures can be approximated as

$$\begin{aligned}s_X^2 &\simeq \sum_{t=1}^{n} \frac{M_t^2}{n} + \sum_{t=1}^{n} \frac{\epsilon_t^2}{n} - \{\sum_{t=1}^{n} \frac{M_t}{n}\}^2. \\ &= \sum_{t=1}^{n} \frac{M_t^2}{n} + \sigma^2 - \{\sum_{t=1}^{n} \frac{M_t}{n}\}^2.\end{aligned}$$

Rearranging this equation, yields an estimate of $\sigma^2 = \text{var}(X_t)$

$$\sigma^2 \simeq s_X^2 - \sum_{t=1}^{n} \frac{M_t^2}{n} + \{\sum_{t=1}^{n} \frac{M_t}{n}\}^2.$$

It is, therefore, possible to estimate $\text{Var}(X_t)$ from monthly averaged data. The variance of the noise process $\{Z_t\}$ can now be estimated using equation (6) as

$$Var(Z_t) = (1 - r^2)\{s_X^2 - \sum_{t=1}^{n} \frac{M_t^2}{n} + \{\sum_{t=1}^{n} \frac{M_t}{n}\}^2\}. \qquad (7)$$

There are now two possible methods for applying this theory to predict the error variance for an AR(1) model with lag 1 correlation r, from a years monthly averaged data:

month	mean daily maximum temperature	variance of daily maximum temperatures
Jan	$\overline{T}_1$	s_{z1}^2
Feb	$\overline{T}_2$	s_{z2}^2
Mar	$\overline{T}_3$	s_{z3}^2
.	.	.
.	.	.
.	.	.
Dec	$\overline{T}_{12}$	s_{z12}^2

Method 1

Let the years average daily maximum temperature = $\overline{Z}$

$$\overline{Z} = \frac{\overline{T}_1 + \overline{T}_2 + \ldots + \overline{T}_{12}}{12}$$

and the years variance of daily maximum temperatures = s_z^2, it can easily be shown that

$$s_z^2 = \frac{\sum(s_{zi}^2) + \sum(\overline{T}_i^2)}{12} - \overline{Z}^2$$

Where,

s_{zi}^2 = the variance of daily maximum temperatures for month i

$\overline{T}_i$ = the mean of daily maximum temperatures for month i

Let T_{ij} be the expected maximum temperature for day j of month i, estimated by linear interpolation of the $\overline{T}_i$.

So,
$$Var(T_{ij}) = s_{ij}^2 = s_z^2 + \frac{365\overline{Z}^2 - \sum(T_{ij}^2)}{365}$$
$$= \frac{\sum(s_{zi}^2) + \sum(\overline{T}_i^2)}{12} - \overline{Z}^2 + \frac{365\overline{Z}^2 - \sum(T_{ij}^2)}{365}$$
$$= \frac{\sum(s_{zi}^2) + \sum(\overline{T}_i^2)}{12} - \frac{\sum(T_{ij}^2)}{365} = \sigma^2$$

Now,
$$Var(Z_t) = Var(T_{ij})(1 - r^2)$$
$$= \{\frac{\sum(s_{zi}^2) + \sum(\overline{T}_i^2)}{12} - \frac{\sum(T_{ij}^2)}{365}\}(1 - r^2)$$

When this method was applied to each data set, estimates of the error standard deviation were obtained. These are displayed in table 8, with the true error standard deviations obtained by fitting the full AR(1) models presented in brackets.

Table 8. Estimates of the error standard deviation for the adjusted AR(1) model using method 1, for data from 5 East African sites.

Site	estimated error standard deviation (truevalue)	
	Max. temps	Min. temps
Chipata 1986	1.96 (2.02)	1.41 (1.37)
Chipata 1987	2.12 (2.13)	1.63 (1.51)
Muguga 1968	1.47 (1.45)	1.15 (1.08)
Kizimbani 1984	1.21 (1.02)*	0.98 (0.90)
Zanzibar 1986	1.51 (1.17)*	1.31 (1.25)

* - poor estimate

Most estimates of the error standard deviation are good, except for two. Estimation inaccuracies arise in two ways. Firstly, the approximations neccesary in producing the formula for the variance estimate, equation (7), will create inaccuracies. Secondly, the average of the expected extreme temperatures for each month will not equal the observed monthly average extreme temperature. This is due to the linear interpolation

between month midpoints. There appears to be no simple, suitable method of interpolation to estimate the expected daily maximum or minimum temperatures whilst preserving the observed monthly mean. Those datasets with the largest estimation inaccuracies of the error standard deviation are those in which there is the biggest departure between successive monthly mean extreme temperatures. This increases inaccuracies in both the ways described above.

Method 2

An alternative approach is to treat each month seperately, and to obtain an estimate of the error variance for each month.

Let $Var(Z_{tj}) = Var(Z_t)$ for month j.

$$Var(Z_{tj}) = Var(\overline{T}_i)(1 - r^2)$$

$$= \{s_{zj}^2 + \frac{n\overline{Z}_j^2 - \sum(T_{ij}^2)}{n_j}\}(1 - r^2)$$

where,

s_{zj}^2 = the variance of daily maximum or minimum temperatures for month j,

$\overline{Z}_j$ = the mean of daily maximum or minimum temperatures for month j,

T_{ij} = the expected maximum or minimum temperature for the ith day of month j,

n_j = the number of days in month j.

When this method was applied to the Chipata 1987 monthly averaged data, the estimates of the error standard deviation for each month displayed in table 9 were obtained.

Table 9. Estimates of the error standard deviation for the adjusted AR(1) model using method 2, for data from Chipata in 1987.

	error standard deviations - S.d(ϵ_{ij})	
month	Max. temps	Min. temps
Jan	1.84	0.63
Feb	1.63	0.68
Mar	1.56	0.89
Apr	1.63	1.66
May	2.35	1.91
Jun	2.83	1.55
Jul	1.69	1.74
Aug	2.11	1.77
Sep	1.88	1.73
Oct	3.14	2.50
Nov	1.60	1.64
Dec	2.42	1.04
mean =	2.05	mean = 1.47
true =	2.13	true = 1.51

It should be noted that the mean of the error standard deviations for each month is very close to the actual error standard deviation when the AR(1) model is fitted to the true data. The validity of this method, however, is dubious because the lag 1 correlation is not estimated seperately for each month. A vast number of years data would be required for estimating the lag 1 correlation for each month. Because of its impractability, and due to its increased complexity, this method is abandoned.

Default values of lag 1 correlation and error variance

It is clear from the argument presented above that, given an estimate of the lag 1 correlation, the error variance can be accurately estimated from the within month variances presented in the monthly averaged data (using method 1). Thus, if a default value of the lag 1 correlations for maximum and minimum temperatures can be found to give reasonable development fractions estimates, then only the monthly averaged data would suffice to run simulations from. This is the objective, as monthly averaged

data is the only readily accessible form of climate data available to users of the model.

Taking the average of the lag 1 correlations for maximum and minimum temperature for the five sites gives mean lag 1 correlations of 0.462 and 0.431 for the adjusted maximum and minimum temperature sequences respectively. Using the monthly averaged data along with these mean lag 1 correlations, the estimates of model error standard deviation are obtained (method 1 above). These estimates are presented in table 10.

Table 10. Estimates of the error standard deviation for the adjusted AR(1) model using method 2, for data from 5 sites in East Africa, when the lag 1 correlations for the maximum and minimum temperature models are assumed 0.462 and 0.431 respectively.

	error standard deviations - S.d(ϵ_{ij})	
Dataset	max. temp.	min.temp.
Muguga 1968	1.98	1.30
Chipata 1986	2.21	1.71
Chipata 1987	2.32	1.87
Kizimbani 1984	1.16	0.93
Zanzibar 1986	1.38	1.26

Using these parameters, ten simulations at each site were performed, and values of the expected tick development time, E, obtained. These are displayed and summarised in table 11.

Table 11. Expected developmental times, E, for ticks at each site, using climatic data generated from AR(1) models using lag 1 correlations of 0.462 and 0.431 for adjusted maximum and minimum temperatures respectively.

	Dataset				
	Muguga	Chipata	Chipata	Kizimbani	Zanzibar
	1968	1986	1987	1984	1986
	267.95	96.58	89.41	73.86	73.65
	275.20	102.93	86.31 75.93	73.87	
	271.30	98.83	89.20	76.86	74.44
	268.82	100.07	91.58	77.67	74.03
	276.73	100.41	87.58	75.27	73.48
	272.85	102.19	90.15	77.10	74.43
	279.91	104.53	84.52	77.36	74.03
	272.73	100.41	85.33	77.67	74.10
	274.69	101.35	91.92	75.75	74.45
	293.81	110.80	94.78	78.58	73.88
mean	275.40	101.81	89.08	76.41	74.04
st. dev.	7.38	3.84	3.21	1.37	0.33
95% C.I.	(270.11, 280.68)		(86.78, 91.38)		(73.80, 74.28)*
		(99.06, 104.56)		(75.43, 77.39)	
true value	277.39	99.73	90.42	76.63	74.40

Only one of the 95% confidence intervals for the mean does not contain the true value, that being for simulations from the Zanzibar airport data (marked with the asterisk). However, the magnitude of this error is in the order of only one day, which is negligable as far as the model is concerned. The adjusted AR(1) model with default lag 1 correlations and estimated error variances therefore appears to produce very satisfactory results. In fact, comparison of these results with those for when an AR(1) model was fitted seperately to each dataset, presented earlier in table 6, suggests that the mean and standard deviation of the predicted expected developmnet time, E, is very sim-

ilar under both approaches. Only for the data from Muguga in 1968 is there a large difference in the standard deviation of these predictions. It would appear, therefore, that the default parameters provide an adequate approximation in the absence of site-specific parameter estimates.

6.6 CONCLUSIONS

Most models discussed in the literature concentrate on daily rainfall levels, daily temperatures being estimated once the sequence of rain or no-rain days is predicted. These models are unsuitable for modelling ticks, as temperature is the crucial factor required, and daily data for predicting rainfall sequences is rarely available.

The extreme value distribution method for predicting maximum and minimum tempertatures (Gumbel, 1952) provides a rainfall-independent method. However, development times estimated from temperature data predicted by this model appear consistently underestimated.

The proposed method, using an AR(1) model to predict a sequence of adjusted temperatures, appears to give rise to development times close to those expected. Moreover, the model appears robust enough to allow the use of default lag 1 correlations of 0.462 for maximum temperatures and 0.431 for minimum temperatures.

7. ECFXPERT: AN INTEGRATED MODEL

"Machines are worshipped because they are beautiful,
and valued because they confer power;
they are hated because they are hideous,
and loathed because they impose slavery."

Bertrand Russell, *Sceptical Essay.*

ECFXPERT is an integrated computer model designed for the investigation of *Rhipicephalus appendiculatus* tick populations, the disease East Coast fever (ECF) and its control. The model is designed to be used by a wide range of users from many disciplines in helping to answer differently motivated questions concerning ticks and the disease. A tick ecologist, for example, may be interested in investigating the factors that control various seasonal patterns exhibited by ticks, or the consequences of global warming on tick populations. A parasitologist may wish to explore the effects and importance of carrier status in recovered cattle. Alternatively, a farm manager might be interested in determining the most effective and economical method of disease control at a given location. ECFXPERT provides the facility to explore these questions. The model can also be used as a planning tool to determine effective research programmes by performing computer experiments to assess the suitability of a research thrust, and as an aid to experimental design.

Because it is intended that the model should be accessible to users from diverse areas of interest, the package is supported with comprehensive up-to-date data concerning all aspects of the disease. This enables all users to effectively understand and employ the models, and to interpret the results. In fact, the motivation in constructing such a package is that it would not just be of interest to scientists working in the area, but that planners and managers on local and national levels would find it a useful tool in decision making. It is therefore important to design the package in such a way that it can be used as effectively by experts and non-experts alike. Certainly, the opinions of scientists involved in ECF research is of major importance in critically evaluating the models and establishing its shortcomings and strengths. Shortcomings can be dealt with and strengths built upon, allowing the model to evolve into a useful and accurate

tool for studying disease control. If nothing else is achieved, the process of modelling a system will at least highlight those areas where knowledge is lacking, and where further research is required to complete our understanding of the problem. However, the model should not stop there. Once accepted by experts, it should be made available to the people involved in making decisions, such as composing reliable national dipping strategies, or cattle movement and importation laws. The consequences of such decisions involve great financial risk. For example, currently the governments of most African countries where ECF is a problem spend millions of dollars each year in maintaining intensive dipping strategies. Many experts now believe this to be a massive waste of resources. In fact, recommendations following the International Tick Symposium, ICIPE, Nairobi (1990) suggested that dipping should be reduced because intensive tick control reduces disease challenge, and consequently reduces resistance to disease. This can have devastating effects in areas where dipping is terminated or where ticks become resistant to acaricides. Possibly the most effective control is to reduce tick numbers sufficiently to prevent fatal disease, but allow mild infections which maintain disease resistance. The degree of tick control required to permit such a situation is likely to be finely balanced, and is a question that should be addressed by mathematical models if they are to be of practical value. The motivation behind ECFXPERT is that it will evolve into a state from where such powerful results can be extracted. To allow this, however, scientists and managers need to view models not as the hideous constructions of mathematicians, but in the light of their potential value. Present scepticism is a result of mathematical models being created to produce interesting or beautiful mathematics, not to effectively describe the complexity of the system under study. These models are not of interest to non-mathematicians. ECFXPERT offers the alternative approach, aimed not to produce elegant mathematics, but to generate improved understanding of the natural process.

7.1 ECFXPERT ENVIRONMENT AND KNOWLEDGE BASE

ECFXPERT runs on IBM and compatible microcomputers, and provides a user-friendly environment for performing computer experiments. The models are completely menu-driven, and on entering the package the user can select to run either the tick, ECF, dipping, or drug models, or to view a demonstration. Associated with each model are data screens containing default values for each model parameter. Screen editors allow these parameters to be viewed and edited. In addition, different climatic datasets can be selected, or created and saved within the package.

Expert knowledge available to the user is stored in three ASCII text files – a help file, a dictionary and a bibliography. Help messages are associated with every parameter contained in the data entry screens of each model, and provide current knowledge to assist in the choice of parameter value. Keywords, indicating areas where more information is available, appear highlighted on a particular message. Thus, in a hypertext-like manner, a user can progress through a series of help screens, increasing their knowledge on a particular aspect of the disease. Keywords and their associated messages are stored in the dictionary, which can easily be updated and extended – providing a growing and developing pool of knowledge available to educate the user. In a similar way, specific references to relevant literature and scientific papers are made available on request, or can be viewed in the bibliography which lists all scientific literature important in constructing the models and in understanding the disease.

Output screens provide graphical plots of numbers of ticks in each stage each day of the year, and dot-plots of weekly changes in the numbers of cattle to become infected, and die. Simple univariate summary statistics are displayed throughout runtime which provide useful and meaningful indices of disease risk. Statistics thought to distinguish different geographical sites as disease risks include: the percentage of the tick population questing, the percentage of infected questing ticks, and the average development times of ticks through their various developmental stages. A comprehensive summary of data describing the course of a particular simulation is stored in an output file for later study and analysis.

7.2 PROGRAMMING DETAILS

A major constraint in the development of the computer programs, was that the model was required to be fast and efficient enough to effectively simulate the biological processes in a length of time that will retain the attention of the user. Users will lose interest in models that are too slow, or badly presented.

In the process of programming, two main problems arose: how to present on screen the yearly profiles of ticks graphically, given the year to year changes in tick numbers; and how to efficiently store data on the tick population in such a way that each tick can be individually followed through its life cycle, and vast numbers of ticks can be dealt with.

Dynamic scaling of the tick population graph

Tick populations vary in size from year to year and from simulation to simulation. If the scaling of the graph is fixed, then a decaying tick population would be shown as a mass of lines close to the x-axis, and an expanding tick population would disappear off the top of the graph.

To optimise the scaling of the tick population graph, eggs and larvae are scaled differently to nymphae and adults to allow for the vast difference in the number of ticks in each stage, and the scalings are adjusted at the beginning of each year depending on the state of the tick population in the previous year. The algorithm that appeared most effective is as follows:

1. Record last years maximum counts of eggs, larvae, and nymphae.
2. Adjust the y-axis scaling by positioning last years nymphal peak three quarters of the way up the scale.
3. Scale down the number of larvae by positioning last years larval peak at the top of the new scale, and deducing the appropriate scaling factor for larvae.
4. Scale down the number of eggs in an identical way to the larval scaling.

A problem arises in choosing a suitable starting scale for the first year of the simulation experiment. This is chosen from experience, but is not too critical as it may take the tick population some years to stabilise into a steady state.

Data structures for handling the tick population

The majority of data handled in the simulation program is concerned with the tick population. The herd is assumed small enough (less than 200 animals) to present no real problems, and information on the age and status of each animal in the herd is stored in an array of records. The fecundity of ticks is required to be between 4000 and 6000 eggs per female in oviposition, so the total number of ticks present at any one time in a typical simulation experiment is likely to be in the order of many thousands. It is important, therefore, to choose data structures that will enable the program to be most time and memory efficient. The data structures used in the simulation of the tick life cycle are illustrated below in Figure 1.

The length of time spent in the feeding stages is constant for each stage (Branagan, 1978). The numbers of ticks feeding in each stage can, therefore, be stored in a single 1-[D] array of length equal to the time spent in that stage. At the beginning of each

day, ticks that have completed feeding are removed from the end of the array, and the other elements moved down one place. The number of newly attached ticks is placed in the first entry in the array. This number of newly attached ticks is calculated by generating a random variable from a Binomial(n,p) distribution, where n is the number of questing ticks of the appropriate stage, and p is the daily attachment probability. Efficient generation of random variables from the Binomial distribution was discussed in chapter 5.

Questing ticks will remain questing until they either die or attach. The number of ticks in each questing stage is stored as a single variable, which is incremented daily by newly developed ticks, and decremented daily by newly attached ticks.

Developing ticks can be handled as cohorts because ticks entering a developmental phase on the same day will become fully developed on the same day in the future. Each cohort will represent the number of engorged ticks, or eggs laid, arriving on any one day. The numbers of ticks in each developmental phase are stored in a circular list of sufficient length to never become totally full. Newly entering ticks are placed at the bottom of the list, newly developed ticks are removed from the top of the list. Pointers are kept assigned to the first element and last element of the list, and are adjusted whenever entries are removed or added. The number of entries in the list is recorded so as it is obvious whether the list is empty or full.

Associated with each block of ticks is a constant which enables the fraction of development completed by the start of any day to be established. A cumulative sum of each days development fraction for each developmental stage is kept throughout the simulation. When a new batch of ticks enters a developmental phase, they are assigned a developmental value, d, equal to the cumulative sum of development fractions up to that day, $S(day)$. Hence, when the sum of development fractions minus the developmental value becomes at least 1, then the tick batch has developed. I.e. When $S(day+n)-d \geq 1$, for some integer n, the ticks have developed.

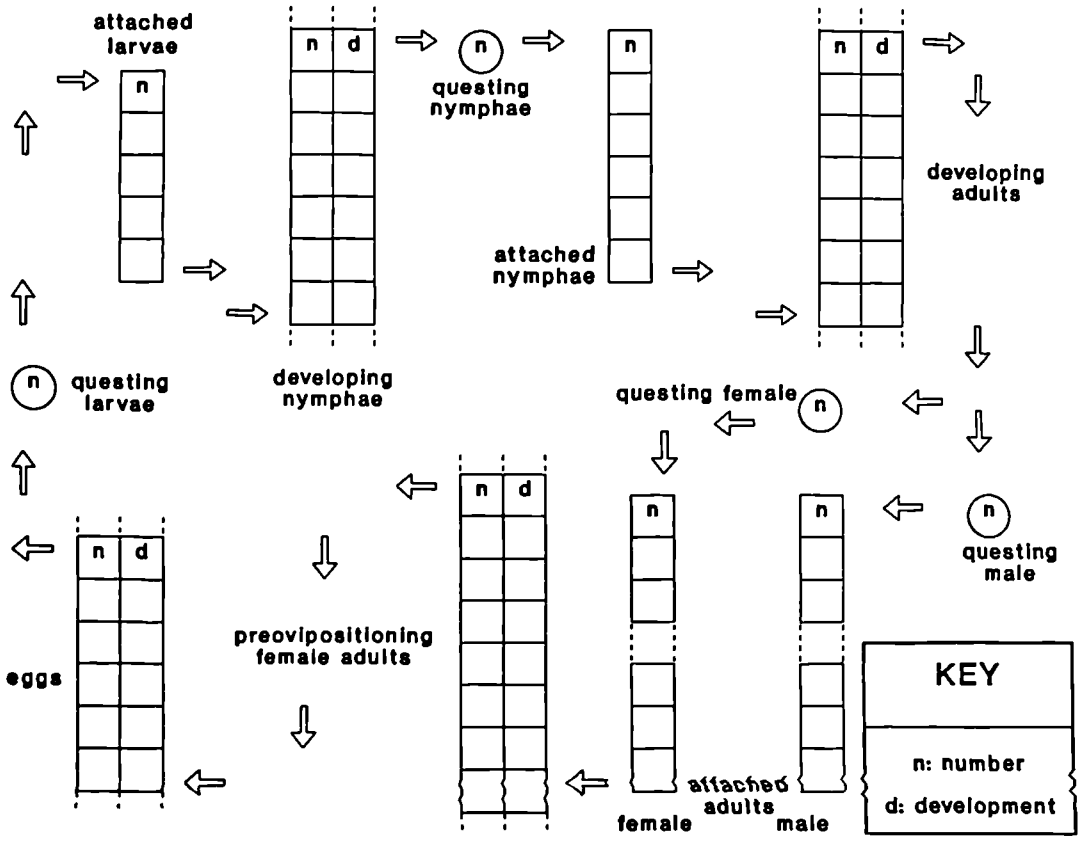

Figure 1. *Data structures employed by the tick life cycle model.*

The advantages of storing data in this way are great, as they facilitate the speed and simplicity of the program. Firstly, storing ticks in cohorts allows random events, such as the number of ticks surviving a particular day in a particular cohort, to be more efficiently simulated by using Poisson or Normal approximations to the Binomial distribution. Groups of developing ticks are stored in the order of most developed at top of list, least developed at the bottom of the list. This allows fast and efficient searching for developed ticks. Also, development fractions are only calculated once for all the ticks in a phase, rather than individually for each group of ticks. The numerical integration required to calculate development fractions is costly, and this enables the model to run faster.

7.3 THE ECFXPERT PACKAGE

ECFXPERT is supplied on a single 3.5 or 5.25 inch diskette and will run on IBM compatible microcomputers with 640K RAM and a VGA colour monitor. The package comes complete with up-to-date bibliography and dictionary files containing current scientific knowledge concerning the disease. These files are named BIB.TXT and ECFXPERT.DIC respectively. Help messages are stored in the text file ECFXPERT.HLP. Also supplied are a dozen or more climatic data sets, containing temperature and rainfall statistics for sites in Kenya, Tanzania, Zambia, and Zimbabwe. These are contained in files named with the extension .CLI. The package allows the facility to create and save new climatic data sets within ECFXPERT. Summary statistics describing the course of a simulation are stored in the text files TKSTAGES.TXT and TKATT.TXT for the tick model, and ECFOUT.TXT, DIPOUT.TXT and CHEMOUT.TXT for the ECF model, dipping model and chemotherapy models respectively. Summary statistics for the tick model consist of weekly predicted numbers of eggs, larvae, nymphae and adults and weekly predicted numbers of attached larvae, nymphae and adults. For the other models, these summary statistics consist of monthly numbers of questing ticks, yearly numbers of new ECF cases and yearly numbers of ECF fatalities. To use ECFXPERT simply copy the files from the diskette into a directory on the hard disk of your computer and type ECFXPERT.

The package was designed and assembled by G. Gettinby and W. Byrom at the University of Strathclyde for the Overseas Development Administration, U.K. The authors gratefully acknowledge the following persons and organisations for their advice and cooperation:

D. Berkvens,	T. Dolan,	J. Doyle,
E. Flach,	S. Hazelwood,	N. McHardy,
I. Morrison,	S. Morzaria,	R. Newson,
A. Norval,	B. Perry,	N. Short,

Cooper Pitman-Moore Animal Health Ltd., Berkhamsted, U.K.

International Laboratory for Research on Animal Diseases, Nairobi, Kenya.

The results of the models do not neccesarily represent the specific views of those people who generously contributed to the discussions.

8. RESULTS

"The roots of education are bitter,
but the fruit is sweet."

Aristotle, *Life.*

In the following sections, the results of a number of computer experiments are presented. These experiments were performed to help validate the ECFXPERT models, and to investigate the effects of certain parameters on model predictions. In all experiments, unless otherwise stated, the tick attachment rate was assumed 0.04, the herd was assumed to contain all immune cattle but offspring would be fully susceptible until challenged with the disease, and immune cattle were assigned carrier status with a probability of 0.05 of infecting feeding ticks. The herd parameters reflected an expanding herd commencing with only 30 members, with high growth and takeoff rates. In the absence of the disease, over 700 new cattle could be expected to be produced by the herd in a twenty year period, and of these around 300 would remain for their first year at least.

Within each simulation, various statistics were recorded to describe the behaviour of the tick population and the disease. Statistics thought useful in describing the tick population were the seasonal occurrence of the attached stages, which also correspond to periods of possible disease outbreak, and the number of questing ticks present each month of the year. Questing tick totals were summarised as mean, maximum and minimum monthly totals for each year of each simulation, and describe the yearly and within year changes in tick challenge. Tick data from the first five years of each simulation were discarded, as it was observed that this period of time was required for the tick population to stabilise. Statistics recorded to assess disease prevalence were the number of incidences of disease in a particular simulation, and the proportion of these infections that resulted in fatalities. All Statistical tests, comparing predictions under different conditions, were performed on the results using 5% or less significance levels.

8.1 VALIDATION OF MODELS

Many studies at different geographical locations report observations on the seasonal abundance of attached ticks. These reports can be used to help validate the tick model. The development fractions technique has already been shown to be satisfactory (King *et al.*, 1988) by comparison of predicted development times with field observations (Branagan, 1973b). Unfortunately, validation of the ECF model is not straight forward. Field tests of the model at different sites where ECF is endemic are required.

The observed occurrence of attached ticks

Four tick surveys reported in the literature were investigated:

Mwanza, Tanzania ($2°S, 33°E$): Larvae, nymphae and adults are present throughout the year (McCulloch *et al.*, 1968).

Nyabubinza, Tanzania ($3°S, 33°E$): Peak numbers of adults, larvae and nymphae occur from October to March, February to August and May to November respectively (Yeoman, 1966).

Nanduba, Zambia ($16°S, 28°E$): Adults occur between November and June, larvae between February and August, and nymphae between March and October. Moreover, two peaks of nymphs appeared to occur in May and July (MacLeod and Colbo, 1976).

Lake McLlwaine, Zimbabwe ($18°S, 31°E$): Adults occur between November and June. Larvae and nymphae occur in high numbers between March and December, and May and January respectively (Short and Norval, 1981a).

Model predictions

The model was seen to produce very satisfactory predictions at three of the four sites considered. Figures 1a, 1b, 1c and 1d illustrate the predicted abundance of attached larvae (thin solid line), nymphae (broken line) and adults (thick solid line) at Mwanza, Nyabubinza, Chipata and Lake McLlwaine respectively. Chipata ($13°S, 32°E$) was chosen in place of Nanduba, as climatic data were not available for this site. Predictions for Mwanza using the ECFXPERT tick model are good. It is predicted that ticks of each stage will be found attached to animals throughout the year. At Nyabubinza predicted adult and larval presence is very close to that observed. Two peaks of nymphae are predicted, one from January to April, the other from May to October. The second peak correlates well with observations, the first peak not being reported.

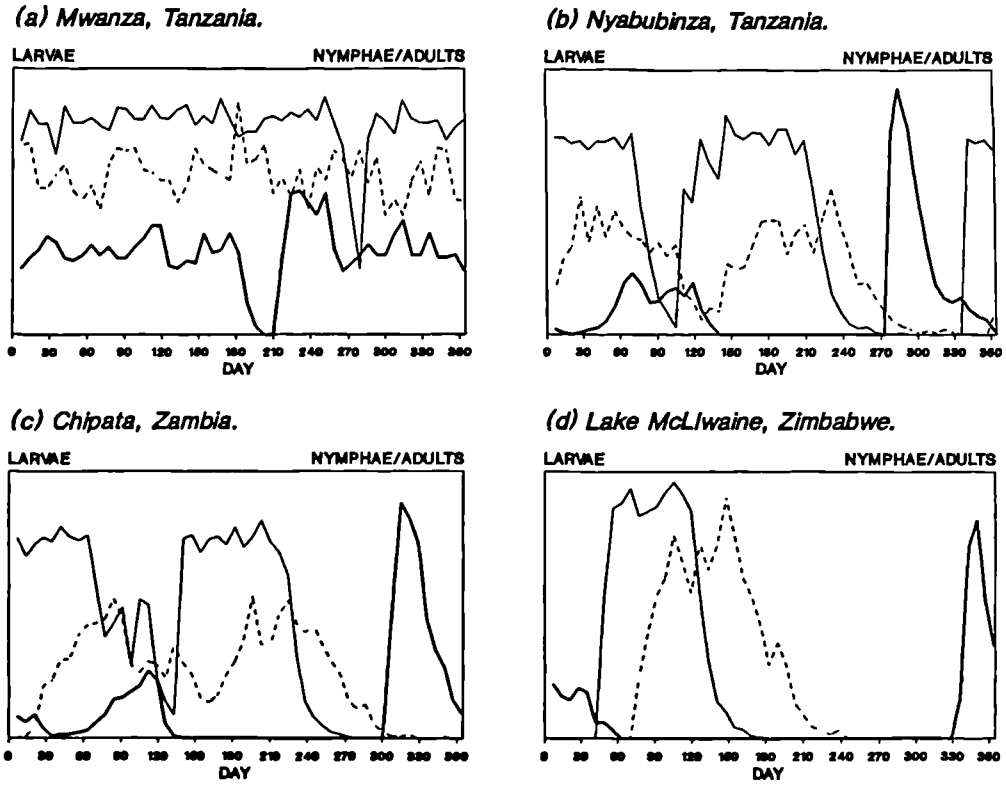

Figure 1. *Predicted seasonal occurrence of attached ticks at four sites.*

At Chipata, the predicted seasonality of attached ticks in all stages follows closely to that observed for Nanduba. The observed bimodal nymphal distribution is also predicted, maxima occurring between March and May, and July and August. Predictions for Lake McLlwaine show that the time of appearance of attached ticks in each stage is consistent with observations. However, attached ticks are observed on animals for much longer periods than those predicted. This could possibly be overcome by reduction of the questing tick attachment probability, causing peaks to become more elongated.

8.2 THE OBSERVED VARIATION IN MODEL OUTPUT

To illustrate the natural variation exhibited by the model, a computer experiment comprising of ten simulations of the ECF model over a 20 year horizon at Chipata was performed. Ten simulations were observed to be sufficient in producing reliable estimates of the mean and variance of predicted statistics. In this experiment, all recovered cattle were assumed carriers, each with a probability of 0.05 of infecting feeding ticks.

Yearly variation in the distribution of attached ticks

Figure 2 illustrates the variation in the numbers of larvae and nymphae attached to animals within a single 20 year simulation. The thin solid line, thick solid line and broken line represent output from the fourth, seventh and tenth years of the simulation respectively. The general position and height of the peaks is similar from year to year, although much variation is seen to occur which may have an effect on disease. Little year to year variation in the distribution of attached adults was observed.

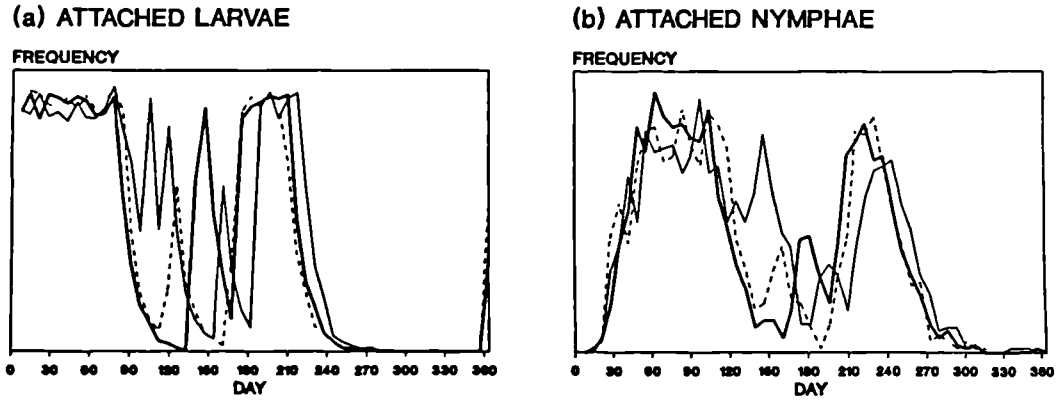

Figure 2. *Predicted variation in attached ticks at Chipata.*

Yearly variation in the duration of developmental periods

Expected modal development times can be calculated by dividing 365 by the sum of development fractions for each day of the year. The observed modal development times may not be equal to those expected because of the seasonality observed at Chipata, however, this statistic does give an indication of the variation seen in model output.

Within a single 20 year simulation the expected mode duration of the pre-eclosion, larva to nymph moult, nymph to adult moult, and pre-oviposition phases were seen to vary from 43 to 46 days, 13 to 14 days, 22 to 24 days and 8 to 9 days respectively.

Variation in disease incidence over a 20 year period

The disease incidence varied substantially from year to year within a single 20 year simulation. In all years, most susceptible cattle contracted the disease, but the proportion of infections that were fatal varied from none in some years, to almost all infected cattle in other years. Results of the computer experiment showed that the proportion of infections that were fatal in each 20 year simulation varied from 0.246 to 0.406. The mean proportion of infections in 20 years resulting in fatal disease reactions was 0.301, with standard deviation 0.050.

8.3 THE EFFECTS OF THE TICK ATTACHMENT PROBABILITY ON TICK POPULATIONS AND ECF

The effects of changing the tick attachment probability was investigated by performing computer experiments using meteorological data for Chipata, where ticks exhibit strong seasonality (Figure 1c), and for Mwanza, where ticks of each stage are present throughout the year (Figure 1a). At both sites computer experiments comprising of 10 simulations, each of 20 years, were performed for a range of attachment probability values: 0.045, 0.04 [default], 0.03, 0.025 and 0.02. At each site an attachment probability of 0.045 produced a tick population that was rapidly increasing, the number of ticks exceeding as many as 1000 million before the end of a single 20 year simulation. Attachments of 0.04 and 0.03 appeared to produce fairly steady state tick populations at both sites.

Attachment rates of 0.025 at Chipata caused extinction of the tick population within the 20 year simulation 8 out of 10 times. In one case, extinction was attained as early as day 70 in year 8. Extinction of the tick population was observed for all 10 simulations at Chipata when the attachment rate was as low as 0.02.

However, at Mwanza, the effects of lowering the daily attachment rates to 0.025 and 0.02, did not cause extinction of the tick population in any of the simulations performed. This is because conditions for ticks are more favourable at Mwanza, and adult ticks exhibit little quiescence and so the attachment probability is less critical.

Statistical analysis was performed on measurements of disease severity for predictions from each site. Analysis was confined to comparing the groups with attachment rates of 0.04, 0.03 and 0.025. In those simulations that continued for the full 20 years at Chipata, the mean numbers of ECF cases were 247, 212 and 166 per simulation when attachment rates were 0.04, 0.03 and 0.025 respectively. A multiple range test suggested that the incidence of disease was highest when the tick attachment rate was 0.04, and lowest when the tick attachment rate was 0.025. However, the mean proportion of infections that were fatal in each group did not appear to be significantly different ($p = 0.886$).

For predictions at Mwanza, the mean numbers of infections arising in simulations when the tick attachment rate was 0.04, 0.03 and 0.025 were 215, 309 and 231 respectively. In the case when the attachment rate was 0.03 there appeared significantly more infections than in the other two cases. This is a strange result. The mean proportions of infections resulting in fatalities were not significantly different between groups

($p = 0.752$), being 0.325, 0.314 and 0.313 for groups with attachment rates of 0.04, 0.03 and 0.025 respectively.

8.4 THE EFFECTS OF INFECTIVE PERIOD AND CARRIER STATUS ON DISEASE

Using data for Mwanza and Chipata, it was observed that when the infectious period of recovering cattle was 5 days this was not sufficient to maintain the disease. Typically cattle and ticks ceased to become infected within 2 years, resulting in extinction of the parasite.

The infectious period of cattle that recover was increased to 20 days, which was more in line with expert opinion, although no published data were available to estimate this parameter. In this case, disease challenge was maintained for a longer period, but in all simulations dissappeared within the first 5 years.

It is clear that infection cannot be maintained simply from a short infectious period in cattle that are infected. In this case the timing of the infectious period becomes critical, and because it may not always correspond to a period of high tick challenge, the parasite is doomed to eventual extinction.

Carrier status was introduced, whereby cattle that recover become immune to the disease, but maintain small numbers of parasites in their bloodstream which can be transferred to feeding ticks. In this case, disease challenge was maintained throughout all simulations up to 20 years. The effects of varying the infectivity rate of carrier cattle is discussed below in section 8.9.

There exists much disagreement amongst experts as to the role of carrier status amongst recovered cattle. The model results suggest that carrier status must exist for the infection to be maintained, although this result excludes the possibility of wild hosts providing a reservoir for maintaining transmission of the disease.

8.5 THE EFFECTS OF CLIMATIC CHANGE ON TICK POPULATIONS AND ECF

To investigate the effects of climatic change on ticks and disease, two sites were considered: Chipata and Mwanza. At each site, mean monthly maximum and minimum temperatures were reduced by 5 degrees, 2 degrees, and 1 degree, not changed, and increased by 1 degree, 2 degrees and 5 degrees respectively, producing a total of 7 computer experiments for each location. Each computer experiment comprised of ten simulations of the ECF model over a 20 year horizon. All recovered cattle were assumed

carriers, each with a probability of 0.05 of infecting feeding ticks.

Effects on the distribution of attached ticks

When temperatures were reduced by 5 degrees at Mwanza, the tick population soon became extinct due to the predicted period of quiescence in adult ticks extending over the whole year. Similar reduction in temperatures at Chipata predicts adults to be inactive for 11 months in the year. In some cases this was sufficient to cause extinction of the tick population. Figures 3 and 4 contrast the change in the yearly distribution of attached ticks when temperatures were reduced by 2 degrees and increased by 5 degrees at Chipata and Mwanza. Larvae are represented by a thin solid line, nymphae by a broken line and adults by a thick solid line. These Figures can be compared to Figures 1c and 1a showing the distribution of attached ticks at Chipata and Mwanza predicted using the default climatic data for each site.

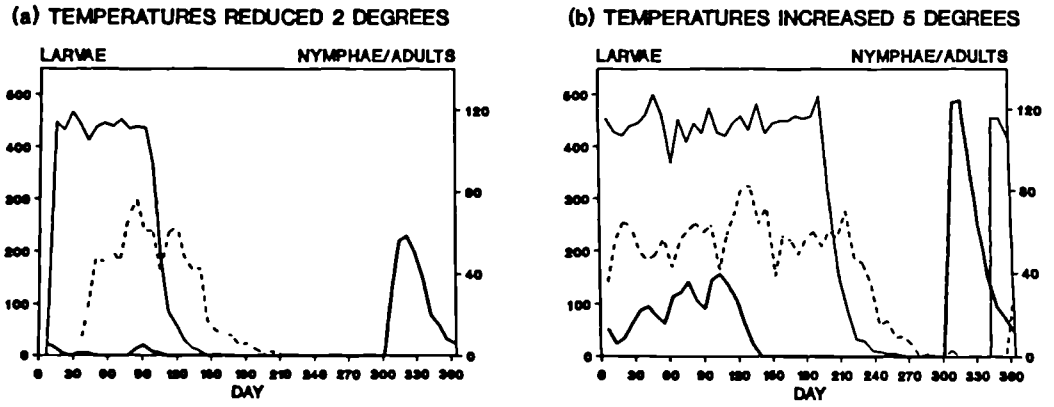

Figure 3. *The effect of temperature change on the seasonal distribution of attached ticks at Chipata.*

When temperatures were reduced by 2 degrees at Chipata, the distribution of attached larvae and nymphae changed from being bimodal (Figure 1c) to having a single mode (Figure 3a). The period of time larvae and nymphae were observed attached to animals was reduced significantly: larvae were observed for 5 months instead of 9 months, nymphae for 6 months instead of 10 months. The distribution of attached adult ticks remained very similar. When temperatures were increased by 5 degrees, the bimodality of the distribution of larvae and nymphae again disappeared (Figure 3b), but the period of time for which ticks of these stages were observed was maintained. Again, the distribution of adult ticks remained similar.

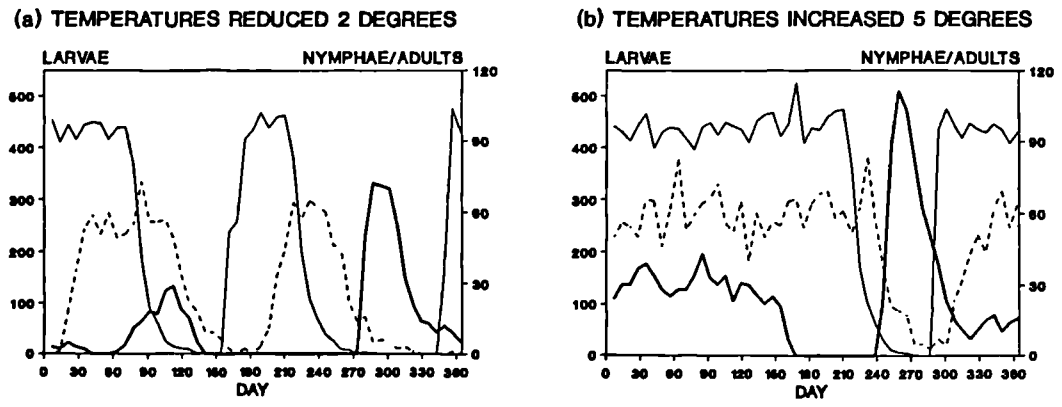

Figure 4. *The effect of temperature change on the seasonal distribution of attached ticks at Mwanza.*

Reduction of temperatures by 2 degrees at Mwanza, caused the distribution of attached ticks to change from ticks of all stages being observed all year round (Figure 1a) to bimodal patterns (Figure 4a). Larvae were predicted to occur in high numbers between December and March, and June and August; nymphae between February and May, and August and September; and adults between October and December, and March and April. When temperatures were increased by 5 degrees (Figure 4b), a short period of quiescence in adult ticks between June and August caused attached adults to be absent during these months. This consequently caused larval numbers to drop between August and October, and nymphal numbers between September and October.

Effects on the development times of ticks

Figure 5 shows the expected modal development times for the pre-oviposition, nymphal moult, larval moult and pre-eclosion phases, predicted for each computer experiment performed at Mwanza.

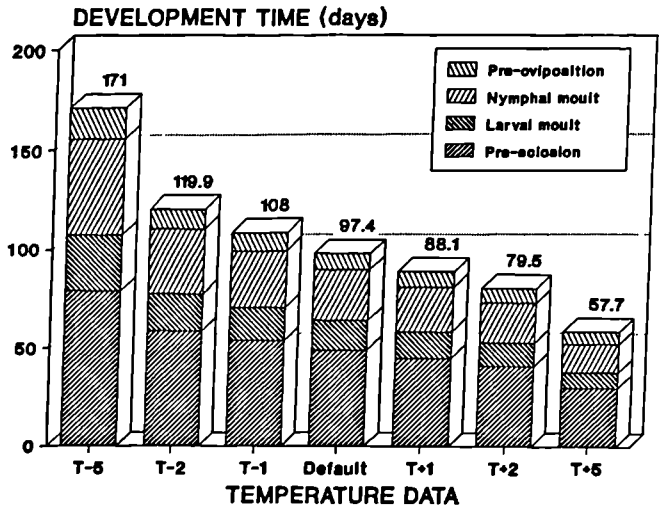

Figure 5. *The effect of temperature change on the development times of ticks at Mwanza.*

In each case, as temperatures increase, development times decrease. The sum of expected mode developments for the four phases was reduced from 171.0 to 57.7 days over the range of temperatures considered. At Chipata, a similar reduction in development times was observed, from 157.3 to 50.3 days over the same temperature range.

Effects on the timing and prevalence of disease

Ticks contract infection whilst feeding in larval and nymphal stages, and transmit infection to cattle whilst feeding as nymphae and adults. The timing of disease outbreaks therefore corresponds with periods of nymphal and adult feeding.

Under the default climatic data for Chipata, infections can occur all year round, although are most likely between mid-February and mid-April, July and September, and November and December (Figure 1c). A reduction of temperatures by 1 degree has little effect on the timing of disease, but a reduction of 2 degrees, however, has a significant effect: infections are not observed between August and October, and the main periods of disease outbreak are February to May and November to December (Figure 4a). Increasing temperatures at Chipata has little effect on the timing of disease (Figure 4b).

At Mwanza, infections can occur all year round under the default climatic data (Figure 1a). Reducing temperatures by 1 degree has little effect on the timing of infections, the disease is still present all year round. When temperatures are reduced by 2 degrees, infections can still occur at any time of the year, but are more likely between February and mid-May, and mid-July and November (Figure 5a). Increasing

temperatures at Mwanza appears to have no significant effect on the timing of disease.

For each site, the proportion of infections that were fatal after 20 years of simulations using the default climatic data, temperatures reduced by 2 degrees and temperatures increased by 5 degrees, were tested for differences using one-way analysis of variance. At Chipata there appeared to be no significant difference ($p = 0.682$) in the proportion of infections causing death after ten simulations under each of the three different climatic scenarios.

However, at Mwanza the proportion of infections that were fatal under the default data appeared to be higher than under the reduced or increased temperature data, using a multiple range test. This observation, however, was not quite statistically significant ($p < 0.061$). The mean proportions of infections that were fatal were 0.298, 0.299 and 0.325 for experiments with temperatures reduced by 2 degrees, increased by 5 degrees and not changed, with standard deviations of 0.0272, 0.0229 and 0.0307 respectively. A possible explanation for the difference is the appearance of periods of quiescence when the temperature data are changed. When temperatures are reduced by 2 degrees, adult ticks are predicted inactive between May and September, and when temperatures are increased by 5 degrees adults are predicted to quiesce between June and August. This will affect the survival of adult ticks, which may produce the observed changes in disease prevalence.

8.6 THE EFFECTS OF GRASS LENGTH ON TICK POPULATIONS AND ECF

Four computer experiments comprising 10 simulations over a 20 year horizon were performed at Mwanza and Chipata under short and long grass habitats. In each experiment recovered cattle were assumed carriers with an infective probability of 0.05.

The results for each site were quite different. At Chipata under long grass conditions, tick populations exhibited strong seasonality (Figure 1c) due to the long period of adult quiescence between May and October. In short grass conditions, the dry season corresponded with the timing of maximum questing activity of larval ticks. This reduced the number of larvae to such an extent that in all 10 simulations for short grass habitats the tick population became extinct within 6 years. In some cases extinction was as rapid as 2 years. This could suggest that in such strongly seasonal locations, heavy grazing may have a detrimental effect on ticks and disease.

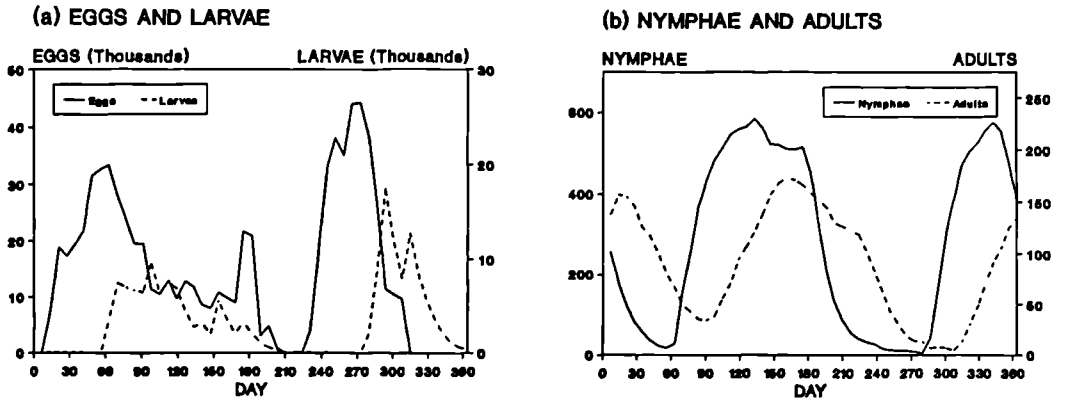

Figure 6. *Predicted distribution of the total tick population in short grass habitats at Mwanza.*

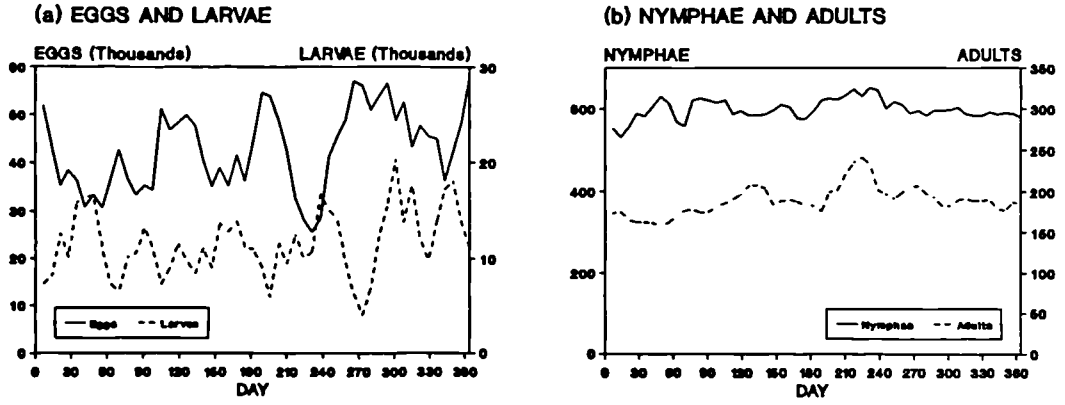

Figure 7. *Predicted distribution of the total tick population in long grass habitats at Mwanza.*

At Mwanza, however, the effects of short grass were not so catastrophic, but just as dramatic. Figures 6 and 7 present the predicted yearly distribution of eggs, larvae, nymphae and adults for ticks in short and long grass habitats respectively. These Figures illustrate the total numbers in each stage, not just the numbers of attached ticks. Figure 7 shows that eggs, larvae, nymphae and adults are present throughout the year in long grass habitats. However, Figure 6 shows that when the grass is short, seasonality is observed. This seasonality is produced by the level of rainfall in July being low, causing egg and larval numbers to be reduced due to desiccation. This consequently effects nymphal and adult numbers which are predicted to occur in two waves each year. The observed behavioural differences in the tick population have an influence on disease. In long grass habitats, disease was predicted to occur at any time of year. However, in short grass habitats, disease was unlikely to occur in

October. Moreover, in long grass habitats the proportion of infections that were fatal in 20 years of simulations appeared higher ($p < 0.051$) than in short grass habitats. The proportion of infections that were fatal had means 0.325 and 0.299 with standard deviations of 0.0307 and 0.0202 for long and short grass habitats respectively.

8.7 THE EFFECTS OF DIPPING ON TICK POPULATIONS AND ECF

For ticks at each site, Mwanza and Chipata, four different dipping strategies were investigated by computer experimentation and compared to the predictions when no dipping was performed. Different acaricides were investigated by changing the efficacy and residual period parameters, and different strategies investigated by changing the number of days between successive dips. The dipping strategies considered were:

Strategy	Dipping interval	Residual period	Efficacy
[A]	15 days	3 days	30%
[B]	15 days	3 days	50%
[C]	30 days	6 days	30%
[D]	30 days	6 days	50%

For each site, 10 simulations comprising a 20 year period were performed under each dipping strategy and for the no dipping case. Recovered cattle were assumed to have carrier status, with a probability 0.05 of infecting feeding ticks.

Computer experiments at Mwanza predicted that the mean proportions of infections that were fatal were 0.325, 0.298, 0.318 and 0.300 for the no dipping case, dipping strategy [A], dipping strategy [C] and dipping strategy [D] respectively. It was impossible to analyse the data from dipping strategy [B] as in all but one of the 10 simulations the tick population became extinct. Analysis of variance showed no significant difference in the proportion of infections that were fatal in the dipping and no dipping cases ($p = 0.247$). The mean number of infections that were recorded over 20 years under each scenario were 215, 252, 266 and 257 for the no dipping case, dipping strategy [A], dipping strategy [C] and dipping strategy [D] respectively. Analysis of variance of these data suggested the surprising result that no significant difference in the number of infections occurring in the no dipping and dipping cases could be observed ($p = 0.221$). These results support the theory that only one tick is required to transmit the disease, and that the infection vectored by one infected tick is sufficient to produce fatal ECF.

The predicted yearly means of monthly questing tick totals from years 6 to 20 in each of the ten simulations under each of the five treatment groups for Mwanza

were analysed using a repeated measures design. The interaction between year and dipping strategy was not significant, suggesting that similar patterns of questing ticks could be observed through time in the predictions for each group. The mean monthly totals of questing ticks at Mwanza were 27001, 13857, 547, 17987 and 11117 for the no dipping case, dipping strategy [A], dipping strategy [B], dipping strategy [C] and dipping strategy [D] respectively. The predictions for dipping strategy [D] represent a 98% decrease in the size of the tick population. A multiple range test indicated that the numbers of questing ticks predicted under each dipping strategy were all significantly different. Strategy [B] was the most effective in reducing tick numbers, then strategy [D], then strategy [A], then strategy [C]. Each strategy was a significant improvement over the no dipping case. Similar patterns were obtained from the maximum and minimum monthly numbers of questing ticks.

At Chipata, where ticks are predicted to exhibit seasonal behaviour rather than be present throughout the year as at Mwanza, predictions indicated that the mean proportions of infections that were fatal were 0.301, 0.302, 0.283 and 0.304 for the no dipping case, dipping strategy [A], dipping strategy [C] and dipping strategy [D] respectively. As before, the data from dipping strategy [B] were unable to be analysed as in all of the 10 simulations the tick population became extinct. The tick population became extinct once out of the 10 simulations under dipping strategy [A], and four times out of 10 under dipping strategy [D]. Only the infections data corresponding to simulations where the tick populations persisted for the full 20 year period were used in the analysis, which again indicated that dipping had no significant effect on the proportion of infections producing fatal disease ($p = 0.663$). The mean total number of infections occurring over 20 years under each scenario were 246, 195, 189 and 163 for the no dipping case, dipping strategy [A], dipping strategy [C] and dipping strategy [D] respectively. The data suggested that under dipping strategies [C] and [D] there may be fewer infections than under dipping strategy [A], and that dipping strategy [A] may permit fewer infections than the no dipping case ($p < 0.065$). This result is not quite significant, but is different to that for simulations at Mwanza, that clearly indicated no differences between the groups ($p = 0.221$).

Repeated measures analysis on the mean monthly totals of questing ticks predicted for Chipata again indicated that the interaction between year and dipping strategy was not significant. The mean monthly total numbers of questing ticks in each group were 65, 2741, 3815, 6628 and 11386 for dipping strategy [B], dipping stategy [D],

dipping stategy [A], dipping stategy [C], and the no dipping case respectively. The predictions for dipping strategy [D] represent a 99.4% decrease in the size of the tick population when compared to the predictions for the no dipping group. A multiple range test indicated that all dipping strategies significantly reduced the mean monthly total number of questing ticks. Analysis also suggested that dipping stategy [B] was the most effective in reducing the monthly total of questing ticks, then dipping strategy [D], then dipping strategy [A], and then dipping strategy [C]. Similar patterns were obtained from the mean minimum and maximum monthly totals of questing ticks. This result is analogous to that obtained from predictions using the data for Mwanza.

Figure 8 shows the mean monthly number of questing ticks for each year under each scenario at Chipata. The differences between the five groups are clearly illustrated, and it is interesting to note that the tick population appears to have achieved a steady state in each case.

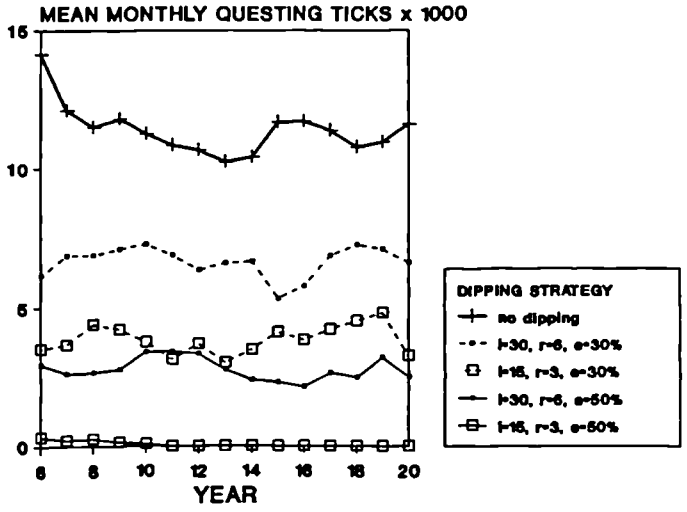

Figure 8. *Predicted changes in the numbers of questing ticks under each dipping strategy at Chipata.*

It is interesting that for simulations for both sites strategy [A] appears better than strategy [C], and strategy [B] appears better than strategy [D]. Strategies [A] and [C] both employ an acaricide of 30% efficacy, but in strategy [A] the acaricide is assumed active for only half the time of strategy [C], but is administered twice as regularly. The same is true of strategies [B] and [D], only the acaricide efficacy is increased to 50% in these cases. One might expect, therefore, that the net effects of strategies [A] and [C], and [B] and [D], would be the same. However, the predicted differences can be explained by considering the proportion of the tick population that is likely to be affected by the

acaricide under each strategy. As mentioned in chapter 5, female ticks normally spend a period of 9 days attached to a host whilst engorging and mating. When the dipping period is 15 days and the residual effect of the acaricide is 3 days, only those female ticks attaching one or two days after the chemical has ceased to be active will avoid its effects. However, when the dipping period is 30 days and the residual effect increased to 6 days, female ticks attaching between 1 and 23 days after the acaricide has ceased to be efficacious will not be affected by the chemical. This represents a much higher proportion of the female tick population that are not challenged by the acaricide, and may go on to produce eggs.

8.8 THE EFFECTS OF CHEMOTHERAPY ON DISEASE

The effects of drug treatment of infected cattle were considered for two drugs, parvaquone and buparvaquone, administered at the manufacturers recommended doses, $1 \times 20mg/kg$ and $1 \times 2.5mg/kg$ respectively. The parameters describing the action of each drug were estimated from clinical trials data supplied by Dr. N. McHardy at Cooper Pitman-Moore Animal Health Ltd. and are as follows:

Parvaquone at $1 \times 20mg/kg$***:***

Increase in the infective period of treated cattle that die: $\times$ 2.863 days,

Probability that the treatment is unsuccessful: 0.033,

Probability that treated cattle that recover become infectious to feeding ticks: 0.286.

Buparvaquone at $1 \times 2.5mg/kg$***:***

Increase in the infective period of treated cattle that die: $\times$ 2.472 days,

Probability that the treatment is unsuccessful: 0.208,

Probability that treated cattle that recover become infectious to feeding ticks: 0.552.

Computer experiments were performed to investigate drug action at Mwanza and Chipata. At each site, 10 simulations were repeated under three scenarios: no treatment of infected animals, treatment of infected animals with parvaquone (clexon) and treatment with buparvaquone (butalex). Simulations were recorded over a 20 year horizon and recovered cattle were assumed to have carrier status with a probability 0.05 of infecting feeding ticks. Oneway analysis of variance was performed on the two statistics describing predicted disease prevalence at each site: the number of infections observed within the herd in each 20 year period and the proportion of these infections that resulted in fatalities. The results of the statistical analysis are as follows.

For cattle at Mwanza, the mean proportions of infections that were fatal were 0.325, 0.008 and 0.064 for the no treatment, parvaquone treatment and buparvaquone treatment groups respectively. A multiple range test indicated that both drugs significantly reduced the proportion of infected cattle that died, and also that parvaquone was significantly more effective in reducing fatalities than buparvaquone. The mean numbers of infections in the 20 year periods were 215, 404 and 417 for the no treatment, parvaquone treatment and buparvaquone treatment groups respectively. A multiple range test also suggested that significantly more infections were observed amongst the herd when treating infected animals with drugs, than when not treating infected animals. This result is somewhat of a red-herring, as drug treatment allows more cattle to survive, and the herd to expand at a greater rate – hence more infections are observed as there are more cattle present.

At Chipata, similar predictions were obtained. The mean proportions of infections that were fatal were 0.301, 0.009 and 0.061 for the no treatment, parvaquone treatment and buparvaquone treatment groups respectively. Again, using a multiple range test it appeared that both drugs significantly reduced the proportion of infected cattle that died, and also that parvaquone was significantly more effective than buparvaquone. The mean numbers of infections recorded in the 20 year periods were 246, 288 and 302 for the no treatment, parvaquone treatment and buparvaquone treatment groups respectively. Analysis of variance suggested that the number of infections occurring in the groups treated with drugs could be larger than in the no treatment group ($p < 0.06$), for the same reasons as discussed above.

The results of simulations for both sites clearly illustrate the benefits of chemotherapy on ECF control. However, the result that parvaquone is more effective in control than buparvaquone should be treated with great caution. The data used in evaluating parameters for each drug were based on laboratory trial results using the same *T. parva* (Muguga) parasite strain. However, host differences in each trial are not accounted for, as many trials concerned the testing of just one of the two drugs. In fact, the data for buparvaquone includes the results of one trial which gave poor results and where parvaquone was not used. Obtaining standardised data for comparison of the two drugs is vital, as the model prediction that parvaquone is superior to buparvaqoune is at variance with field trial results (McHardy, personal communication).

8.9 THE EFFECTS OF THE CARRIER INFECTIVITY RATE ON DISEASE

To investigate the effects of the infectivity of carrier cattle, a computer experiment was performed using data for Chipata. The ECF model was used to test five different values of the carrier infectivity rate – 0.4, 0.2, 0.1, 0.05, 0.025. The infectivity rate was assumed at most 0.4, as this is the literature estimate for the infectivity rate of cattle suffering from the disease (Purnell *et al.*, 1973). For each scenario, ten simulations each over a 20 year horizon were performed, and the resulting predicted numbers of ECF infections fatalities were recorded. The results were as follows.

When the carrier infectious probability was 0.4, the herd became extinct due to severe ECF three times out of the ten simulations, and twice out of ten when the infectious probability was 0.2. In the other three scenarios, none of the predicted disease outbreaks were not severe enough to cause loss of the herd. In those simulations where the herd survived the full 20 year period, the mean number of incidences of disease in 20 years was 184, 245, 242, 256 and 249 for the cases when the carrier infectious probability was assumed 0.025, 0.1, 0.05, 0.4 and 0.2 respectively. There appeared to be no significant differences between the groups ($p = 0.062$). It is possible, however, that when the infectious probability is 0.025 there are fewer infections than in the other cases, which follows from a multiple range test at a significance level of 10%. The mean proportion of infections that were fatal over 20 years of simulations were 0.299, 0.301, 0.311, 0.347 and 0.442 for the groups with infectious probabilities 0.025, 0.05, 0.1, 0.2 and 0.4 respectively. A multiple range test indicated that the proportion of infections that resulted in death of the host was significantly higher when the carrier infectious probability was 0.4 than in the other groups. It is interesting that the proportion of fatalities in the other groups increases with the infectious probability. This is as might be expected, although the predicted differences were not statistically significant.

8.10 CONCLUSIONS

As mentioned in an earlier chapter, one aim of building a complicated model of a complex system is to investigate areas where knowledge concerning the system is lacking. One such area is the attachment rate of ticks, which is a parameter rarely attempted to be measured experimentally. The results of section 8.3 suggest that when between 3% and 4% of questing ticks are able to attach each day, this leads to a fairly steady state tick population, at least for the sites under study. Below this attachment rate, tick populations are predicted to decline and eventually disappear; above this rate popula-

tions are predicted to expand uncontrollably. The attachment rate of ticks is unlikely to be a simple figure, such as 4%, but is more likely to be controlled by a number of factors. In particular, age and breed differences are seen to influence tick burdens. It would be interesting to design experiments to investigate, and attempt to quantify, the effects of host age and breed on tick pick-up rates.

Another area of uncertainty that was investigated by the model was the role of carrier status in the disease dynamics. These results are presented in detail in sections 8.4 and 8.9. Predictions indicated that carrier status must exist for the infection to persist in cattle. It is clearly very difficult to ensure parasite transmission from animal to tick if only clinical cases are infectious. The infectious period of an animal suffering from East Coast fever is likely to be less than 3 weeks. This would require a large number of ticks to attach within a short period of time, to ensure successful parasite transmission from the infected animal to the tick population, and then eventually back from the tick population to another animal. It is not in the interests of the parasite, which has survived successfully for such a long period of time, to live so dangerously. Although many experts state that recovered animals are capable of transmitting infection to feeding ticks, the literature does not contain any data quantifying the infectivity of these animals. Clearly, the carrier state in recovered animals is plays a vital role in the mechanism of the disease, and in the interests of disease control, should be understood more completely.

Finally, the model has also proved useful in considering the relative impact of different acaricidal dipping strategies on tick populations and the disease (section 8.7). The dangers of switching from fortnightly dipping to monthly dipping regimes has been clearly illuminated by the model predictions. Many developing countries, faced with the inhibitive costs of tick control, are forced to reduce dipping. This, however, could have more serious financial consequences when both ticks and tick-borne diseases increase in prevalence.

To conclude, the philosophy behind building ECFXPERT has already proved its worth, but further extensions and development of the ECFXPERT models are likely to produce even more powerful results.

9. DISCUSSION

"All streams flow into the sea,
yet the sea is never full.
To the place where streams come from,
there they will return again."

Ecclesiastes 1:7, (N.I.V.).

This thesis has investigated the application of a number of different modelling techniques to processes in nature. Each approach has involved obtaining a degree of understanding of the natural process, then based on this producing a model to increase understanding. In each chapter, the approaches have been quite different. In chapter 2, simple deterministic models for the dynamics of specific parasites were constructed. These models were theoretical, being based only loosely on scientific knowledge specific to each parasite. This produced models that are general enough to facilitate application to other parasite systems. However, although general and simple, these models do allow valuable insights into the dynamics of parasite systems. The single species model highlighted the dramatic differences in the predicted behaviour of population size through time between parasites having low survival and high fecundity, such as nematodes, and parasites having high survival and low fecundity, such as the protozoan gut parasite *Entamoeba histolytica*. The earlier observation is important in understanding that high levels of nematode infestation within a herd or flock under observation, may not always correlate with periods of climatic favourability. There is always an unpredictable element to such biological systems, which means that favourability models, such as the M_t index discussed in chapter 1, may occasionally be misleading. The two species commensalism model highlighted the dependence of parasite systems on the state and behaviour of their corresponding host populations. When applied to different species of tsetse flies, the model predicted that *Glossina palpalis* are likely to maintain a relatively constant population size, whereas the population of *Glossina mortisans* is likely to be more changeable. Observations such as this are of great practical value, even though they arise from very simple models. Clearly, tsetse fly control methods would have to be species specific.

It is clear that the model simplicity does not always mean that the model will not produce powerful results. The models in chapter 2 have yielded results of a fairly simple nature, but results that are by no means obvious. The models have, therefore, been valuable as understanding has been increased. Over the last decade, such discrete analytical models have been revisited by researchers because of the discovery of their interesting chaotic properties. Mathematical techniques do not extend far enough to provide the means to satisfactorily analyse such models. Some theory does exist concerning simple maps, $A_n = f(A_{n-1})$ where f is continuous, such as if the system has a period point of period 3, then it must have periodic points of all other periods (see Devaney, 1989). However, mathematics is, as yet, unable to deal with the overall complexity arising from such simple mathematical structures. The development of new models encourages the concurrent development of theory required to analyse the new models. Perhaps in the next decade, new exciting breakthroughs in mathematics will allow increased understanding of these models. However, due to the advancing power of computing methods, it has become attractive and fashionable to analyse models by simulation alone. It was through simulation that the interesting and unpredicted properties of non-linear dynamical systems were discovered, but it is only through mathematics that these properties can be fully understood. Simulation has highlighted the need for increased understanding, but does not provide this understanding in itself.

The models presented in chapter 4 are likewise discrete and also display complicated behaviour, but were developed as models that could be applied only to *Theileria parva*, the parasite responsible for East Coast fever in cattle. Models were constructed around a set of rules taken from published results and expert opinion. In this way, a sufficient set of rules could be established that described the dynamics of the parasite through all its developmental stages. This rule set provided the basis for the models. Rules were translated into a programming language, and the model took life. It was observed that each model was described by a set of difference equations, and that certain behaviour could be explained by observing the nature of the graph of the initial population state against the subsequent population state. This has direct similarities with the models described in chapter 2, the only difference being that in this case the exact mathematical structures of the models are unknown due to the complexity of the rule sets composing each model. Mathematical techniques, therefore, have limited value, and simulation is required for the complete analysis of each model. Bifurcation maps provide a useful way of displaying the behaviour of each model over a range of

conditions, and enable the comparison of different models. Model behaviour exhibited strong similarities with that observed for the models in chapter 2, being composed of areas of periodicity and areas of chaos. The models were extended to consider the effects of chemotherapy, and it was observed that the nature of the graph of initial to subsequent numbers of infected ticks provided a useful tool in comparing the relative benefits of different drugs. This is a useful observation, and enforces the importance of mathematics in model analysis. Attempting to translate a very complex model into a structure similar to that produced by mathematical models of much simpler structure, facilitates a more detailed understanding of the predicted outcomes than just simulation alone. Due to the increased specificity of these models, the resulting predictions produced more detailed conclusions concerning the parasite. The relative benefits of breeding stocks of cattle for resistance could be compared to the benefits of drug treatment of susceptible cattle when challenged with disease. Interesting and surprising conclusions were made concerning the control of the infection at different parameter values.

The chaos theme was extended further through into the stochastic models for East Coast fever presented in chapter 5. These models implemented an algorithm for generating streams of uniform random numbers which formed a basis for all model decisions. Such a generator would be of the form $X_{n+1} = f(X_n) \bmod m$ (see Morgan, 1984), where m and the parameters of the function f are chosen carefully so as to produce a sequence of values $\{X_n\}$ that are in chaos. It follows, therefore, that the output of the simulation models presented is chaotic. This is supported by the results of simulations using each model presented in chapter 8. Under a specific parameter set, the model was run ten times, each time starting at a different position in the sequence of predicted random numbers $\{X_n\}$. In each case, a different sequence of events was predicted, suggesting chaos. This predicted variation enabled statistical comparison of different scenarios, such as the efficacy of different control regimes. This is an element absent in the previous deterministic modelling approaches, and is of vital importance to a model which is to be used in decision making at local or national levels. When linked with an economic component, the financial risks and gains of different disease control strategies will become apparent. Without the economic component, however, ECFXPERT has yielded interesting predictions that do increase understanding of the disease. For example, the importance of carrier status in the disease dynamics has been illuminated, which remains an area of uncertainty amongst experts. The model

itself is only a first approximation to the true field situation, and further modelling and validation is required before a useful management tool is produced. Factors such as host immune response to ticks and parasite, the effects of temperature on the success of the parasite within the tick, and the implementation of a possible tick vaccine may be important to a future version of the model.

The requirement of models to be continually changed and adjusted to consider different hypotheses, or to mimic more complex situations, highlights a great problem to those involved in modelling. The time involved in taking a complex system, such as that describing East Coast fever, and condensing it into a number of components that can be modelled together is immense. ECFXPERT required over 3 years development time, and alterations and extensions to the model may also prove costly. A large amount of the time spent developing the model was spent on the programming and testing of the computer code. There is a great demand for modelling software that will enable the programming and testing time to be drastically reduced.

At Strathclyde University, such a piece of software is being developed by S. Hazelwood and G. Gettinby, called a Network Flow Simulator. The package provides a user friendly environment for defining and simulating discrete time models. The aim is that any population, or group of populations, that can be expressed in the form of a network can be modelled by the simulator. The user divides the population into stages, and defines links between stages and appropriate time delays and survival rates associated with each stage. The simulator then converts relationships into a high level programming language and simulates. This piece of software has already proved useful in producing a climate driven model for anthelmintic resistance amongst nematodes infecting sheep (Gettinby, Hazelwood and Armour, in press). This model was of similar structure to that reported by Gettinby, Soutar, Armour and Evans (1989), but required only a fraction of the time to create. Adaptations and changes to the model can also be undertaken rapidly. The benefits of this approach are paid for in the reduced speed of simulation, as the package is not moulded to a specific biological system, and in the possible inflexibility of the structure of the package when dealing with diversely different systems. These problems, however, are of minor nature, and can be addressed as the software is implemented and developed further. The Network Flow Simulator is an exciting breakthrough and should provide a much needed modelling tool.

REFERENCES

Anderson, R.M., 1978. Population dynamics of snail infection with miracidia. Parasitol., **77**, 201–224.

Anderson, R.M. and May, R.M., 1979. Prevalence of schistosome infections within molluscan populations: observed patterns and theoretical predictions. Parasitol., **79**, 63–94.

Anderson, R.M. *et al.*, 1982. Transmission of *Schistosoma mansoni* from man to snail: experimental studies of miracidial survival and infectivity in relation to larval age, water temperature, host size and host age. Parasitol., **85**, 339–360.

Anon., 1975. Cattle tick in Australia. Inquiry by the cattle tick commission. Australian Government Publishing Service, Canberra.

Bailey, N.T.J., 1975. The mathematical theory of infectious diseases and its applications. Charles Griffin and Company Ltd.

Balashov, Y.S., 1968. Bloodsucking ticks (*Ixodoidea*) – vectors of disease to man and animals. Nauka Publishers, Leningrad. Translation T500, NAMRU 3, Cairo, Egypt. Miscellaneous Publications of the Entomological Society of America, **8**, 161–376.

Ball, F., 1985. In "The population dynamics of rabies in wildlife" (Bacon, P.J., ed.). pp. 197–222. Academic Press, London.

Box, G.E.P. and Jenkins, G.M., 1976. Time series analysis: forecasting and control. Holden-Day Inc.

Branagan, D., 1969. The maintenance of *Theileria parva* infections by means of the Ixodid tick, *Rhipicephalus appendiculatus*. Trop. Anim. Hlth. Prod., **1**, 119–130.

Branagan, D., 1973a. Observations on the development and survival of the Ixodid tick *Rhipicephalus appendiculatus*, Neumann, 1901, under quasi-natural conditions in Kenya. Trop. Anim. Hlth. Prod., **5**, 153–165.

Branagan, D., 1973b. The developmental periods of the Ixodid tick, *Rhipicephalus appendiculatus*, Neumann, 1901, under laboratory conditions. Bull. Entomol. Res., **63**, 155–168.

Branagan, D., 1978. In "Weather and parasitic animal disease" (Gibson, T.E., ed.), pp. 126–140. WHO Technical Note no.159, World Meteorological Organisation.

Bruhn, J.A., Fry, W.E. and Fick, G.W., 1980. Simulation of daily weather data using theoretical probability distributions. J. Appl. Meteorol., **19**, 1029–1036.

Chao-Kuang, H. and Levine, H.D., 1977. Degree-day concept in development of infective larvae of *Haemonchus contortus* and *Trichostrongylus colubriformis* under constant and cyclic conditions. Am. J. Vet. Res., **38**, 1115–1119.

Cowdry, E.V. and Ham, A.W., 1932. Studies on East Coast fever: the life cycle of the parasite in ticks. Parasitol., **24**, 1–49.

Devaney, R.L., 1989. An introduction to chaotic dynamical systems. Addison-Wesley Publishing Company Inc.

Devroye, L., 1986. Non-uniform random variate generation. Springer-Verlag, New York.

Dietz, K., 1988. Density-dependence in parasite transmission dynamics. Parasitol. Today, **4**, 91–97.

Dolan, T.T. *et al.*, 1984. Dose dependent responses of cattle to *Theileria parva* stabilate. Int. J. Parasitol. **14**, 89–95.

Dolan, T.T., 1989. Theileriosis: a comprehensive review. Rev. Sci. Tech. Off. Int. Epiz., **8**, 11–36.

Donnelly, J. and MacKellar, J.C., 1970. The effect of weather and season on the incidence of redwater fever in cattle in Britain. Agric. Meteorol., 7: 5–17.

Duffus, W.P.H., 1976. Theileriosis (Henson, J.B. and Campbell, M., eds.). p. 28. IDRC, Ottawa, No. 086e.

Duggan, A.J., 1970. In "The African Trypanosomiases" (Mulligan, H.W., ed.) pp.41-88. George Allen and Unwin Ltd., London.

FAO, 1984a. Agroclimatological data Africa, Vol I. Rome, Food and Agriculture Organisation of the United Nations.

FAO, 1984b. Agroclimatological data Africa, Vol II. Rome, Food and Agriculture Organisation of the United Nations.

Fawcett, D. *et al.*, 1985. Sporogony in *Theileria* (Apicomplexa: *Piroplasmida*). A comparative ultrastructure study. J. Submicrosc. Cytol., **17**, 299–314.

Fisher, R.A. and Tippett, L.H.C., 1928. Limiting forms of the frequency distribution of the largest or smallest member of a sample. Proc. Cambridge Phil. Soc., **2**, 180–190.

Fivaz, B.H., 1984. Studies on the immunity of the ox and rabbit to *Rhipicephalus appendiculatus* (Neumann). Ph.D. Thesis, University of Zimbabwe.

Gabriel, K.R. and Neumann, J., 1957. On a distribution of weather cycles by length.

Quart. J. R. Meteorol. Soc., **83**, 375–380.

Gabriel, K.R. and Neumann, J., 1962. A Markov chain model for daily rainfall occurrence at Tel Aviv. Quart. J. R. Meteorol. Soc., **88**, 90–95.

Gettinby, G., Hope-Cawdery, M.J. and Grainger, J.N.R., 1974. Forecasting the incidence of fascioliasis from climatic data. Int. J. Biometeorol., **18**, 319–323.

Gettinby, G. and McLean, S., 1979. A matrix formulation of the life cycle of liver fluke. Proc. Royal Irish Academy, **79**, 155–167.

Gettinby, G., Bairden, K., Armour, J. and Benitaz-Ushr, C., 1979. A prediction model for bovine ostertagiasis. Vet. Record, **105**, 57–59.

Gettinby, G., and Gardiner , W.P., 1980. Disease incidence forecasts by means of climatic data. Int. J. Biometeorol., **24**, 87–103.

Gettinby, G., 1987. A computer model with expert rules for the control of African cattle diseases. In "Interactions in artificial intelligence and statistical methods" (Phelps, B., ed.) pp.73–84. Technical Press, Aldershot.

Gettinby, G., Newson, R.M., Calpin, M.J., and Paton, G., 1988. A simulation model for genetic resistance to acaricides in the African brown ear tick *Rhipicephalus appendiculatus* (Acarina: *Ixodidae*). Prev. Vet. Med., **6**, 183–197.

Gettinby, G., Soutar, A., Armour, J. and Evans, P., 1989. Anthelmintic resistance and the control of ovine ostertagiasis: a drug action model for genetic selection. Int. J. parasitol., 19: 369–376.

Gettinby, G. and Byrom, W., 1989. The dynamics of East Coast Fever: a modelling perspective for the integration of knowledge. Parasitol. Today, **5**, 68–73.

Gettinby, G., Hazelwood, S. and Armour, J. (in press). Computer models applied to drug resistance in parasites. In "Resistance of parasites and antiparasite drugs" (Boray, J.C., ed.).

Gibson, T.E., 1978. Weather and parasitic animal disease. World Meteorological Organisation, Geneva, WHO Technical note no. 159.

Goult, R.J. *et al.*, 1973. Applicable mathematics. The MacMillan Press Ltd.

Gumbel, E.J., 1944. Ranges and midranges. Annals Math. Soc., **15**, 415.

Gumbel, E.J., 1952. Statistical theory of extreme values and some practical applications. US Department of Commerce, National Bureau of Standards, Applied Mathematics Series **33.**,

Hugh-Jones, M., 1989. Applications of remote sensing to the identification of the habitats of parasites and disease vectors. Parasitol. Today, **8**, 244–251.

Irvin, A.D., 1983. Clinical and diagnostic features of East Coast fever *(Theileria parva)* infection of cattle. Vet. Record, **113**, 192–198.

Jarrett, W.F.H. *et al.*, 1969. *Theileria parva*: kinetics of replication. Exp. Parasitol. **24**, 9–25.

King, D. *et al.*, 1988. A climate-based model for the development of the Ixodid tick, *Rhipicephalus appendiculatus*, in East Coast fever zones. Vet. Parasitol. **29**, 41–51.

Leslie, P.H., 1945. On the use of matrices in certain population mathematics. Biometrika **35**, 183–212.

Lessard *et al.*, 1990. Geographic information systems for studying the epidemiology of cattle diseases caused by *Theileria parva*. Vet. Record, **126**, 255–262.

Lewis, E.R., 1976. Application of discrete and continuous time network theory to linear population models. Ecology, **57**, 33–47.

MacDonald, G., 1965. The dynamics of helminth infections, with special reference to schistosomes. Trans. R. Soc. Trop. Med. Hyg. 59,489-506.

MacLeod, J. and Colbo, M.H., 1976. Ecological studies of Ixodid ticks (Acari, *Ixodidae*) in Zambia. I. Cattle as hosts of the larvae of *Amblyomma variegatum* and *Rhipicephalus appendiculatus* Neumann. Bull. Entomol. Res., **66**, 65–74.

MacLeod, J. *et al.*, 1977. Ecological studies of Ixodid ticks (Acari: *Ixodidae*) in Zambia. III. Seasonal activity and attachment sites on cattle with notes on other hosts. Bull. Entomol. Res., **67**, 161–173.

May, R.M., 1976. Simple mathematical models with very complicated dynamics. Nature, **261**, 459–467.

Maynard-Smith, J., 1968. Mathematical ideas in biology. The University Press, Cambridge.

McCulloch, B. *et al.*, 1968. A study of the life history of the tick *Rhipicephalus appendiculatus* – the main vector of East Coast Fever – with reference to its behaviour under field conditions and with regard to its control in Sukumaland, Tanzania. Bull. Epizoot. Dis. Afr., **16**, 477–500.

Mehlhorn, H. and Schein, E., 1984. The Piroplasms: life cycle and sexual stages. Adv. Parasitol., **23**, 37–103.

Miller, L.H. *et al.*, 1977. Immunity to blood parasites of animals and man. pp. 1–132. Plenum Press, New York.

Milligan, P.J.M. and Baker, R.D., 1988. A model of tsetse transmitted animal trypanosomiasis. Parasitol., **96**, 211–239.

Molineaux, L. and Gramiccia, G., 1980. The Garki project. World Health Organisation, Geneva.

Mollison, D., 1981. In "The mathematical theory of the dynamics of biological populations II" (Hiorns, R.W. and Cooke, D.L., eds.). pp. 99–107. Academic Press, London.

Mollison, D., 1987. Population dynamics of mammalian diseases. Symp zool. Soc. Lond., **58**, 329–342.

Morgan, B.J.T. 1984. Elements of simulation. The University Press, Cambridge.

Morrison, W.I. *et al.*, 1981. *Theileria parva*: kinetics of infection in the lymphoid system of cattle. Exp. Parasitol., **52**, 248–260.

Morrison, W.I. *et al.*, 1986. In "Parasite antigens: towards new strategies for vaccines" (Pearson, T.W., ed.). pp. 167–213. Marcel Dekker.

Mount, G.A. and Haile, D.G., 1989. Computer simulation of population dynamics of the American Dog tick (Acari: *Ixodidae*). J. Med. Entomol., **26**, 60–76.

Murray, M. and Gray, A.R., 1984. The current situation on animal trypanosomiasis in Africa. Prev. Vet. Med., **2**, 23–30.

Newson, R.M., 1984. Survival of *Rhipicephalus appendiculatus* (Acarina: *Ixodidae*) and persistence of *Theileria parva* (Apicomplexa: *Theileridae*) in the field. Int. J. Parasitol., **14**, 483–489.

Nicks, A.D. and Harp, J.F., 1980. Stochastic generation of temperature and solar radiation data. J. Hydrol., **48**, 1–17.

Ollerenshaw, C.B. and Rowlands, W.T., 1959. A method of forecasting the incidence of fascioliasis in Anglesey. Vet. Record, **71**, 591–598.

Pegram, R.G. and Banda, D.S. (in press). Ecology and phenology of ticks in Zambia: development and survival of free-living stages. Exp. Appl. Acar.

Punyua, D.K., 1984. Development periods of *Rhipicephalus appendiculatus* Neumann (Acarina: *Ixodidae*) under field conditions. Insect Sci. Appl., **5**, 247–250.

Purnell, R.E. *et al.*, 1974. *Theileria parva*: variation in the infection rate of the vector

tick, *Rhipicephalus appendiculatus*. Int. J. Parasitol., **4**, 513–517.

Purnell, R.E., 1977. East Coast Fever: some recent research in Africa. Adv. Parasitol., **15**, 82–132.

Radley, D.E. *et al.*, 1974. East Coast Fever: quantitative studies of *Theileria parva* in cattle. Exp. Parasitol., **36**, 278–287.

Rechav, Y., 1982. Dynamics of tick populations (Acari : *Ixodidae*) in the Eastern Cape Province of South Africa. J. Med. Entomol., **19**, 679–700.

Reichenow, E., 1940. Der Entwicklungsgang des Kustenfiebererreges in Rinde und in der ubertragenden Zecke. Archiv fur Protistenkunde, **94**, 1–56.

Richardson, C.W., 1981. Stochastic simulation of daily precipitation, temperature and solar radiation. Water Resour. Res. **17**, 182–190.

Richardson, C.W., 1984. WGEN: a model for generating daily weather variables. USDA-ARS ARS-8. Washington DC: US Department of Agriculture.

Richie, T.L., 1988. Interactions between malaria parasites infecting the same vertebrate host. Parasitol. **96**, 607–639.

Ripley, B.D., 1987. Stochastic Simulation. Wiley.

Ripley, B.D., 1988. Uses and Abuses of Statistical Simulation. Math. Prog., **42**, 53–68.

Rogers, D., 1988. A general model for the African trypanosoiases. Parasitol., **97**, 193–212.

Short, N.J. and Norval, R.A.I., 1981. Regulation of seasonal occurrences in the tick *Rhipicephalus appendiculatus* Neumann, 1901. Trop. Anim. Hlth. Prod., **13**, 19–26.

Short, N.J. and Norval, R.A.I., 1981. The seasonal activity of *Rhipicephalus appendiculatus* Neumann 1901 (Acarina : *Ixodidae*) in the highveld of Zimbabwe, Rhodesia. J. Parasitol., **67**, 77–84.

Short, N.J., 1986. Effects of climate on the development, behaviour and survival of the free-living stages of *Rhipicephalus appendiculatus*, *Boophilus decoloratus* and *Boophilus microplus*. M. Phil. Thesis, University of Zimbabwe.

Soulsby, E.J.L., 1982. Helminths, arthropods and protozoa of domesticated animals. Bailliere, Tindall.

Stagg, D.A. *et al.*, 1984. Superinfection of established *Theileria*-infected bovid cell lines with *Theileria parva* sporozoites. Annals Trop. Med. and Parasitol., **78**, 335–337.

Sutherst, R.W. and Dallwitz, M.J., 1979. In "Proceedings of the fourth international congress on acarology" (Piffl, E., ed.). pp. 557–564. Akademiai Kiado, Publ. Hse. Sci., Budapest, Hungary.

Sutherst, R.W. and Maywald, G.F., 1985. A computerised system for matching climates in ecology. Agric. Ecosystems Environ., 13: 281–299.

Tatchell, R.J. and Easton, E., 1986. Tick (Acari: *Ixodidae*) ecological studies in Tanzania. Bull. Entomol. Res., **76**, 229–246.

Tatchell, R.J., 1987. Tick Control in the context of ECF immunization. Parasitol. Today **3**, 7–10.

Theiler, A., 1904. East Coast fever. J. R. Army Med. Corps, **3**, 599–620.

Thomas, R.J. and Starr, J.R., 1978. Forecasting the peak of gastrointestinal nematode infections in lambs. Vet. Record, **103**, 465–468.

Tukahirwa, E.M., 1976. The effects of temperature and relative humidity on the development of *Rhipicephalus appendiculatus* Neumann (Acarina, *Ixodidae*). Bull. Entomol. Res., **66**, 301–312.

Von Mises, R., 1936. La distribution de la plus grande de n valeurs. Revue Math. l'Union Interbalcanique, **1**, 1–20.

Walker, A.R. *et al.*, 1981. Assessment of *Theileria* infections in *Rhipicephalus appendiculatus* ticks collected from the field. Z. Parasitenkd., **65**, 63–69.

Woolhiser, D.A. and Pegram, G.G.S., 1979. Maximum likelihood estimation of Fourier coefficients to describe the seasonal variations in parameters in stochastic daily precipitation models. J. Appl. Meteorol. **18**, 34–42.

Yeoman, G.H., 1966. Field vector studies of epizootic East Coast fever: a quantitative relationship between *R. appendiculatus* and the epizooticity of East Coast fever. Bull. Epizoot. Dis. Afr., **14**, 5–27.

Yeoman, G.H., 1967. Field vector studies of epizootic East Coast fever: pasture ecology in relation to *R. appendiculatus* infestation rates on cattle. Bull. Epizoot. Dis. Afr., **15**, 89–113.

Young, A.S. *et al.*, 1988. Integrated control of ticks and tick-borne diseases of cattle in Africa. Parasitol., **96**, 403–432.